TÉCNICO LISBOA

# Design and Optimization for Mobile Networks in Stadium Environments

**Carolina Pereira Lopes**

Dissertation to obtain the Master of Science Degree in

**Electrical and Computer Engineering**

Supervisor: Prof. António Luís Campos da Silva Topa

**Examination Committee**

Chairperson: Prof. José Eduardo Charters Ribeiro da Cunha Sanguino

Supervisor: Prof. António Luís Campos da Silva Topa

Member of Committe: Prof. António José Castelo Branco Rodrigues

**November 2019**

Declaration

I declare that this document is an original work of my own authorship and that it fulfils all the requirements of the Code of Conduct and Good Practices of the Universidade de Lisboa.

*To my beloved parents who always invest in my education and believe in me.*

*To my adorable dog for all the nights and days that kept me company studying.*

*And, especially, to the best buddy anyone could ask for, Francisco Santos (Espanhol) for being tireless in every good and bad moment.*

# Acknowledgements

I would like to start by thanking my dissertation supervisor, Prof. António Topa, for allowing me to work on the theme I proposed and enabling me to freely manage my time based on my working schedules. Also for offering me the honor of having this work presented in the XIII Iberian Meeting on Computacional Electromagnetics international conference in Santander, Spain. This dissertation had Lisbon's *Instituto de Telecomunicações* as its host institution.

A special acknowledgement is given to Eng. Ricardo Santos, who introduced me to the world of telecommunication solutions for special events. He helped me with his prised advices and his tremendous knowledge. Also, I would like to thank the company OMTEL, *Estruturas de Comunicações, S.A.*, that have always been supportive and understanding of the challenging situation that is starting a new chapter in life without entirely having closed the previous one. Furthermost, it was mainly thanks to the company's staff that I was able to use the iBwave Designing Software for simulations. Without them, this work would not have been the same.

For their great friendship during this journey, I would like to thank my dear friend Francisco Santos for all the help and patience demonstrated along these years, my amazing friend Maria Casimiro who was one of the friendships for life that IST gave me and my travel buddy Inês Mataloto for being my partner in the greatest adventure of my life.

Lastly, I would like to thank and show my deep gratitude to my parents and brother for their unconditional love, emotional support, and for all the opportunities they have given me. Without them, I would not be the person I have become.

# Abstract

The main problem addressed in this dissertation is managing the growing demand for data-intensive applications while maintaining high-quality customer experience in a high capacity location. In a large venue like a stadium, a large number of people use their smartphones to share pictures and experiences, such as real-time video and download/upload information. This behaviour creates traffic profiles that differ from those typically seen in an ordinary day network, with higher uplink traffic and more frequent packet transmission. This dissertation has a starting point in the designing of an LTE network solution for stadium *José Alvalade*. The process of radio planning began by obtaining the 3D model of the stadium after doing a site survey. The selection and best mounting positions for the antennas were discussed, and the elements responsible for its operation presented for both a single-operator and multi-operator scenario. The capacity sizing theoretical background was exposed, and the number of sectors necessary to satisfy the nowadays traffic profile and the LTE subscribers was calculated, as so the number of resources needed to support each service type. Considering the 1800 and 2600 MHz band, simulations for measuring signal strength and noise, coverage areas, maximum achievable data rate, LTE overlapping and the needed mobile transmission power were performed and presented. The best solution found was considering 40 sectors for covering the seating area. Only, 20 antennas were used being divided in two layers, both 1800 MHz band and 2600 MHz band. A brief approach was made to the physical and financial limitations when designing a real solution. Using data from the past, two forecast cases for the traffic demand growth were assumed, and an estimation of the expiration date of the final solution was presented.

# Keywords

Growing Demand, High-quality Experience, Traffic Profiles, Radio Planning, Capacity Sizing, Simulations

# Resumo

O principal desafio desta dissertação é acompanhar o crescente uso de aplicações extremamente exigentes no que diz respeito a consumo de dados e, ao mesmo tempo, garantir boa qualidade de experiência aos utilizadores em locais com milhares de pessoas. Em estádios, um grande número de espectadores usa os respetivos smartphones para partilhar fotografias e experiências, como vídeos em tempo real e para realizar descargas/cargas de informação. Esse comportamento cria perfis de tráfego que diferem dos do dia-a-dia, com maior tráfego de *uplink* e transmissão de pacotes mais frequente. A dissertação tem como ponto de partida o *design* de uma rede 4G única para o Estádio José Alvalade. Após uma visita técnica ao estádio, o modelo 3D foi obtido e o planeamento de rádio começou. O estudo do local mais indicado para montar as antenas foi descrito e os elementos responsáveis foram apresentados, tanto para cenários onde apenas um operador é considerado, como para cenários onde os três operadores são tidos em conta. O pensamento técnico por detrás do dimensionamento de capacidade foi exposto e o número de sectores necessários para satisfazer o consumo de dados, de todos os utilizadores que têm acesso à tecnologia LTE, foi calculado. O número de recursos alocados para tal também foi calculado. Considerando a banda dos 1800 MHz e dos 2600 MHz, foram realizadas simulações para medir a intensidade do sinal e ruído, as áreas de cobertura, a taxa de dados máxima alcançável, as zonas de sobreposição de sectores e a potência de transmissão dos equipamentos móveis necessária para estabelecer uma ligação *uplink*. A melhor solução encontrada apresenta 40 sectores a cobrir as bancadas. No entanto, apenas 20 antenas foram utilizadas uma vez que cada uma apresenta dois sectores, um na banda dos 1800 MHz e outro na banda dos 2600 MHz. Uma breve abordagem foi feita às limitações físicas e financeiras do projeto real. Tendo por base resultados do passado, foram consideradas duas previsões da crescente exigência do tráfego móvel e uma estimativa para a viabilidade da solução proposta foi apresentada.

# Palavras-chave

Crescente uso de aplicações extremamente exigentes, Boa Qualidade de Experiência, Perfis de Tráfego, Planeamento de Rádio, Dimensionamento de Capacidade, Simulações

# Table of Contents

# List of Figures

# List of Tables

# List of Acronyms

| | |
|---|---|
| 3D | Three-Dimensional |
| 16 - QAM | 4 bits per symbol Quadrature Amplitude Modulation |
| 2G | $2^{nd}$ Generation of Mobile Communications |
| 3G | $3^{rd}$ Generation of Mobile Communications |
| 3GPP | Third Generation Partnership Project |
| 4G | $4^{th}$ Generation of Mobile Communications |
| 64 – QAM | 6 bits per symbol Quadrature Amplitude Modulation |
| AMC | Adaptive Modulation and Coding |
| ANACOM | Autoridade Nacional de Comunicações |
| BBU | Baseband Unit |
| BLER | Block Error Rate |
| BPL | Building Penetration Loss |
| BS | Base Station |
| BTS | Base Transceiver Station |
| CA | Carrier Aggregation |
| CC | Component Carrier |
| CCEs | Control Channel Elements |
| CP | Cyclic Prefix |
| CQI | Channel Quality Indicator |
| CSFB | Circuit Switch Fall Back |
| DAS | Distributed Antennas System |
| DC | Directional Coupler |
| DL | Downlink |
| DSP | Digital Signal Processor |
| E2E | End-to-End |

| | |
|---|---|
| eICIC | Evolved Inter-cell Interference Coordination |
| FDD | Frequency Division Duplex |
| FFR | Fractional Frequency Reuse |
| FTP | File Transfer Protocol |
| GBR | Minimum Guaranteed Bit Rate |
| HB | Horizontal Beamwidth |
| HD | High Definition |
| HetNet | Heterogeneous Network |
| HO | Handover |
| IC | Interference Control |
| ICIC | Inter-cell Interference Coordination |
| IFLB | Inter-Frequency Load Balancing |
| ITS | Intelligent Transportation System |
| KPI | Key Performance Indicator |
| KQI | Key Quality Indicator |
| LB | Load Balancing |
| LBA | Load Balancing Action |
| LoS | Line-of-Sight |
| LPN | Low-Power-Nodes (same as small cells) |
| LTE | Long Term Evolution |
| LTE – A | LTE – Advanced |
| LTE – B | LTE – Broadcast |
| M2M | Machine-to-Machine |
| MADR | Maximum Achievable Data Rate |
| MBMS | Multipedia Broadcast Multicast Service |
| mErl | miliErlangs |
| MIMO | Multiple-Input Multiple-Output |
| mmWave | Milimiter Wave |
| MNOs | Mobile Network Operators |
| MooD | MBMS-operation-on-Demand |
| MOS | Mean Opinion Score |
| MT | Mobile Terminal |
| MU-MIMO | Multiple User MIMO |
| NR | New Radio |

| | |
|---|---|
| ODF | Optical Distribution Frame |
| OFDMA | Orthogonal Frequency Division Multiplexing |
| PBCH | Physical Broadcast Channel |
| PDCCH | Physical Downlink Control Channel |
| PDSCH | Physical Downlink Shared Channel |
| PPs | Power Points |
| PRACH | Physical Random Access Channel |
| PRB | Physical Resource Blocks |
| PUCCH | Physical Uplink Control Channel |
| PUSCH | Physical Uplink Shared Channel |
| QCI | QoS Class Identifier |
| QoE | Quality of Experience |
| QoS | Quality of Service |
| QSPK | Quadrature Phase Shift Keying |
| RACH | Random Access Channel |
| RB | Resource Block |
| RE | Resource Element |
| RI | Radio Installation Points |
| RLB | Radio Link Budget |
| RF | Radio Frequency |
| RFU | Radio Frequency Unit |
| RRU | Radio Remote Unit |
| RSRP | Reference Signal Received Power |
| Rx | Receiving |
| SC – FDMA | Single Carrier Frequency Division Multiple Access |
| SINR | Signal-to-Interference-plus-Noise-Ratio |
| SISO | Single-Input-Single-Output |
| SMS | Short Message Service |
| SNR | Signal to Noise Ratio |
| TB | Transport Blocks |
| TTI | Transmission Time Interval |
| Tx | Transmission |
| UE | User Equipment |
| UL | Uplink |

| | |
|---|---|
| VB | Vertical Beamwidth |
| VoIP | Voice over Internet Protocol |

# List of Symbols

| | |
|---|---|
| $\alpha_{pd}$ | Average Power Decay |
| $B_{ch}$ | Channel Bandwidth |
| $Blocking$ | Blocking rate per service |
| $B_{RB}$ | Bandwidth of one RB |
| $C$ | Channel Capacity |
| $CellSubscriptionCapacity$ | Achievable Downlink Data Rate |
| $Connection_{duration}$ | Duration of the connection |
| $d$ | Distance |
| $data_{rate}$ | Data Rate |
| $datarate_{average}$ | Data Rate Average |
| $duty_{cycle}$ | Duty Cycle |
| $Efficiency$ | Spectral Efficiency |
| $G_r$ | Gain of Receiving Antennas |
| $G_t$ | Gain of Transmitting Antennas |
| $IbCeiling$ | Maximum Load Difference |
| $IbThreshold$ | Minimum Load Difference |
| $L_0$ | Path Loss in Free Space Propagation |
| $LoadDiff$ | Load Difference |
| $L_{p\ ind}$ | Penetration Attenuation |
| $L_{p\ outd}$ | Outdoor Path Loss |
| $L_{ptotal}$ | Reference Path Loss |
| $LTE_{sub}$ | LTE subscribers |
| $LTE_{subscribersyear}$ | Number of LTE subscribers in 2018 |

| | |
|---|---|
| $LTE_{subscribersyear}$ | Number of LTE subscribers estimated for the year to predict |
| $M$ | Modulation Order |
| $M_F$ | Fading Margin |
| $n$ | Number of Tx/Rx antennas |
| $NumIFLBrelations$ | Number of IFLB relations |
| $N_{RB}$ | Number of RBs |
| $N_{streams}$ | Order of MIMO configuration |
| $N_{sub-carrier/RB}$ | Number of sub-carriers per RB |
| $N_{symbols/subframe}$ | Number of OFDM symbols per sub-frame |
| $P_r$ | Received Power |
| $P_t$ | Transmitted Power |
| $QCIsubscriptionQuanta$ | Minimum Acceptable Downlink Data Rate |
| $R$ | Instantaneous Data Rate |
| $RE$ | Resource Elements |
| $\mathrm{RadioFrame}_{\mathrm{length}}$ | Radio Frame length |
| $Throughput_{2018}$ | 2018 Throughput |
| $Throughput_{newsubscription}$ | Throughput correspondent to the extra LTE subscribers |
| $Throughput_{total}$ | Total Throughput |
| $Throughput_{year}$ | Throughput per service for each year |
| $t_{TTI}$ | Time Transmission Interval |
| $Tx_{delay}$ | Transmission Delay |

# Chapter 1

# Introduction

This chapter gives a brief overview of the optimization of the mobile network for overhead situations. Before establishing work targets and original contributions, the scope and motivations are brought up. As irrefutable proof that the problem exists in the case study stadium.

## 1.1 Motivation

Twenty years ago, phones and events did not mix. If a person desired to document an event, it had to hire a photographer and wait days to see the results. Today, everyone has a phone in their pocket and can share the event immediately on social media. The age of the smartphone is actually changing the experience of events and the events themselves. Figure 1.1 exemplifies this changing, before the beginning of a football match at stadium *José Alvalade* a person is streaming a South American football match in his smartphone.

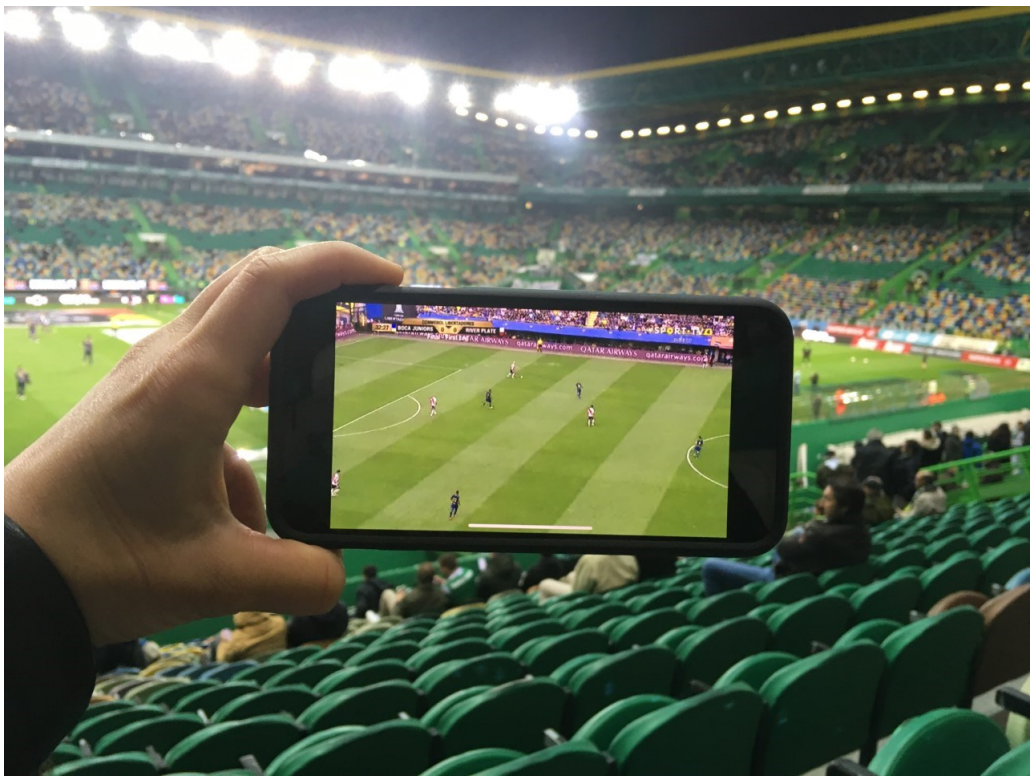

*Figure 1.1 - Photography taken of a person streaming a football match in a stadium environment.*

According to [Eric17], at the 2016 sports event in Rio de Janeiro, social networking, video streaming and web browsing dominated the traffic. Messaging was also prominent, presumably due to the posting of pictures and videos. There was four times more data traffic carried by networks when compared to the 2012 event in London [Data13].

One year later, in the world championship for aquatic sports in Hungary, there was a similar distribution. However, social networking and video streaming categories were even more dominant. The different application categories' share of traffic at both events can be seen in the following graphs, Figure 1.2 and Figure 1.3.

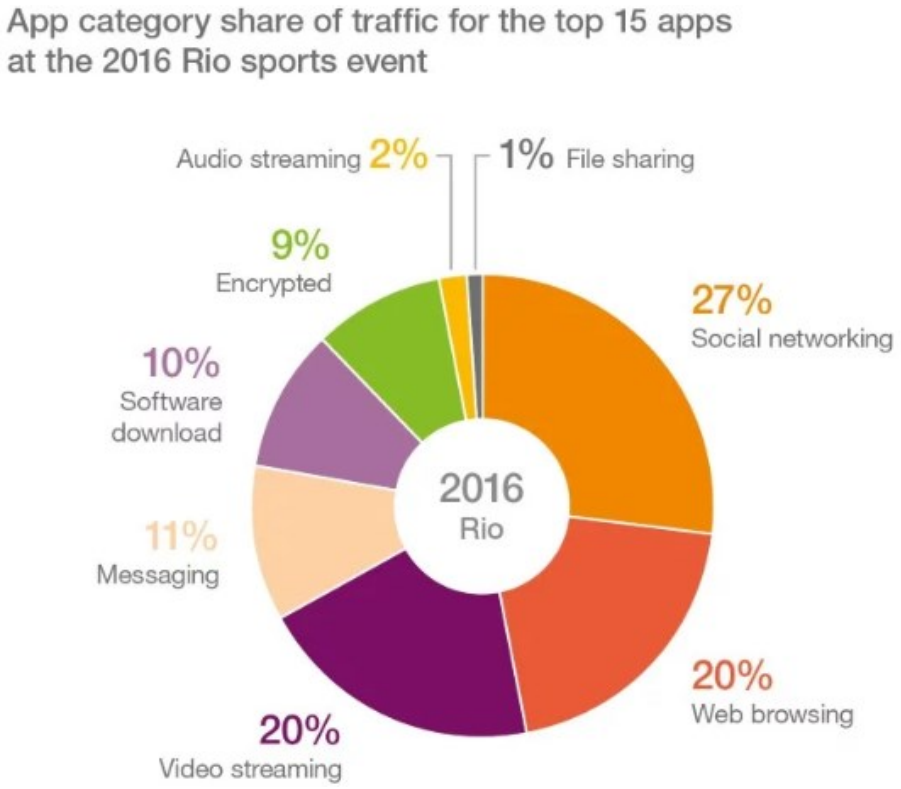


*Figure 1.2 - Application category share of traffic at the 2016 Rio sport event (extracted from [Eric17]).*

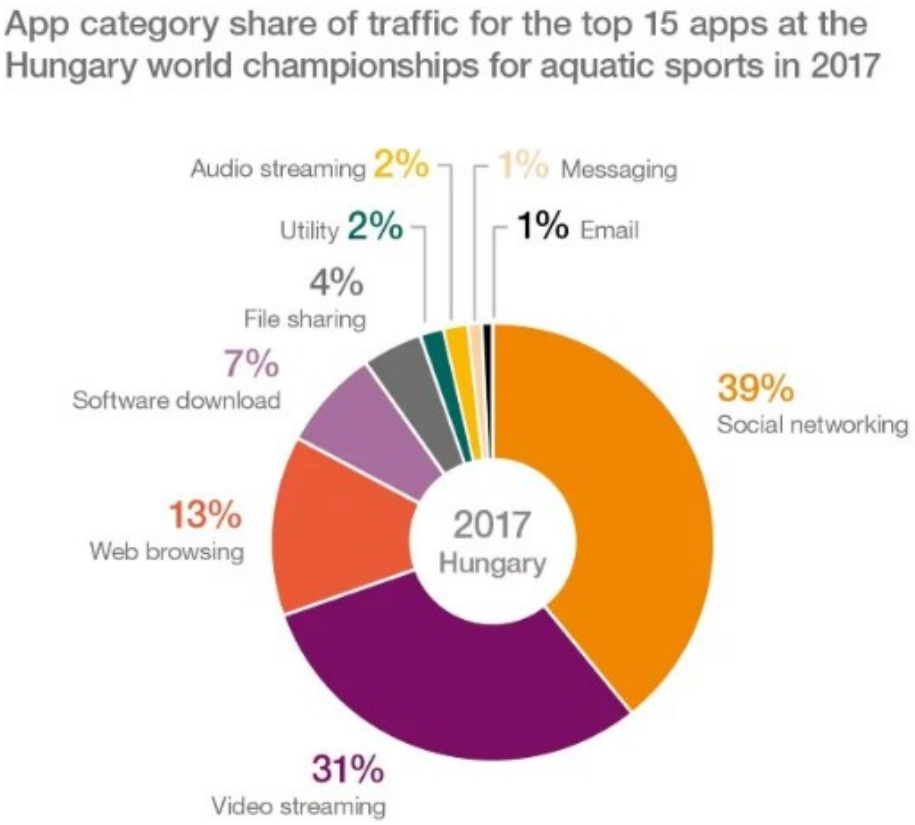


*Figure 1.3 - Application category share of traffic at the 2017 Hungary sport event (extracted from [Eric17]).*

Data from the recent major event above, placed at Hungary in 2017, shows that daily mobile data traffic in areas associated with the event was as high as ten times average volumes. The growth in mobile traffic at events, challenges operators and event organizers to provide ever better content at events, i.e., finding a way of boosting mobile phone capacity and high-quality coverage at mass events.

Besides the constant changing in the data traffic at events situations, the high quality of experience that will be required in the next three to five years by the spectators are the reasons to study the existing solutions for sporting events and how to design better wireless networks in stadiums environments.

This dissertation tries to find an optimum solution for a specific stadium environment by adapting techniques and practises used in other stadiums.

## 1.2 Problem Description

Nowadays, when users are at a music festival, sporting event or another mass event they might see their phones showing there is a signal available, yet nothing is getting through. Although subscribers (users') are more forgiving in those situations. If it takes several attempts to make a successful call through mobile applications like WhatsApp/Skype, download/upload a photo or share real-time video in social networks, it will leave a mark on operators' reputation and can affect subscribers' future choices.

Mass events attract tens of thousands of visitors that generate mobile traffic comparable to the traffic generated in a medium-sized city requiring ten or more base stations to service, at the same time. To prevent network degradation, preparation is essential, so it is vital to possess correct and detailed information on where and when an event will take place and what is the expected attendance. For those reasons, it is critical to have in account that each case is different, and the solution is unique.

When a Long Term Evolution (LTE) network is designed and optimised, these services focus on improving the performance of both indoor solution for the stadium and outdoor coverage solution of the surrounding areas. The aim is to provide Quality of Experience (QoE) to the users in events situations. This report addresses this problem, aiming at providing an assessment for a specific scenario and potential implementation guidelines.

The problem in the addressed case study is real. Figure 1.4 presents two speed test results obtained on the 3rd of February 2019 at the stadium *José Alvalade*, in Lisbon with a smartphone using two different applications, during the half-time of one match. Despite the use of two different applications, the result was the same. The congestion was evident, making it impossible to use mobile data, providing a poor QoE.

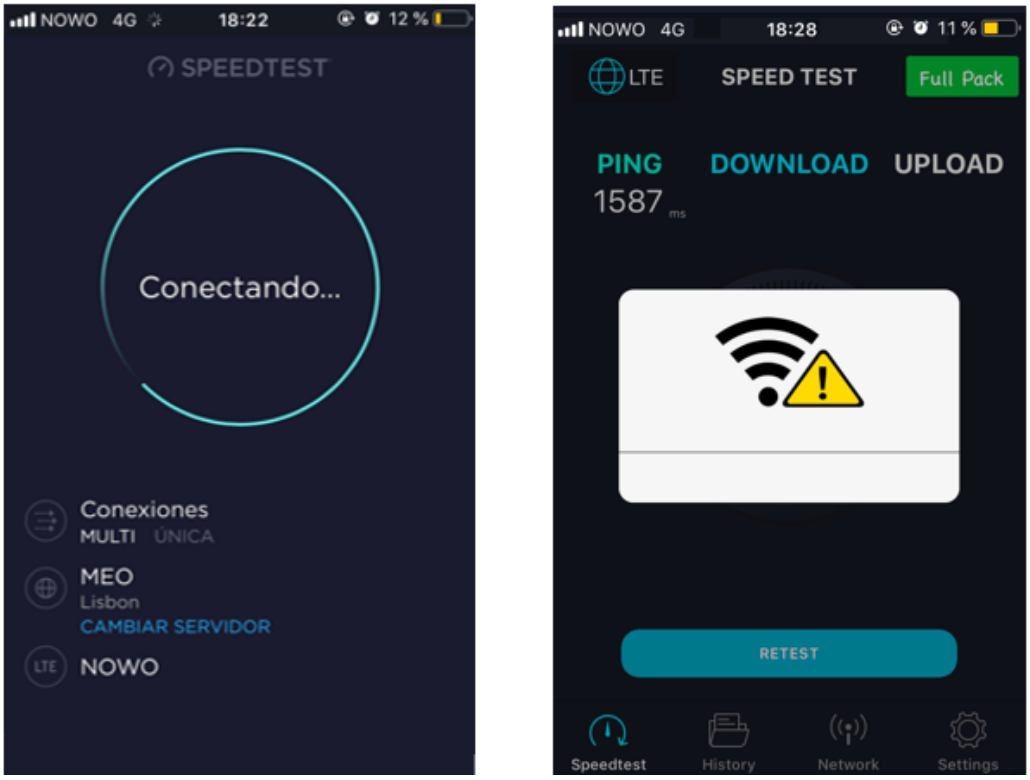


*Figure 1.4 - Speed Test results obtained using the application Speedtest (right printscreen) and OiMeçoInternet (left printscreen) for iOS operating system.*

This dissertation seeks to find an optimum solution for stadium *José Alvalade* environment by simulating different antenna models and adapting techniques and practises used before but now having in consideration the Portuguese spectators' characteristics.

# Chapter 2

# Fundamental Concepts and State of the Art

This chapter provides an LTE overview, mainly focussing on the network, the coverage and capacity aspects, and the performance parameters. It is made a connection between the fundamental concepts and the mass event approach. A brief state of the art is also presented.

## 2.1 Radio Interface

This section presents an overview of some essential points of the radio interface for LTE and parallelism with the LTE requirements for mass events situations, the content presented is based on [Syed09], [HoTo11] and [Yout17].

It is known that LTE operates in different arrangements of frequency and bandwidth, depending on the region where it is implemented. Accordingly, to [ANAC16], the three frequency bands chosen for LTE were 800 MHz, 1800 MHz and 2600 MHz. It is important to refer that LTE can coexist with the previous $3^{rd}$ Generation of Mobile Communications (3GPP) technologies, so some bands can be used simultaneously by LTE and by other technologies. There are a large number of allocations or radio spectrum that have been reserved for Frequency Division Duplex (FDD), for traditional cellular operators who already have established 2G and 3G services, it is popular to have the spectrum “paired” as FDD.

Connecting multiple devices to a single access point requires multiple access schemes. LTE network uses Orthogonal Frequency Division Multiple Access (OFDMA) for downlink (DL) and Single Carrier Frequency Division Multiple Access (SC-FDMA) for uplink (UL). In UL the signal looks like a single carrier modulated at a higher data rate. The main difference between this access technique and OFDMA is the lower power consumption for signal generation. The basic parameters .e.g. sub-frames and Transmission Time Interval (TTI) were matched with those of the DL.

In FDD, the downlink (DL) and the uplink (UL) radio frames are not at the same carrier. The radio frame is called type 1 by the 3GPP and has 10ms length (duration), these are divided into ten sub-frames, each sub-frame being 1.0ms long, shown in Figure 2.1. Each sub-frame is further divided into two slots, each with a duration of 0.5ms. One sub-frame is also the TTI. The physical layer of LTE is by default, in the time domain, divided in TTIs and in order to achieve the requirements of low latency tend to evolve to shorter TTIs.

By default, the frequency domain is divided into equally sized Physical Resource Block (PRB) of 12 sub-carriers with 15 kHz resulting in a 180 kHz minimum bandwidth allocation. One slot can be a combination of 7 or 6 Resource Elements (REs), depending on if a Cyclic Prefix (CP) length is used. The length of the CP has a fundamental role: if it is too short, it becomes impossible to avoid the multipath reflection delay spread and, in another hand, if it is too long, it narrows the data throughput capacity. Scheduling is the process of allocating resources according to their need and priority. A scheduling block is a group of two Resource Blocks (RBs), to a single user, so the quantity of scheduling blocks is proportional to the data speed required by the user.

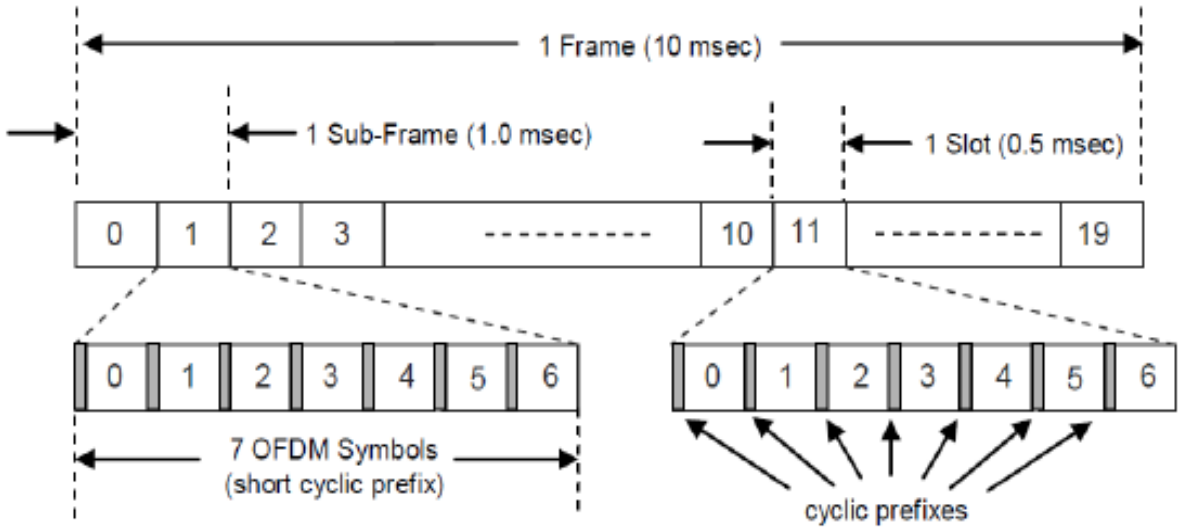


*Figure 2.1 - Frame Structure Type 1 with short CP (extracted from [Share16]).*

Some Reference Symbols (RSs) are inserted, in a fixed location, to synchronise, demodulate and to evaluate the LTE channels. The symbols are used for Multiple-Input Multiple-Output (MIMO) operations. LTE-A supports 8x8 MIMO in DL and 4x4 UL. According to [Bryd13], MIMO can be sub-divided into three main configurations: the transmit diversity where the same signal is sent from different antennas with the same coding, exploiting the gains from independent fading between antennas. The spatial multiplexing is a different configuration, consists of sending signals from two or more different antennas with different data streams. And finally, MIMO also relies on Pre-Coding, which exploits transmit diversity by weighting information streams, i.e., the transmitter sends the coded information to the receiver in order to estimate radio channel conditions and maximise the received Signal-to-Noise Ratio (SNR). At stadium situations, 4G/LTE with MIMO is being deployed in some cases because it allows multiple signals to be sent and received on the same radio channel and supports four frequency bands. In the LTE capacity sizing chapter, the theme MIMO is presented with greater detail.

The Adaptive Modulation and Coding (AMC), as well as too many other 3GPP systems, was proposed in order to improve system capacity and also coverage reliability, the modulation scheme and the coding rate may be adapted according to the channel conditions. In this situation, the transmitter based on the variations of the received signal quality tries to match the data rate for each user. LTE uses QPSK, 16-QAM and 64-QAM modulation schemes: 64-QAM carries 6 bits per symbol, whereas QPSK and 16-QAM carry 2 and 4 bits per symbol, respectively. These last two schemes are available in all devices, while support for 64-QAM in UL is a User Equipment (UE) capability, and can only be supported by some devices, Table 4.1 presents a resume of the UE category.

According to [Fuji13], a “collision” happens if more than one UE transmit on the same frequency and at the same time, so to avoid interference: LTE uses OFDMA for DL and SC-FDMA for UL, as was mentioned before. For OFDMA systems, multiple techniques can be used to dodge a collision, i.e., tryo to avoid each other either in the frequency domain or in the time domain.

In order to transport data and signalling messages, LTE uses three types of channels: the Logical, the

Physical and the Transportation ones. Logical channels are defined by the type of information it carries. They can be classified into control or traffic channels. The control channels are used to transmit plain control information, and the traffic channels, are used to carry the data between the UE and the network. The transportation channels define how and with what characteristics the information is transmitted. At last, the physical channels are defined by the physical resources used to transmit the data. They are divided into Physical Downlink Shared Channel (PDSCH), Physical Broadcast Channel (PBCH), Physical Downlink Control Channel (PDCCH), Physical Uplink Shared Channel (PUSCH), Physical Uplink Control Channel (PUCCH) and Physical Random Access Channel (PRACH). The transmission of data in the PDSCH is made in units known as Transport Blocks (TBs).

According to [NSN13], during extreme mass events, control plain processing capacity, RACH capacity and inter-cell interference continue to represent a challenge. PRACH collisions can occur in LTE. If two terminals select the same PRACH resource, unnecessarily high power is needed for the PUSCH, which causes massive inter-cell interference.

It is possible to avoid cell-edge user interference by using Fractional Frequency Reuse (FFR). ODFMA can be seen as dividing the bandwidth into multiple smaller units, the sub-carriers. FFR is the process of grouping them, using dynamic allocation, making this interference mitigation technique efficient for modern cellular networks due to its low complexity, low coordination requirements and resource allocation flexibility.

## 2.2 Coverage and Capacity

When designing a dedicated solution, the main objectives are to determine the areas that need to be covered and to calculate the number of serving sites required to cover the target areas, while fulfilling the capacity and coverage goals and requirements. This section presents a basic description of LTE's coverage and capacity, establishing a connection with the mass events' situation.

### 2.2.1 Coverage

When one talks about coverage, is important to know that it refers to the range of a network, coverage estimation calculates the area where the base station can be "heard" by the users (receivers). There are two different ways of defining coverage: geographic coverage is the percentage of the territorial area where the service is available, and population coverage is the percentage of the population to whom the service is available. When designing a dedicated solution to an event situation, the main concern is the percentage of the population to which the service is available.

Radio link budget (RLB) is of central importance to coverage planning in LTE, taking the interference caused by traffic into account, the calculation of the maximum path loss is based on the required Signal Interference-to-Noise Ratio (SINR) level at the receiver. The minimum received signal and maximum path loss, in both DL and UL, are converted into cells radius. According to [Corr13], cells are usually classified into different categories depending on the cell's radius, the relative position of the Base Station

(BS) antennas and its respective transmitted power. As can be seen in Table 2.1, there are four categories: macrocells (which could be large or small), microcells, picocells and femtocells. According to [Fuji13], with identical conditions, the throughput from one cell is the same regardless of cell sizes. It also means that total capacity is inversely proportional to the square of the cell radius (lower radius cell, increasing maximum capacity).

*Table 2.1 - Cell's radius and transmitted power for different cell categories (based on [Pire15]).*

| **Cell Category** | **Radius [km]** | **Maximum transmitted power [dBm]** |
|---|---|---|
| Macrocells | > 1 | 44 |
| Microcells | 0.1 – 1 | 38 |
| Picocells | < 0.1 | 24 |
| Femtocells | < 0.05 | 20 |

Compared with the macrocell site, microcells have a shorter distance and a more direct signal path between the serving site and the UE, which leads to a loss reduction around 20 to 40 dB.

The coverage area radius of a cell is estimated as follows:

$$R_{\max[km]} = 10^{\frac{P_{t[dBm]}+G_{t[dBm]}-P_{r[dBm]}+G_{r[dBi]}-L_{ptotal[dB]}-M_{F[dB]}}{10\alpha_{pd}}} \quad (2.1)$$

Where:

- $P_t$ is the transmitted power;
- $G_t$ and $G_r$ are the gain of the transmitting and receiving antennas, respectively;
- $P_r$ is the minimum receiving power required by the UE;
- $L_{ptotal[dB]}$ is the path loss;
- $M_{F[dB]}$ refers to the fading margin;
- $\alpha_{pd}$ is the average power decay.

According to [Corr13], at indoor situations, there is the need to add an attenuation to the signal, coming from penetration into indoors. So the path loss can be calculated, based on (2.3) result:

$$L_{ptotal[dB]} = L_{p\ outd[dB]} + L_{p\ ind[dB]} \quad (2.2)$$

Where:

- $L_{p\ outd[dB]}$ is the outdoor path loss;
- $L_{p\ ind[dB]}$ is the penetration attenuation.

The outdoor path loss is estimated, based on (2.4), as follows:

$$L_{p\ outd[dB]} = L_{0[dB]} + 10\ \alpha_{pd} \log\left(d_{[km]}\right) \quad (2.3)$$

Where:

- $d_{[km]}$ is the distance.
- $L_{0[dB]}$ is the path loss in free space propagation.

The path loss in free space propagation can be calculated as follows, where the distance is equal to 1 km:

$$L_{0[dB]} = 32.44 + 20 \log\left(d_{[km]}\right) + 20\ \log\left(f_{[MHz]}\right) \quad (2.4)$$

The penetration attenuation is given by a model that follows the Log-Normal Distribution for an overall indoor coverage probability.

The LTE system will adapt the modulation scheme used on the radio channel automatically according to the actual radio channel quality. Lower order modulations like QPSK are more robust and can better tolerate higher levels of interference. The coverage range will be bigger. High order modulations such as 16-QAM and 64-QAM will offer better bit rates, although they are more susceptible to errors due to their sensitivity to noise, interference and channel estimation errors, and will have a coverage range close to the antenna. Regarding frequency bands, lower frequencies using 800 MHz band are used in order to provide more extensive coverage range, while higher frequencies in the 1800 MHz and 2600 MHz bands are useful in providing larger capacities. Since the main objective, at events situations, is to have a more concentrated coverage edge and to handle large capacities, high order modulations are a better choice. Therefore the 800 MHz band is not considered, because 2600 MHz and 1800 MHz bands provide up to 20 MHz and 14 MHz of additional capacity, respectively.

The signal of a dedicated solution for an event must be dominant throughout the venue, even if there are areas where the existing macro coverage gives a “five-bar” reading on the phone. Is essential to overcome the residual macro network by a comfortable margin (5~7 dB). Otherwise, the user´s equipment (UE) may be registered with the macro network, a highly undesirable situation because an important requirement is to offload the macro network at the event area. According to [iBwave], the most effective way to reduce the residual macro coverage is to downtilt antennas at nearby sectors that points

towards the venue.

The predominantly outdoor macro networks have limits reaching indoors, mainly where building materials block cellular signals. When we specify for stadium environments, unique characteristics must be taken into account, such as the existence of a roof or not. When stadiums have roofs composed of steel-enforced structures the building penetration losses (BPL) values are lower, and the signal is diffracted which causes little attenuation, thus providing a strong signal in the bowl. If the nearby sectors of the outdoor network, are down-tilted, the signal path will penetrate the concrete wall and significantly attenuates before it reaches the bowl, as shown in the green path of Figure 2.2.

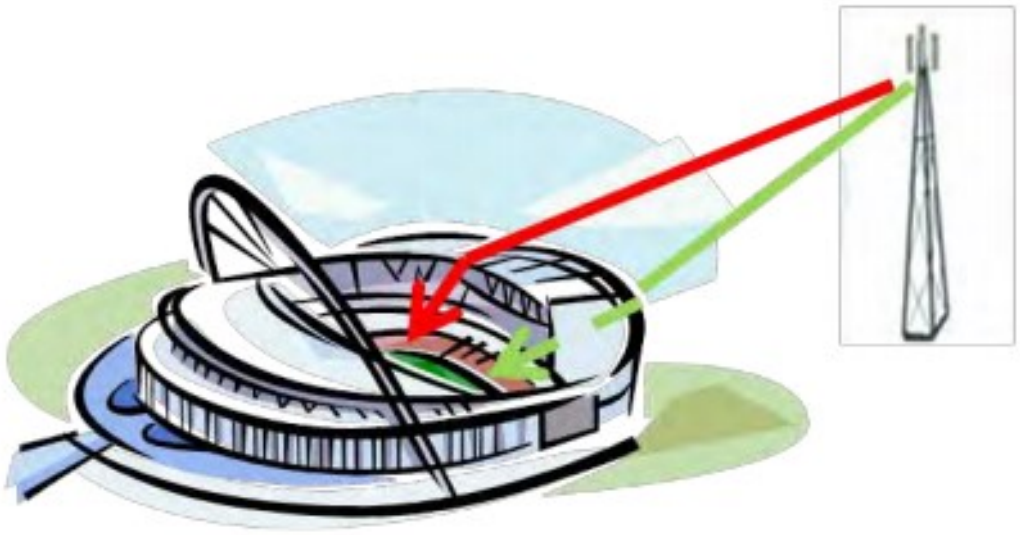

*Figure 2.2 - Down-Tilting Sector Antennas (extracted from [Jevre15]).*

## 2.2.2 Capacity

In LTE, the capacity can be described as the number of users that can be served simultaneously by a serving site for a given service (for example, data). The maximum number of users that can access the network at a given instant depends on the amount of RBs that are required by each user. An approximate number of the amount of RBs can be calculated by using:

$$N_{RB} = \frac{B_{ch[kHz]}}{B_{RB[kHz]}} \cdot \frac{P_{Bch[\%]}}{100} \tag{2.5}$$

Where:

- $B_{ch}$: channel bandwidth;
- $B_{RB}$: bandwidth of one RB, which is 180 kHz;
- $P_{Bch[\%]}$: percentage of the channel bandwidth used. For a 1.4 MHz channel bandwidth is 77% and 90% for the remaining ones.

In *Table 2.2*, is presented the relation between some LTE bands and the corresponding number of RBs.

*Table 2.2 - Number of RBs and sub-carriers associated with each LTE channel bandwidth (extracted from [Pire15]).*

| **Channel bandwidth [MHz]** | 1.4 | 3.0 | 5.0 | 10 | 15 | 20 |
|---|---|---|---|---|---|---|
| **Number of RB** | 6 | 15 | 25 | 50 | 75 | 100 |
| **Number of sub-carriers** | 72 | 180 | 300 | 600 | 900 | 1200 |

In terms of capacity, it is important to compare the number of RBs allocated to each user with the data rate required by each one of them. Having in account that these peak rates are calculated with standard CP length (7 symbols per sub-carrier), it is possible by combining Table 2.3 and Table 2.4, with Table 2.2, to see that the data rate increases with the bandwidth, the number of RBs, the order of the coding scheme and ratio, and the order of MIMO.

*Table 2.3 - Uplink peak data rate, considering no MIMO (extracted from [Alme13]).*

| | | **UL Peak Data Rates [Mbps]** | | | | | |
|---|---|---|---|---|---|---|---|
| | | **Bandwidth [MHz]** | | | | | |
| **MCS** | **Bits/Symbol** | **1.4** | **3.0** | **5.0** | **10** | **15** | **20** |
| **QPSK** $^{1}/_{2}$ | 1.0 | 1.0 | 2.5 | 4.2 | 8.4 | 12.6 | 16.8 |
| **16QAM** $^{1}/_{2}$ | 2.0 | 2.0 | 5.0 | 8.4 | 16.8 | 25.2 | 33.6 |
| **16QAM** $^{3}/_{4}$ | 3.0 | 3.0 | 7.6 | 12.6 | 25.2 | 37.8 | 50.4 |
| **16QAM 1/1** | 4.0 | 4.0 | 10.1 | 16.8 | 33.6 | 50.4 | 67.2 |
| **64QAM** $^{3}/_{4}$ | 4.5 | 4.5 | 11.3 | 18.9 | 37.8 | 56.7 | 75.6 |
| **64QAM 1/1** | 6.0 | 6.0 | 15.1 | 25.2 | 50.4 | 75.6 | 100.8 |

*Table 2.4 - Downlink peak data rate (extracted from [Alme13]).*

| | | | DL Peak Data Rates [Mbps] | | | | | |
|---|---|---|---|---|---|---|---|---|
| | | | Bandwidth [MHz] | | | | | |
| **MCS** | **Bits/Symbol** | **MIMO usage** | **1.4** | **3.0** | **5.0** | **10** | **15** | **20** |
| **QPSK $^1/_2$** | 1.0 | - | 1.0 | 2.5 | 4.2 | 8.4 | 12.6 | 16.8 |
| **16QAM $^1/_2$** | 2.0 | - | 2.0 | 5.0 | 8.4 | 16.8 | 25.2 | 33.6 |
| **16QAM $^3/_4$** | 3.0 | - | 3.0 | 7.6 | 12.6 | 25.2 | 37.8 | 50.4 |
| **16QAM 1/1** | 4.0 | - | 4.0 | 10.1 | 16.8 | 33.6 | 50.4 | 67.2 |
| **64QAM $^3/_4$** | 4.5 | - | 4.5 | 11.3 | 18.9 | 37.8 | 56.7 | 75.6 |
| **64QAM 1/1** | 6.0 | - | 6.0 | 15.1 | 25.2 | 50.4 | 75.6 | 100.8 |
| **64QAM $^3/_4$** | 9.0 | $2 \times 2$ MIMO | 9.1 | 22.7 | 37.8 | 75.6 | 113.4 | 151.2 |
| **64QAM 1/1** | 12.0 | $2 \times 2$ MIMO | 12.1 | 30.2 | 50.4 | 100.8 | 151.2 | 201.6 |
| **64QAM 1/1** | 24.0 | $4 \times 4$ MIMO | 24.2 | 60.5 | 110.8 | 201.6 | 302.4 | 403.2 |

Interference can lead to severe degradation of SINR and spectrum efficiency. This results in lower overall capacity and, consequently, the expected user's throughput will not be achieved. As shown in Figure 2.3, data rates decrease sharply with the reduction of the SINR value, which leads to the reduction of channel capacity.

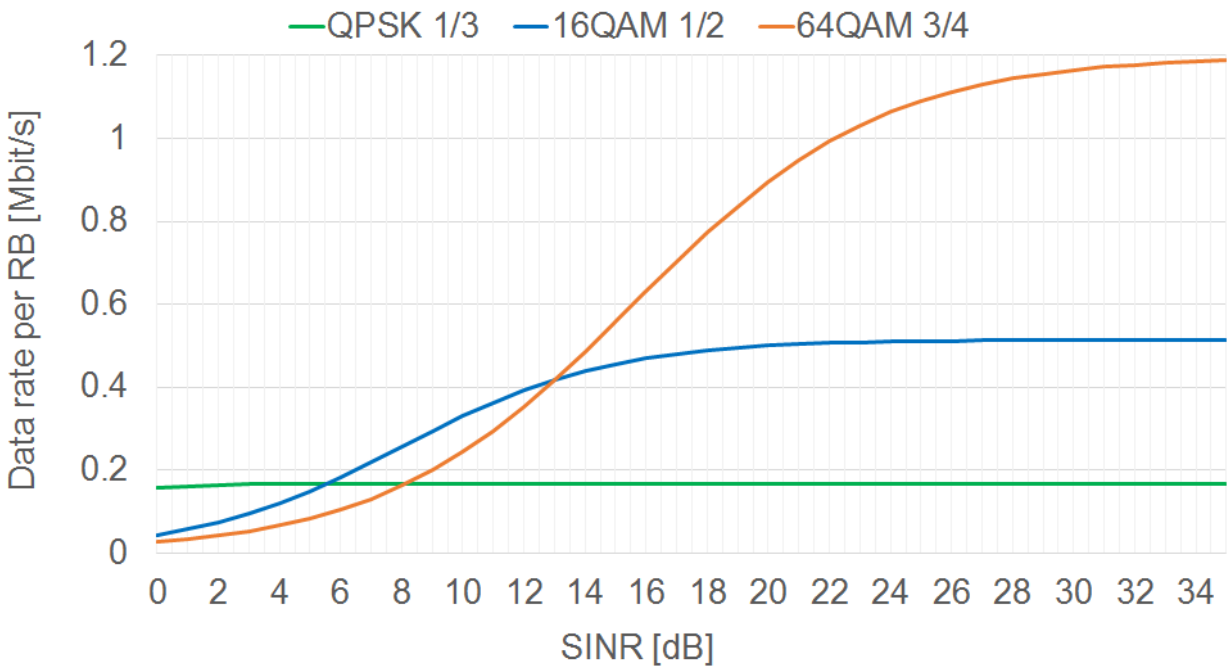


*Figure 2.3 - Throughput per RB in Downlink (DL) vs SINR for different MCS (extracted from [Pire15]).*

According to [NSN13], the mass events capacity depends heavily on the number of cells and network Radio Frequency (RF) planning. In theory, more cells can provide more capacity, but if cell overlapping increases, the additional cells may only increase interference levels. So, to maximize capacity, it is required to minimize, rather than maximize, the coverage footprint of each indoor cell. Therefore, cell dominance areas need to be planned carefully to avoid unnecessary cell overlapping.

With the number of RBs is possible to calculate an estimation of the network capacity, based on (2.5) and (2.7):

$$N_U = \left[\frac{N_{sub-carrier/RB} \cdot N_{RB} \cdot N_{symbols/subframe} \cdot \log_2(M) \cdot N_{streams}}{R_{b/U[Kbps]} \cdot \tau_{TTI[ms]}}\right] \quad (2.6)$$

The physical layer bit rate, $R_{b/U}$, for each user can be calculated as follows:

$$R_{b/U[Kbps]} = \frac{N_{sub-carrier/RB} \cdot N_{RB/U} \cdot N_{symbols/subframe} \cdot \log_2(M) \cdot N_{streams}}{N_U \cdot \tau_{TTI[ms]}} \quad (2.7)$$

And the number of Resource Blocks (RBs) available for each user, as:

$$N_{RB/U} = \left[\frac{N_{RB}}{N_U}\right] \quad (2.8)$$

Where:

- $N_{RB}$ is calculated in (2.5);
- $N_{sub-carrier/RB}$ is the number of sub-carriers per RB (example, 12 for a 15 kHz sub-carrier spacing from Table 2.2;

- $N_{symbols/subframe}$ is the number of OFDM symbols per sub-frame;
- $M$ is the modulation's order;
- $N_{streams}$ is the order of MIMO configuration;
- $\tau_{TTI}$ is the time transmission interval (1ms).

## 2.3 Performance Parameters

### 2.3.1 Services and Applications

The proliferation of network access, in particular on mobile devices, has significantly changed the way users access online services on a day-to-day basis. Along with the increased availability of an always-on Internet, new technologies such as LTE have enabled the use of all types of services, including those that, such as video streaming, come with stringent requirements in terms of network performance and capacity demands. According to [Eric19], mobile video traffic is forecast to grow by around 34 percent annually through 2024 to account for 74 percent of all mobile data traffic. Social networking is also expected to grow – increasing by 22 percent annually over the next six years. According to [EricMT17], the other application categories have annual growth rates ranging from 20 to 32 percent, and so are shrinking as a proportion of overall traffic, because of the stronger growth of video, as shown in Figure 2.4. Consequently, the issue of adequately supporting all those users and all those services is a nontrivial one for network operators, as users expect certain levels of quality to be upheld.

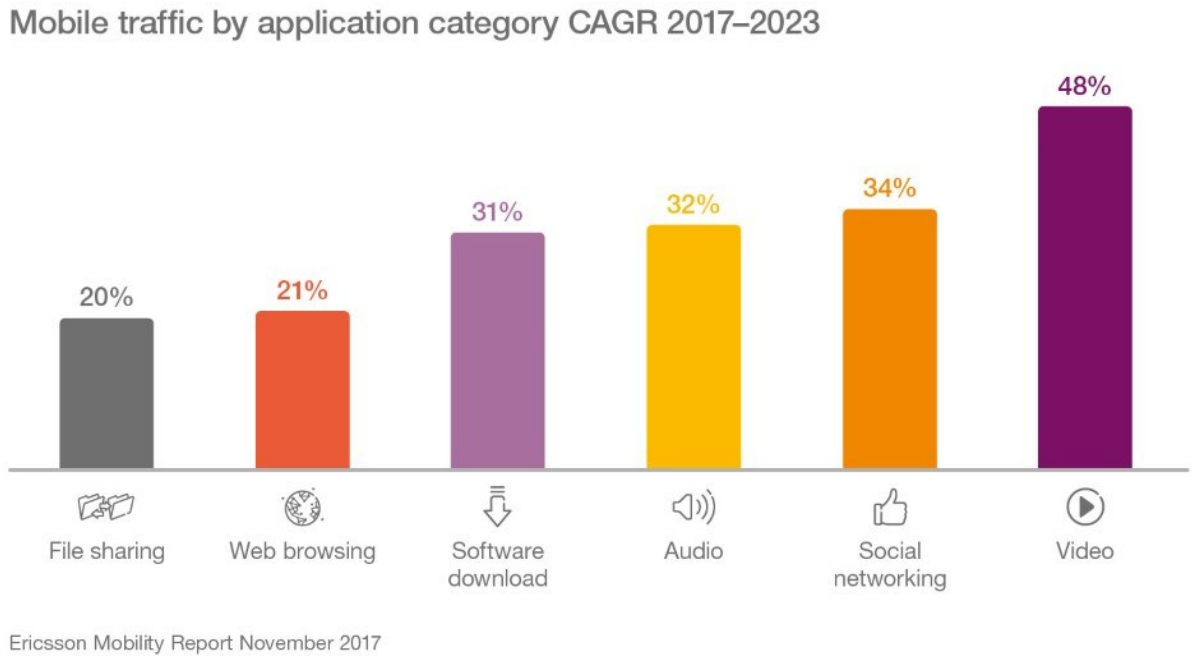


*Figure 2.4 - Mobile Traffic by Application category (extracted from [EricMT17]).*

From a business point of view, network performance, and service quality seen by users is a crucial

differentiation. A good level of perceived quality will help retain users, whereas poor service will lead to high levels of churn for the mobile network operator.

According to [Acce18], to have control over both network performance and user experience, service providers must use instrumentation that combines two types of monitoring: active monitoring that performs end-to-end monitoring between nodes. It relies on probes injected into the network, to calculate Key Performance Indicators (KPIs) and, passive monitoring that analyses every packet through a measurement node (for example, a switch or router), helps providers understand traffic characteristics, and enhances forensics and troubleshooting. Key Quality Indicator (KQI) may be mapped to various Quality of Service (QoS) categories, which gives the degree of QoE.

In order to face these challenges of the different types of applications, and primarily to provide QoS guarantees, 3GPP proposed four different QoS classes related to the desired type of service and quality:

1. Conversational Services: comprises voice and real-time multimedia messaging, in real-time conversations, it is fundamental to preserve time relation (variation) between information entities in the stream and to guarantee low transfer delays. Voice over Internet Protocol (VoIP) and Video Conferencing are examples of this class;
2. Streaming Services: are still dependent on the time relation between both ends of the stream. However, because these services have unidirectional data flows, the delay requirements are not as strict as in Conversational. Video-on-demand is an example of this class;
3. Interactive Services: include web browsing, automatic data base inquiries and server access. This class is applied when one end-user requests data from remote equipment;
4. Background Services: are less delivery-time sensitive by the fact that the destination is not expecting the data within a certain time frame and it can be stored to be read later, e.g. e-mail, SMS, and others.

Although these services and classes were not done explicitly for LTE, they provide some insights into the different natures of traffic. Concerning these QoS classes, different services can be considered: file sharing, web browsing, audio, social networking, voice, music, email, video calling, video streaming and Machine-to-Machine (M2M) applications like smart meters, e-Health, Intelligent Transportation Systems (ITS) and surveillance.

QoS is the ability of the network to provide a service at a guaranteed service level. It includes all functions, mechanisms, and procedures in the wireless networks and terminals that ensure the provision of the negotiated service quality between the Mobile Terminal (MT) and the network. When the network cannot provide the resources that users need, the service configurator will select what kind of treatment the corresponding traffic will experience. According to [SeTB11], those bearers can be classified in Minimum Guaranteed Bit Rate (GBR) bearers, which can be used for applications as VoIP. Also, Non-GBR bearers, which can be used for applications such as web browsing or File Transfer Protocol (FTP) since they do not guarantee any specific data rate. One way of prioritizing is through the QoS Class Identifier (QCI), which is characterized by priority, delay budget, and acceptable packet loss. The QCI label for a bearer determines the way it is handled in the eNodeB, e.g., determines the first service to suffer a reduction in data rates. It is important to mention that in events situations operators always

prioritize voice over data. The standardized QCIs and their characteristics are detailed in Table 2.5.

*Table 2.5 - Standardised QoS Class Identifiers for LTE (extracted from [SeTB11]).*

| QCI | Resource Type | Priority | Packet Delay Budget [ms] | Packet Error Loss Rate | Example Services |
|---|---|---|---|---|---|
| **1** | GBR | 2 | 100 | $10^{-2}$ | Conversional voice |
| **2** | GBR | 4 | 150 | $10^{-3}$ | Conversional video (live streaming) |
| **3** | GBR | 5 | 300 | $10^{-6}$ | Non-conversional video (buffered streaming) |
| **4** | GBR | 3 | 50 | $10^{-3}$ | Real-time gaming |
| **5** | Non-GBR | 1 | 100 | $10^{-6}$ | IMS signaling |
| **6** | Non-GBR | 7 | 100 | $10^{-3}$ | Voice, video, (live streaming), interactive gaming |
| **7** | Non-GBR | 6 | 300 | $10^{-6}$ | Video (buffered streaming) |
| **8** | Non-GBR | 8 | 300 | $10^{-6}$ | TCP-based (e.g. e-mail), chat, FTP, Peer-to-Peer (P2P), file sharing, progressive video, etc. |
| **9** | Non-GBR | 9 | 500 | $10^{-6}$ | — |

### 2.3.2 Quality of Experience

The relation between the Quality of Service (QoS), that operators monitor and manage, and the Quality of Experience (QoE) that the users get is critical for network and service providers. To guarantee that end users receive the quality levels that satisfy them and, at the same time, enabling the efficient use of network resources. Service providers, for instance, can measure the satisfaction in terms of usability, accessibility, retainability, and integrity of the service [SoLC06].

According to [SoLC06], there are two practical approaches to measure QoE in mobile networks: a service level approach using statistical samples and a network management system approach using QoS parameters. Although the measurements rely on statistical samples if the number of observations is correctly selected, the results will get close to achieving a 100% precision. The second method is based on a network management system, which collects KPIs from network elements and compares them with the reference levels. They are better used together.

In respect to QoE metrics, it is crucial to understand the expectations of the end user. As mentioned

before in mass events situations, the expectations are lower because subscribers (users) are more forgiving in those situations, but they have limits too. There will be as many different expectations as there are users, but most of these expectations can be grouped into two main categories: reliability and quality. Reliability is the availability, accessibility, and maintainability of the content, the service network, and the end-user device and application software. Some KPIs related to the reliability are presented in Table 2.6.

*Table 2.6 - QoE KPI according to reliability expectations (extracted from [Pire15]).*

| QoE KPI | Most important measures |
|---|---|
| Service availability (anywhere) [%] | Ratio of territory coverage |
| Service accessibility (anywhere) [%] | Ratio of refused connections |
| Service access time (service setup time) [$s$] | Average call or session setup time |
| Continuity of service connection (service retainability) [%] | Service interruption ratio |

On the other hand, quality refers to the bearer service, the quality of the content, the user device and application software features. Some KPIs related to quality expectations are presented in Table 2.7.

*Table 2.7 - QoE KPI according to quality expectations (extracted from [Pire15]).*

| QoE KPI | Most important measures |
|---|---|
| Quality of session [%] | Service application layer packet loss ratio |
| Data rate [%] | Average bearer data rate achieved as ratio of data rate demanded by application |
| Data rate variation [%] | Bearer stability: data rate variation around negotiated data rate |
| Active session throughput [kbit/s] | Average throughput towards mobile |
| System responsiveness [s] | Average responsive time |
| End-to-end delay [ms] | Average end-to-end delay |
| Delay variation [%] | Jitter |

An important service type at sports event situations is video streaming, it can be either of the person-to-person type, sharing video in real-time, or of the content-to-person type, watching a video from a

website. Mean Opinion Scores (MOS), is a relative scale from 1 to 5 that reflects how a user qualifies the video quality.

Since the human tendency is to avoid perfect ratings, somewhere around 4.3 - 4.5 is considered an excellent quality target. On the low end, video quality becomes unacceptable below an MOS of roughly 3.5 [Twilio19]. Users are more sensitive to variations on the quality of the video than with bad quality all the time.

## 2.4 State of the Art

This section presents previous work developed on 4G solutions for stadium environments, its associated deployment, as well as choices made on capacity, coverage and interference management, showcasing their main conclusions and results obtained through simulations and algorithm analysis. Since each case has a different and unique solution, I will only present one solution with Distributed Antennas System (DAS) and one of four possible solutions with femtocells. The other solutions using femtocells are not exposed in this work since the DAS was the system chosen to deploy.

For the Wembley Stadium Solution [Cham15], an older 2G/3G DAS system was replaced in February 2014 with an active DAS. This takes in raw RF from Radio Frequency Units (RFUs) of macrocell base stations which it converts and combines onto optical fibre cables piped around the stadium. Radio Remote Units (RRUs) close to the antennas re-convert the signal back into RF form.

Two different fixed operators supply backhaul, each providing 2 x 1 Gbps Carrier Ethernet service. A third backhaul supplier was connected to expand the 4 Gbps significantly and adding a further layer of diversity/redundancy with 10 Gbps capacity in the future plan.

A huge frequency spectrum assets are available at 800 MHz, 1800 MHz, 2100 MHz and 2600 MHz. The 800MHz band is not used at Wembley and probably never will be because it is more suitable for broader area/longer range than high capacity. Currently active for LTE are 20 MHz LTE FDD at 1800 MHz, 20 MHz LTE FDD at 2600 MHz and 1 x 15 MHz LTE FDD at 2600 MHz. LTE MIMO is already installed in the main bowl and using Carrier Aggregation can achieve peak speeds of 300 Mbps. The additional 15 MHz band will increase that to around 410 Mbps. These headline rates are theoretical maximums but can deliver as much as 150 Mbps with a Cat 6 device. In a packed stadium, no user is ever going to get that kind of throughput, but there is up to 300Mbps to go around, so this is more about capacity. In an empty, a quick speed-test on a Cat 4 device achieved 83 Mbps down and 47 Mbps up.

Antennas around the stadium are grouped into 24 active sectors. The stadium is segmented vertically, with each sector covering both a segment of the main bowl and the indoor area behind and underneath. The radio planning and the same sectorization is shared with all operators.

Twenty-eight antennas are installed because it is difficult to isolate the end areas that have no roof, with four sectors having a duplicate antenna. To specify the seat, they were centralised on a laser sight attached during the commissioning. Some measurements and calculations were made, then the alignment adjusted by moving the focus to the relevant nearby seat. This made the setup much faster

than the trial and error method sometimes used elsewhere. Is important to refer that once installed, it is difficult and impractical to access the antennas outside pre-scheduled maintenance windows months ahead. In order to reduce inter-sector interference, the roll-off (RF radiation pattern at the edge of coverage) is very tight, only 2-3 degrees.

Using multimode femtocells 4G plus Wi-Fi is a viable solution, but this effectively forms a multilayer Heterogeneous Network (HetNet), which presents challenging inter-layer interference problems between the outdoor-cell layer and indoor-cell layer. In [Fuji13] presents a description of how a stadium environment should be addressed and four solutions are proposed.

The first near-term solution can be immediately implemented, to deploy a HetNet without causing significant inter-layer interference is using different carrier frequencies for the outdoor layer and indoor layer. Assuming the LTE network normally uses 10 MHz channel bandwidth. The microcells located near the stadium (covering the roads and parking lots near the stadium) will use one 5 MHz channel and the femtocells in the stadium use a different 5 MHz channel, with this there will be no interference, but the femtocell capacity will be half.

Using non-overlapping carriers eliminates co-channel interference between the indoor-cell and outdoor-cell layers. The overall capacity can be higher if femtocells use the full bandwidth of 10 MHz and only microcells located near the stadium reduces bandwidth to 5 MHz. Since the major interference is from outdoor-cell-layer to femtocell-layer, so the outdoor-cell layer must reduce its bandwidth, so interference only happens on half of the femtocell carrier.

Femtocell users located near the cell-center can use the full 10 MHz of channel bandwidth. The choice of bandwidth to use for femtocell users, located near the cell edge, depends on the current interference level measured from the outdoor-cell layer. If the interference is not too strong, users can use the full 10 MHz bandwidth. Otherwise, users can allocate RB frequencies to the 5 MHz (Inter-cell Interference Coordination (ICIC) algorithm, which can perform this task).

Knowing only half the femtocell PDCCH will be impacted by the outdoor-cell-layer. DL control information can still be delivered from un-impacted part of control-channel-elements (CCEs) due to the CCE scrambling.

The traffic load in the stadium and the surrounding areas can be dynamic. For example, before the game, most people are driving to the stadium; after the game, most people are leaving the stadium. During these periods, the roads near the stadium and parking lots near the stadium are hectic, so the microcells surrounding the stadium need more capacity, but the indoor femtocells do not need very high capacity. When all users are inside the stadium, the indoor femtocells need high capacity, but the outdoor microcells no longer need high capacity but because people driving are less likely to make video calls or other typical event activity this option only make sense if studies show so.

# Chapter 3

# Radio Planning

This chapter introduces how critical is the selection and mounting of the antennas to ensure proper signal coverage, reduce interference between sectors, obtain high values of SINR and hence higher throughput. The created infrastructure used to support the equipment installation and all the elements responsible for its operation are presented. Such as an explanation of how this solution is multi-operator ready and a brief explanation about the power supplying system.

## 3.1 Site Survey

The site survey is the first action to take when designing a wireless network for a stadium. In the study case stadium, the site survey was done on the 23rd of March 2019. The primarily intuitive engineer step is to use the equipment already deployed modifying the power, the antenna height, the azimuth and the tilt. However, it is not necessary to take a particular test to see that the actual antenna system is not enough for reaching data traffic demands. Figure 1.4 shows that. For this solution, the antenna type properties are fundamental. It is necessary to have more or less the same vertical and horizontal beamwidth so the antenna must be of the panel type, producing an almost square beam pattern. Figure 3.1 shows that the existing antennas have a rectangular shape. Hence, for stadium *José Alvalade*, a new solution for 4G technology will be deployed.

*Figure 3.1 - Photography taken during the site survey showing an antenna of the current solution..*

In the survey, it was evaluated the physical structure, architecture and different morphology. Potential locations to mount the new antennas, run cables and install equipment were identified. Several locations at which to mount the antenna were taken into account and were presented in Annex B2 Figures. The ones that correspond to the final solution antenna positions are presented later in this chapter.

## 3.2 3D Modelling

A proper modelling of the venue is important not only for propagation analysis but to minimize the total costs, e.g. knowing the exact needed distance for materials like coaxial cables or fibre. After importing the CAD files to the iBwave Software, characteristics of the materials that constitute the venue were introduced in the tool, and inclined surfaces were identified. Through the advanced 3D iBwave modelling, a 3D model was generated.

Figure *3.2* corresponds to the extracted 3D stadium model.

Stadiums are multilevel structures that contain different RF propagation environments. In this dissertation, only the seating bowl, i.e. the bleacher is studied. The bleacher is an inclined surface, so it needs to be modelled taking into account the different elevation between rows of seats. Since the only possible location to mount the antennas is the interior part of the rooftop, above the seats, UE will always have a clear Line of Sight (LOS) with the serving antennas.

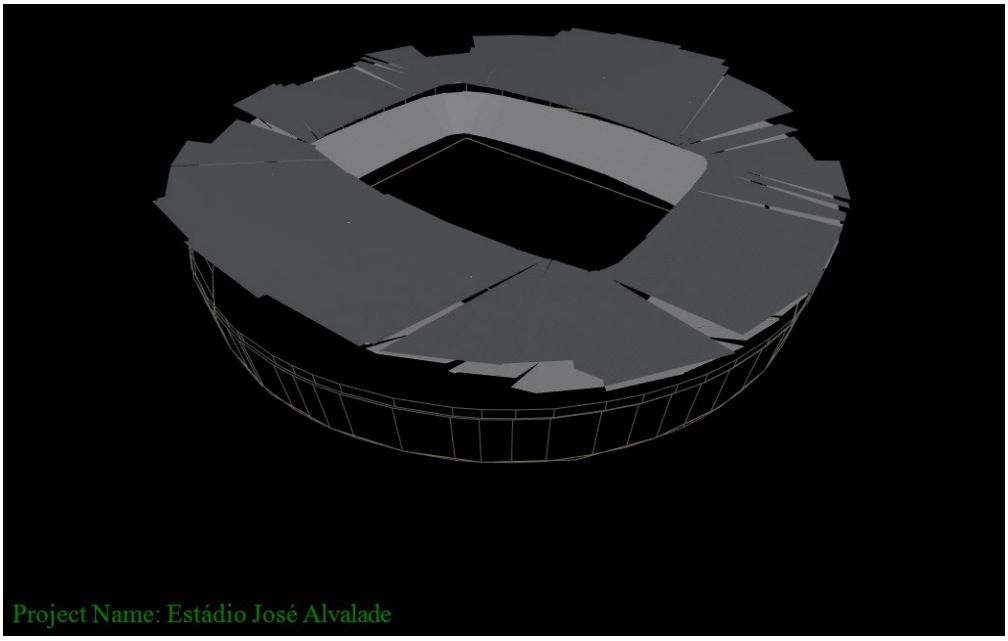


*Figure 3.2 - Stadium 3D model extracted from the iBwave Design Software.*

Underneath the bowl, in the retail area and the VIP area behind the private boxes, the signal is strong because of the proximity of the antennas to the seats however there will be numerous reflected signals due to the concrete walls of the bowl. If the areas isolated from the seating bowls, like team locker rooms, parking zone, shopping area – Alvalaxia, were considered, they would need to have their own antennas for coverage. Since they are not in LoS, and the wall density is much higher than underneath the bowl.

## 3.3 Antennas

Antennas are the essential component of the LTE air interface. When talking about the directivity of an

antenna is possible to define two antenna types, a directional antenna and an omnidirectional one.

Knowing that for this type of high capacity locations, one of the biggest challenges is providing tightly gathered antennas with sufficient capacity and scope without causing interference, in this section, all the antennas mentioned are directional. This type of antenna radiates greater power in one direction so the antenna beam can be focused hence limiting the covered area in the size of a sector. These antenna type beam pattern suggest that the side lobes are very weak, causing little interference to the neighbouring sectors. The antenna placement and selection are explained and reasoned here with the results of the simulations presented in Chapter 5.

### 3.3.1 Antennas Placement

After visiting the stadium, it was concluded that in terms of access for future maintenance and radio efficiency, the best location for mounting the antennas was on the existing rooftop footbridges. Figure 3.3 shows both footbridges.


*Figure 3.3 - Photography taken during the site survey, showing both footbridges.*

Each footbridge is above the beginning of the respective stadium tiers, as shown in Figure 3.5 and Figure 3.6. This position helps separate the area of action in two tiers/rings, the antennas that are placed at the green footbridge will cover the lower tier and the others, placed at the yellow footbridge, will cover

the upper tier, Figure 3.4.


*Figure 3.4 - Original image extracted from [Foot15].*

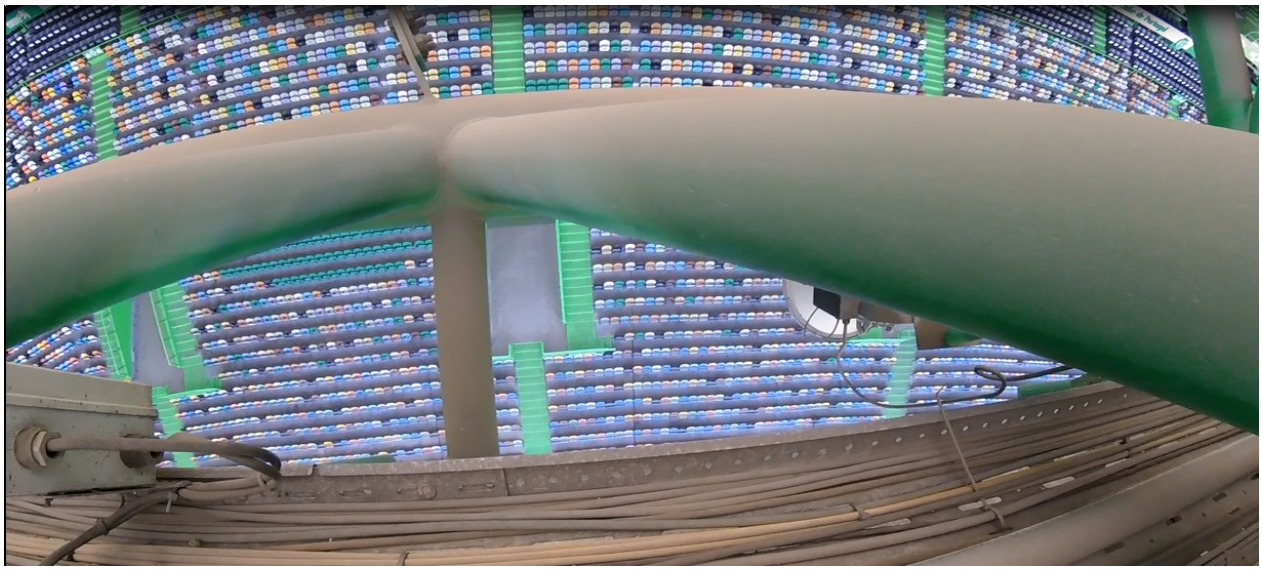

*Figure 3.5 - Photography taken from the green footbridge where is possible to visualize the beginning of the first ring.*

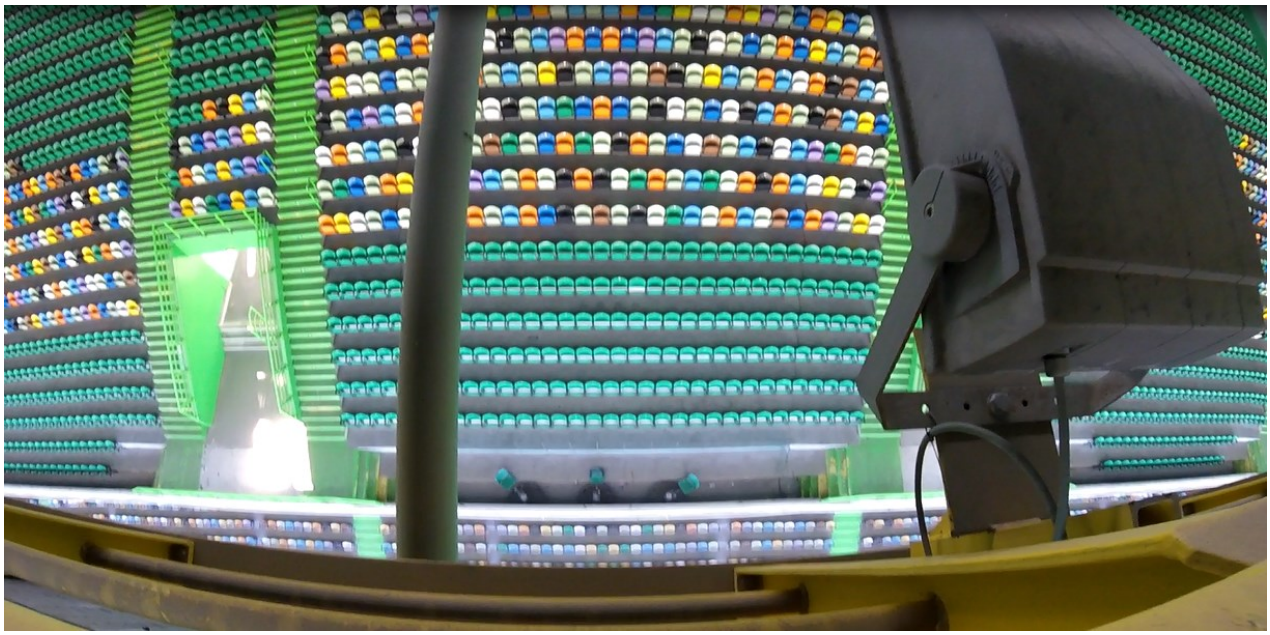

*Figure 3.6 - Photography taken from the yellow footbridge where is possible to visualize the beginning of the second ring.*

The azimuth is the side to side direction that the antenna is pointed, refers to the rotation of the whole antenna around a vertical axis. By definition North is 0º, East is 90º, South is 180º and West is 270º, the reference of this work was the centre of the field and the middle of the goal.

The real north is in the direction of the bleacher named “Bancada Norte” in Figure 3.7. However, the blueprint of the stadium is geo-located only locally, so in order to facilitate the placement of the antennas the azimuth considered is based on the two reference points ignoring the fact that the magnetic compass will not give 0º in the considered direction.

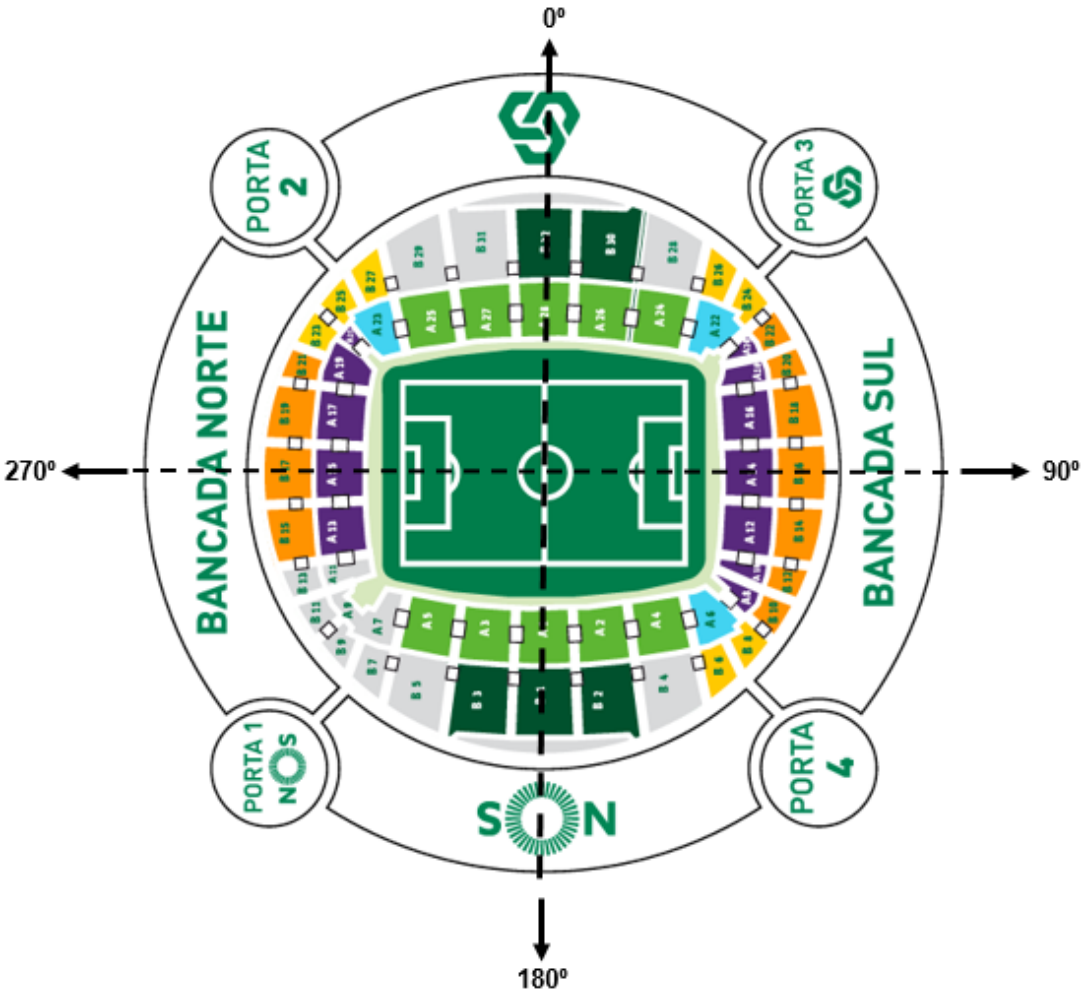


*Figure 3.7 - Original image of the stadium stands layout extracted from [Sport19] with the azimuth overlapped - all the following images present this stadium configuration.*

The first thing to do is to define the position of the antennas that are placed in the middle. So, the location of these will be pointing to the azimuth corresponding to that side of the stadium. Having the middle ones positioned, the others will have those as reference, for example, when looking to Figure 3.8 the antenna A13 with an azimuth of 60 degrees, needs to be mounted 44 meters left of the antenna A11 placed in the middle.

Table 3.1 shows the azimuth and tilt defined for each antenna. The chosen tilt results from the simulations presented in Chapter 5.

It is necessary to take special attention with the position of the antennas that cover the corners so that they are the best servers in the area chosen for that purpose. In that part of the bleacher, the seatings are closer to the rooftop than in the other parts of the stadium, so the yellow footbridge starts after the seating area finish. For this reason, choosing to mount the antenna in that footbridge forces the rotation of the antenna to point to the lawn in order to cover the seating area. The problem is that in this situation the signal would reach the other side of the stadium (diagonal) overlapping signals, so mounting the antenna in the green footbridge was the only option to solve the problem.

*Table 3.1 - Configuration considered for the final solution antennas, shows the azimuth, the tilt defined for each antenna and the input value of the signal source power.*

| Antenna | Sector | Antenna Model | Azimuth (degree) | Tilt (degree) | Signal Source Power (dBm) |
|---|---|---|---|---|---|
| A1 | 1 | CNPLX3055F | 180 | 60 | 49 |
| B2 | 2 | CNPLX3055F | 180 | 20 | 49 |
| A3 | 3 | CNPLX3055F | 185 | 60 | 49 |
| B4 | 4 | CNPLX3055F | 230 | 10 | 49 |
| A5 | 5 | CNPLX3055F | 240 | 40 | 49 |
| A6 | 6 | CNPLX3055F | 270 | 60 | 49 |
| B7 | 7 | CMAX-3030S-D-V53 | 270 | 20 | 49 |
| A8 | 8 | CNPLX3055F | 310 | 45 | 49 |
| A9 | 9 | CNPLX3055F | 355 | 65 | 49 |
| B10 | 10 | CNPLX3055F | 310 | 10 | 49 |
| A11 | 11 | CNPLX3055F | 0 | 65 | 49 |
| B12 | 12 | CNPLX3055F | 0 | 25 | 49 |
| A13 | 13 | CNPLX3055F | 60 | 5 | 49 |
| B14 | 14 | CNPLX3055F | 55 | 10 | 49 |
| A15 | 15 | CNPLX3055F | 65 | 35 | 49 |
| A16 | 16 | CNPLX3055F | 90 | 60 | 49 |
| B17 | 17 | CMAX-3030S-D-V53 | 90 | 20 | 49 |
| A18 | 18 | CNPLX3055F | 120 | 45 | 49 |
| A19 | 19 | CNPLX3055F | 175 | 60 | 49 |
| B20 | 20 | CNPLX3055F | 130 | 10 | 49 |

### 3.3.2 Antenna Selection

In order to choose the most suitable antennas for the solution, first, it is important to understand the distance between the footbridges and the bleacher. Having the 3D modelling of the stadium is possible to simulate in the iBwave software, different positions and models for the antennas, as presented in chapter 5.

Based on the stadium morphology, the number of sectors calculated in subchapter 4.2 and all the simulations done and presented at chapter 5, the ideal position to mount the chosen antennas was the one represented in Figure 3.8.

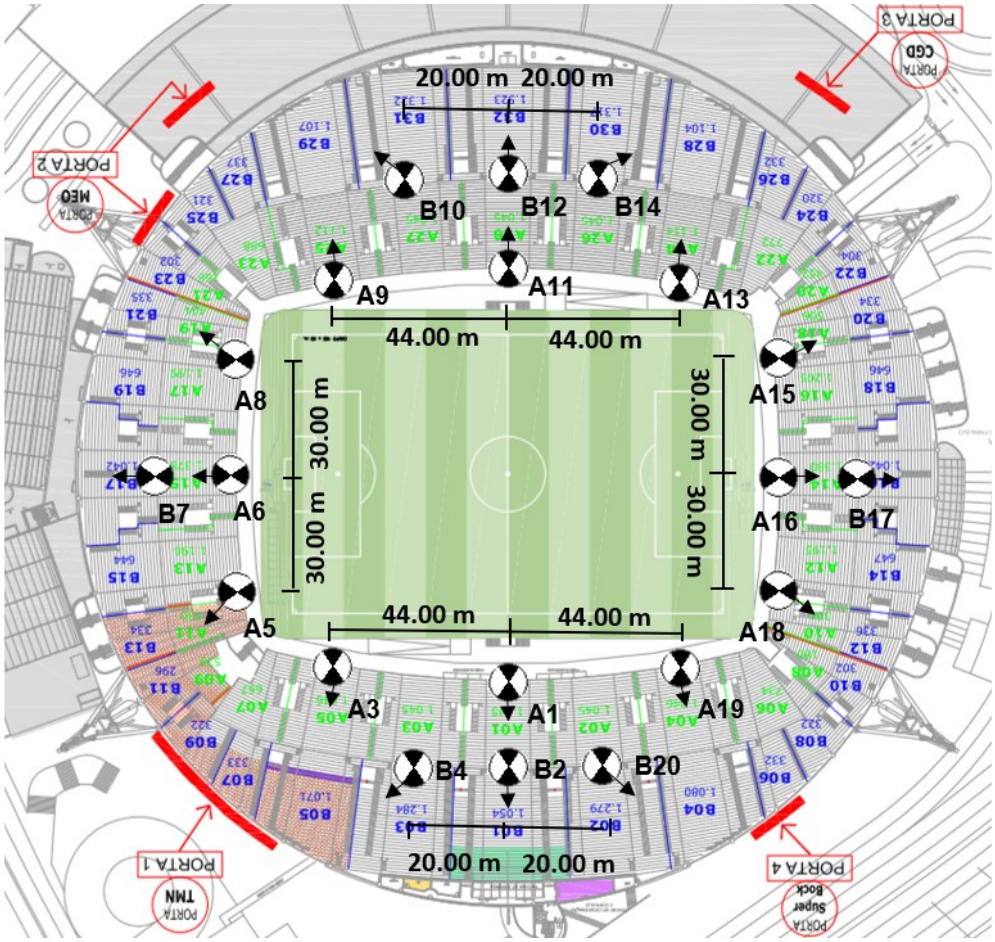


*Figure 3.8 - Antenna final position scheme (created above the plant of the stadium obtained in AutoCAD and based on the iBwave Design Software scheme).*

The antennas responsible for cover the lower tier/ level A were named An and the ones responsible for cover the upper tier/ level B were named Bn. The letter n in the respective nomenclature corresponds to the number of the sector, for example, antenna A1 coverage sector is sector 1.

Figure 3.9 and Figure 3.10 were taken from the blueprint of the stadium so is scaled and shows the position of the antennas that cover the level B (yellow footbridge, yellow antenna) and the ones that cover the first level A (green footbridge, green antenna) comparing to the seatings.

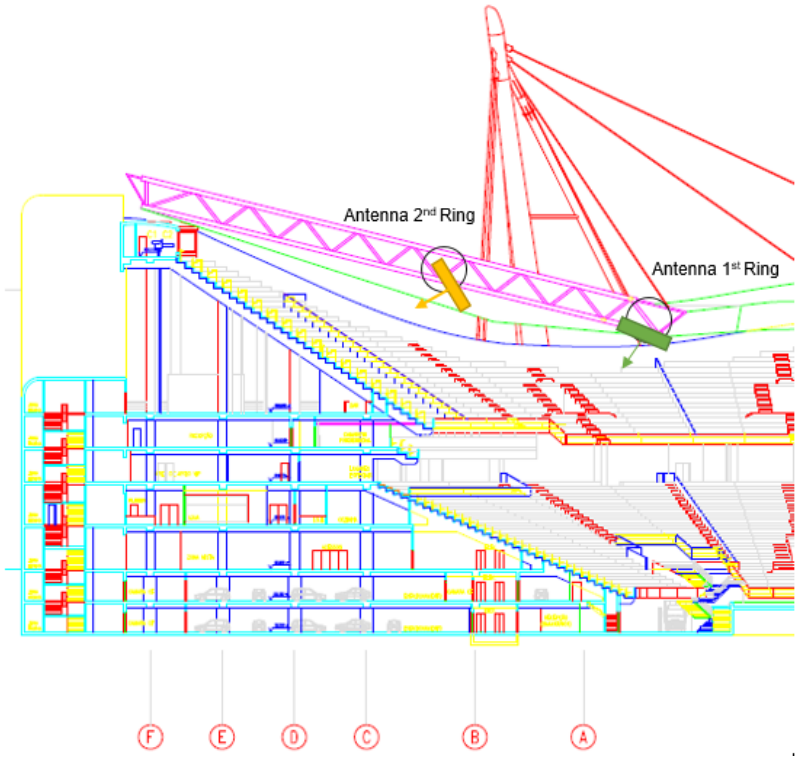


*Figure 3.9 - Antenna fixing scheme representing the antennas A1 and B2 (based on the cut East to West done with AutoCAD).*

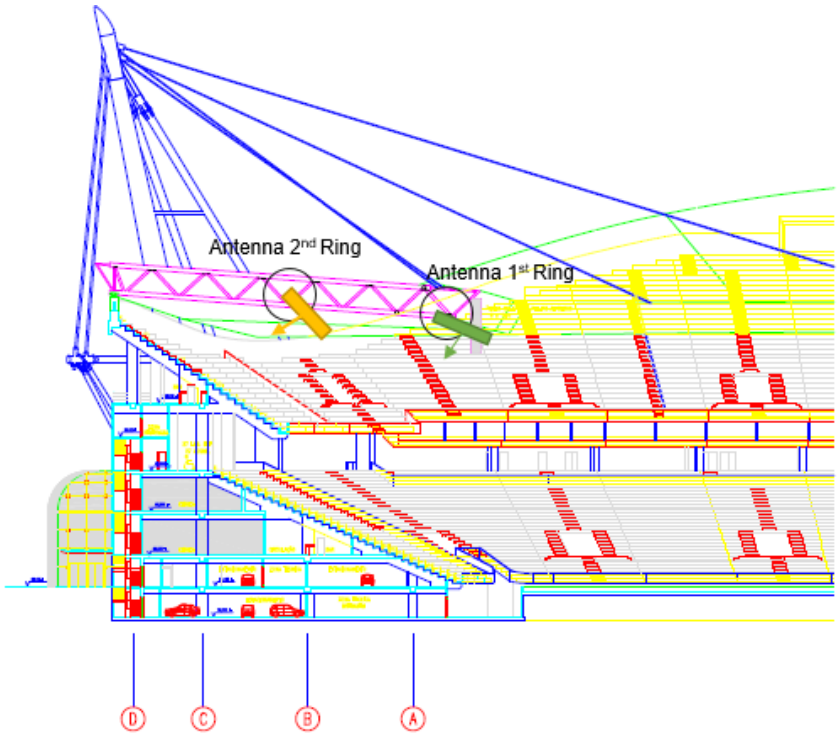


*Figure 3.10 - Antenna fixing scheme representing the antennas A6 and B7 (based on the cut North to South done with AutoCAD).*

The yellow footbridge antennas are especially close to the stadium stand. For this reason, the antennas radiation pattern is very confined in comparison to the ones positioned in the green footbridge. Therefore, a mixed choice of antennas is ideal, i.e., for each position, different characteristics are required so two different types of antennas will be used.

The first thing that is essential to have into account when choosing the antennas is the operating range of frequency bands. In order to increase the capacity, the antennas for this solution work at the 1800 and the 2600 MHz. The dual-band concept means that the antennas operate in two separate bands and so the tri-band in three separate bands. For supporting MIMO 2x2, the antenna needs to have two ports for transmission (Tx) and two ports for receiving (Rx) for each band, if only has two ports the signals need to be combined before using directional couplers.

As shown before in Figure 3.9 and Figure 3.10 antennas that will cover the first ring/ upper tier are farther away from the seats than the others, so is possible to take advantage of the fact that the radiation pattern is not so confined. Owing to the higher number of users and the ring shape the most suitable antenna will have ideally the same degree values for the vertical and horizontal beamwidth. The CommScope CNLPX3055F presents this almost squared radiation pattern. The overlap between cells causes interference, so the area covered by the antenna beams side lobes should be minimized. This antenna was specially designed for stadium environments offering narrow beamwidths that can be reliably shaped into sectors supporting all users without signal overlaps. The antenna includes an internal triplexer for a set of ±45° RF input ports for 2x2 MIMO capabilities and presents an ultra-wideband range of 698–2700 MHz [Annex A - datasheet]. After doing the simulations, this antenna model was chosen for all the positions except two. For the position of the antennas B7 and B17, better results were obtained with another antenna model from CommScope.

The first simulation (simulation 1) was made, using in all positions the CommScope antenna model, specially designed for stadiums. However, as it is possible to observe in Figure 3.11, the relation between signal and noise-interference was not the desired one in the upper tier/level B of the bowl. Consequently, the higher throughput values were achievable in a smaller part of the stand, when comparing to the lower tier/level A. These results are reflected in the legend of percentages presented in Figure 3.12. In level A 71.1% of the bleacher achieves the higher data rate values against the 48.4% achievable in level B.

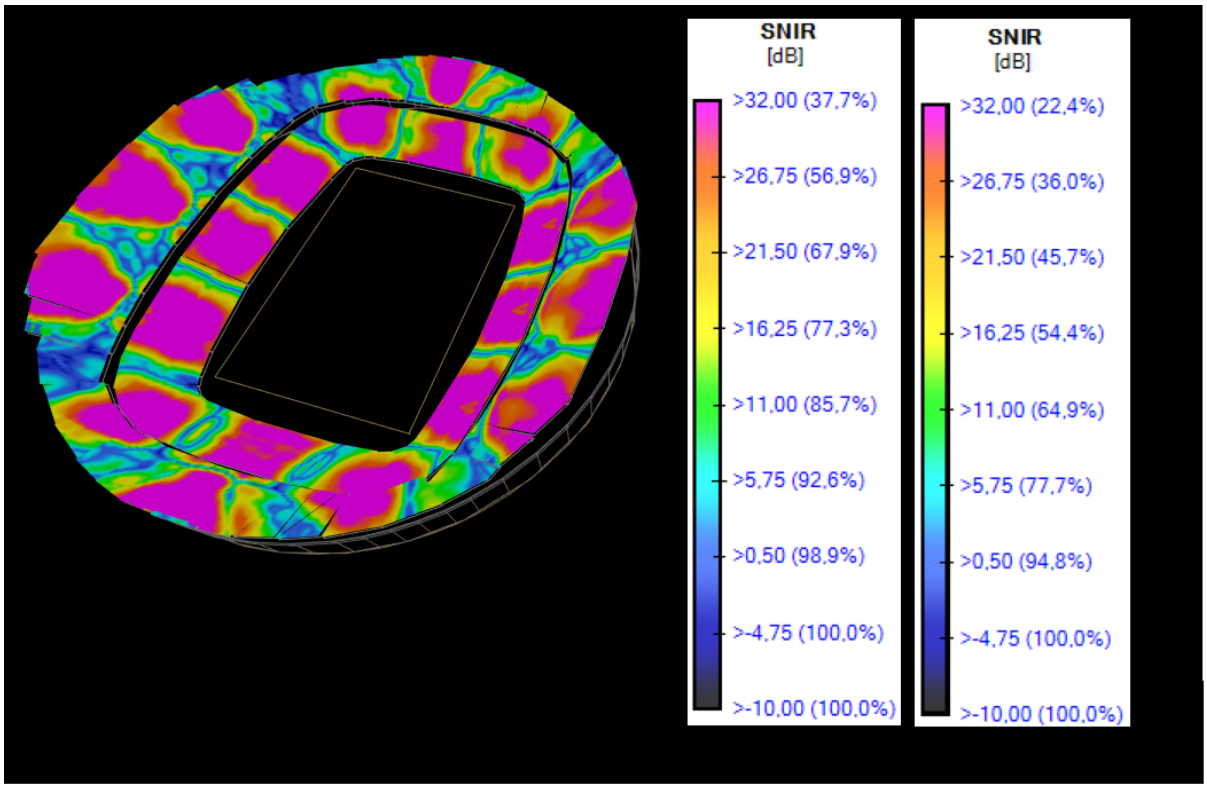


*Figure 3.11 - iBwave SINR output map using only the antenna CNLPX3055F considering the 1800 MHz band (simulation 1).*

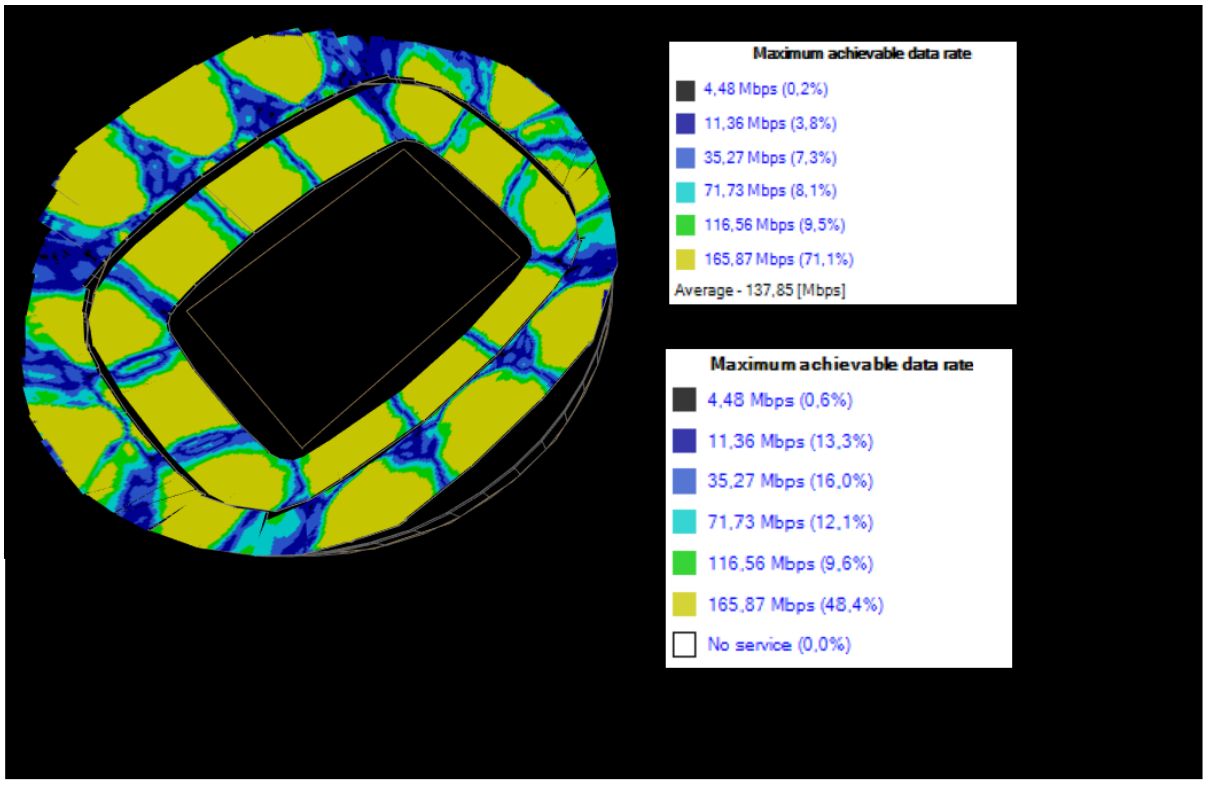


*Figure 3.12 - iBwave MADR output map using only the antenna CNLPX3055F considering the 1800 MHz band (simulation 1).*

By analysing the output maps above, changes need to be done at the level B. For the middle antennas

that will cover the upper tier on the NOS and *Caixa Geral de Depósitos* bleacher. The CommScope model was the best option again. In that part of the stadium, the grandstand is taller being constituted by more seats, so more users. Using an antenna with a larger horizontal beamwidth than the CommScope one, the resulting sector would be responsible for covering a large number of users comparing to the other sectors, in logical terms that is not desirable.

Having in mind that the number of users covered should be identical for every sector, that the interfering zones must be minimized and that the stadium design antenna presented great characteristics, simulations started to be done changing only the antennas position and the respective azimuth. However observing the changes that occurred in the output maps when changing only the position and the azimuth of the CNLPX3055F antenna, it was concluded that the antennas behind the beacons, antennas B7 and B17, should have a narrower beamwidth in order for the signal to not overlap the one emitted by the corner antennas. That is when the antenna CMAX-3030S-D-V53 (datasheet 6 – Annex A) was tested and chosen for the best results and the balance presented between the output maps from both levels/tiers. Figure 3.13 such as Figure 4.5, are just two examples of the excellent results obtained in the final solution simulations.

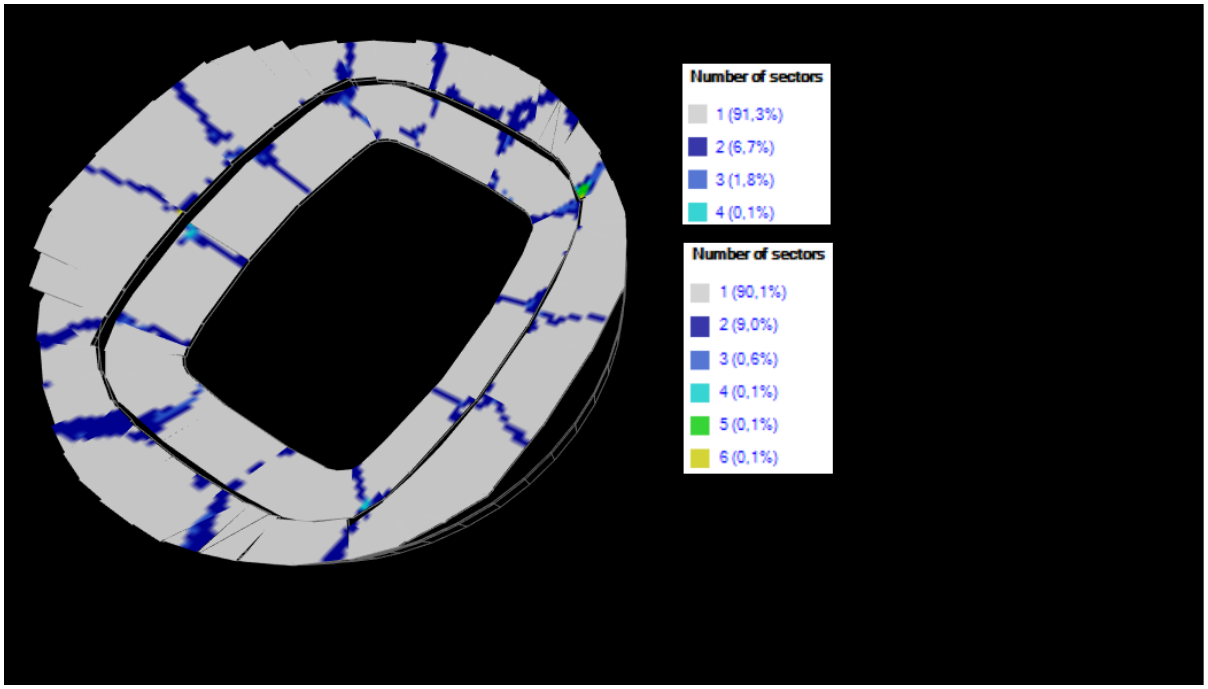


*Figure 3.13 - Final solution iBwave Overlapping Zones output map considering the 1800 MHz band.*

## 3.4 Radio Installation Points

The creation of basic infrastructure to the installation of equipment, as well as, all the elements that support its operation must be taken into account. For this reason, there will be 12 radio installation points (RIs) that need to guarantee energy, transmission and RF. Each RI will be composed by remote radio units (RRU's), coaxial cables, optical fiber, power points (PPs), rectifiers and optical distribution frames (ODF´s) per operator. If in this work, the three operators were taken into account, two 4:4 multi-operator

combiners per antenna should be considered as shown in Figure 3.15, it would be another component at the radio installation points.

### 3.4.1 RRUs and BBUs

High capacity locations users set high “stress” on the Base Transceiver Stations (BTSs) that serve them. Adding more base stations increases cost and can lead to signal interference if the eNodeBs at the base stations are not carefully coordinated.

The BTSs are divided into two parts: the Baseband Unit (BBU) and the Remote Radio Unit (RRU), which allows network operators to maintain or increase the number of network access points while centralizing the baseband processing functions into a “master base station” outside the stadium. [Artiza19].

The RRU acts like a transceiver transmitting and receiving user signals to the base station and vice-versa. This hardware equipment can include a cyclic prefix (CP) module with a CP adder for downlink channel processing, and a CP remover for uplink channel processing, usually known as the RF processing unit. Other tasks are process data, amplify the power and detect standing waves.

Baseband refers to the original frequency range of a transmission signal before it is modulated. The BBU has a Digital Signal Processor (DSP) responsible for the conversion between analog and digital signals. It is also responsible for communication through the physical interface.

Considering all the three operators for the LTE solution, there will be 6 RRU’s per antenna, 2 per operator if each band uses a different radio (separated hardware). In the case of the radio model support, both B3 and B7 band (same hardware), there will be 3 RRU’s per antenna, 1 per operator. Each RRU communicate to the BBU through an optical fiber, per one RRU-BBU connection are required two optical fibers, so per antenna 12 pars of optical fiber are necessary in the first case and a half in the second case. The connection between the two equipment is made via optical fiber because they are placed several meters apart if this connection was made with RF coax cables, the losses would be very critical. RRUs are installed near the antennas in the stadium footbridges at the grandstand roof and the BBUs are installed in the technical room at level -2 of the stadium. Coaxial cables always make the connection between the radio equipment (RRU) and the antennas for that reason the 6 RRU’s per antenna are placed a meter apart from the antenna so that the losses are negligible. Figure 3.16 tries to exemplify that each RI serves the respective antennas described in the name, for example, RI12 serves the antennas A1 and B2, most of them serves two antennas the one placed in the green footbridge and the other placed in the yellow footbridge.

The Optical Distribution Frame (ODF) is a frame used to provide cable interconnections between communication facilities. Can integrate fiber splicing, fiber termination, fiber optic adapters and connectors and cable connections together in a single unit. It can also work as a protective device to safeguard fiber optic connections from damage. Considering the three operators, since the BBU is separated from the RRU several meters apart (vendor recommendation is a maximum of 12 kilometres) and the fiber connection is different for each operator, the use of an ODF is essential first to gather and then to separate the fibers.

It is always a good idea to leave spare fibers in the event of something happening or if later, the operators want to put more equipment. Leaving more fibers enables to scale the capacity with more equipment or to install other future solutions. For example, a Wi-Fi solution if there is both equipment in the footbridge and the technical room or video surveillance solution, the flexibility of the fiber connection allows several usage options.

The radio equipment chosen could have been one that works in both LTE 1800 and LTE 2600 bands avoiding losses introduced by the directional coupler (DC) and the jumper cables that connect the radio to the DC and the DC to the antenna. However, both RF bands are not so closed to each other, and I could not find this ideal RRU model. For that reason, two different radio equipment were considered.

### 3.4.2 Directional Couplers

Using a directional coupler is necessary owing to the fact that the technologies LTE 1800 and LTE 2600 are in different radio equipment. If both technologies were in the same radio equipment (1800+2600), considering only one operator, it would be possible to connect the radio equipment directly to the antenna since the chosen radio has two output ports, the necessary to ensure MIMO 2x2. The combiner is another source of losses so the second option would be ideal for improving the gain. However, as explained both 1800 and 2600 band combination is not usual.

While having two radio equipment and knowing that each radio “feeds” an antenna input port, it is necessary to have at least two 2:1 directional coupler to combine both signals into one output signal that connects to the input port of the antenna. So, the frequency range of the combiner needs to encompass the 1800 band in one input port and in the other the 2600 band. The 2:1 combiner option found did not support LTE technology in both input port, so the second option is to use a 2:2 combiner. Figure 3.14 exemplifies the scheme of one of the sectors that cover the lower tier.

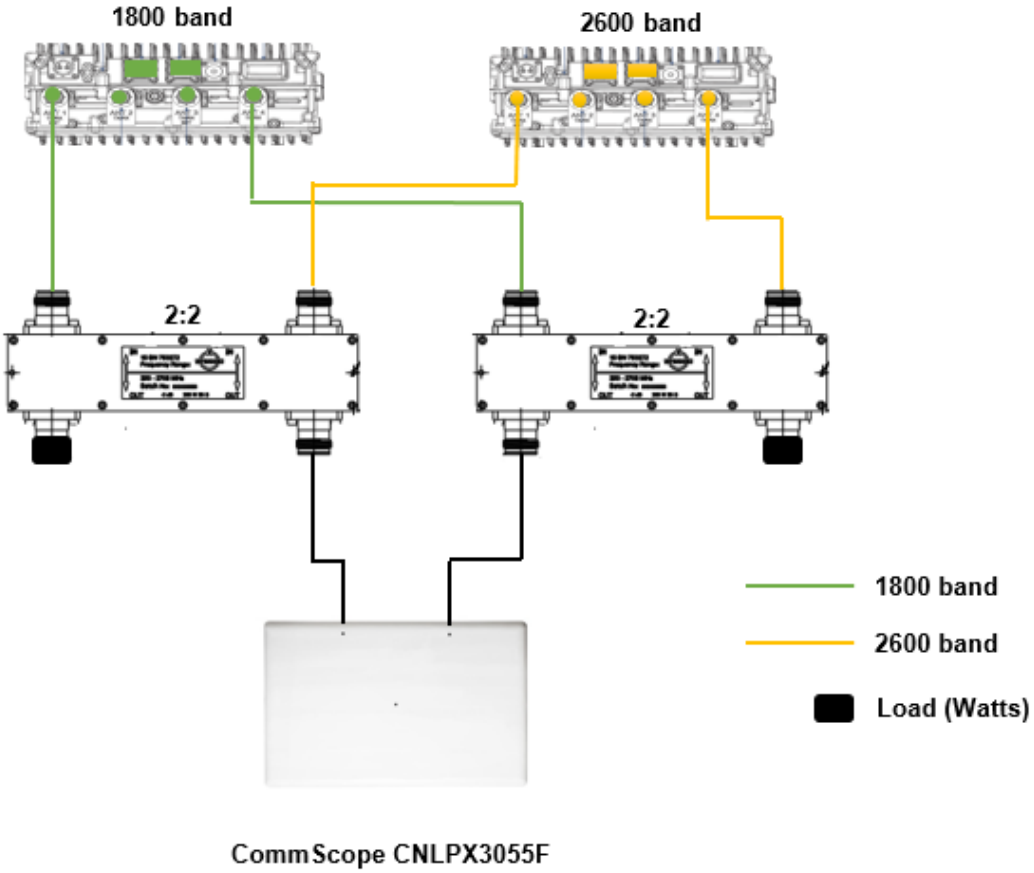


*Figure 3.14 - Scheme of the sector responsible for covering the lower tier.*

If the chosen antenna only has two ports, as in the case of the CommScope antenna [Annex A - datasheet] and the three existing operators in Portugal are considered using different radios per technology, the signals need to be combined before to leave only one cable for each antenna port. In this case, two 3:1 directional coupler would be enough. However, this combination (3:1) is unusual, and the fact that each technology is in different radios makes necessary for each operator to combine the two signals before entering in only one port of the three ports of the directional coupler, this will increase losses.

What happens in the world of telecommunications is that each operator wants to highlight their quality of service compared to the other principally in events situations. In Portugal all events are sponsored, directly or not, by an operator, it is the case of NOS Alive sponsored by NOS, MEO Sudoeste by MEO or Vodafone Paredes de Coura by Vodafone. This leads to a “project leader” operator that will try to undermine the solution of the other operators. So probably the two directional couplers required will have one more input port each for the leader to not have to combine the signals before the directional coupler thus reducing the losses.

A usual combination with four input ports is the 4:4 directional coupler. This option on the edge allows feeding four antennas with MIMO 2x2. For example, for making a horizontal coverage sector with the antennas A1, A3 and A19, the three antennas would have to be all fed by the same two directional

couplers linked to the two radio equipment. So, using a directional coupler with more input and output ports allows scalability to another type of solution in the future.

As mentioned before, using two 4:4 combiners for the solution with two ports antennas and the three operators considered, it would make the project leader have the right to use two input ports and so having an advantage over the others. Figure 3.15 shows this option.

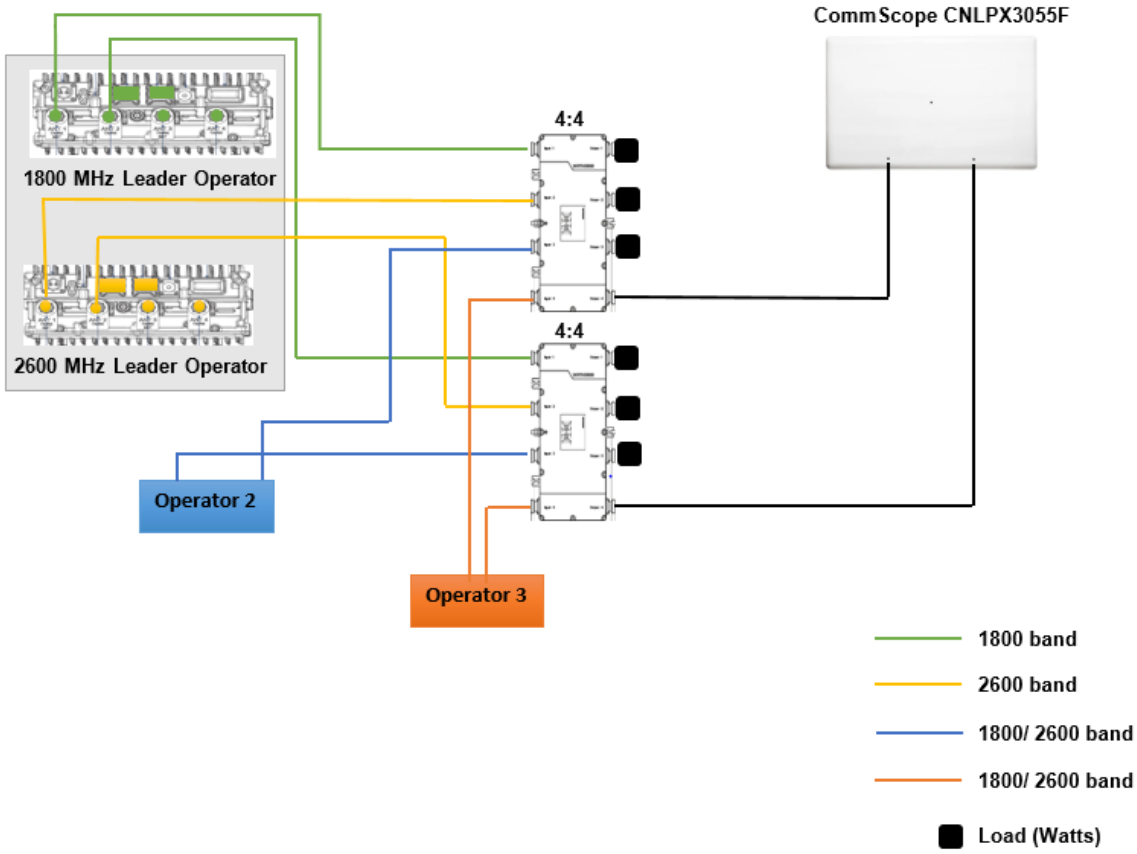


*Figure 3.15 - Scheme of the sector if there is a leading project operator.*

A good practice that is important to follow is when an output port of the directional coupler is left without use is to “lock him” with a load (watts) because since it is injecting signal, it probably would be a signal return.

### 3.4.3 Power Points – General Interest

This topic will not be extensive since it is beyond the purpose of the dissertation. So, for curiosity, it is important to have into account that the equipment requires electrical power to operate. As RRUs operates at 48 V, the 220 V must be converted into 48 V through rectifiers. The power points (PPs) are cabinets where the rectifiers are located. In case the stadium does not have a generator that can guarantee the electrical power needed to supply the equipment in case of something happening, batteries will be placed at PPs. In the presented case study, the electrical supply will be ensured by the connection to the existing electrical panel. If it were necessary to install the batteries, the weight would be much higher, and it would make the project much more expensive. The dashed rectangle

encompasses the antennas fed by each PP. Figure 3.16 shows that for this solution, each stadium stand will have one PP associated due to limitations on cables length. Both PP1 and PP3 will feed six antennas and PP2 and PP4 will feed four antennas.

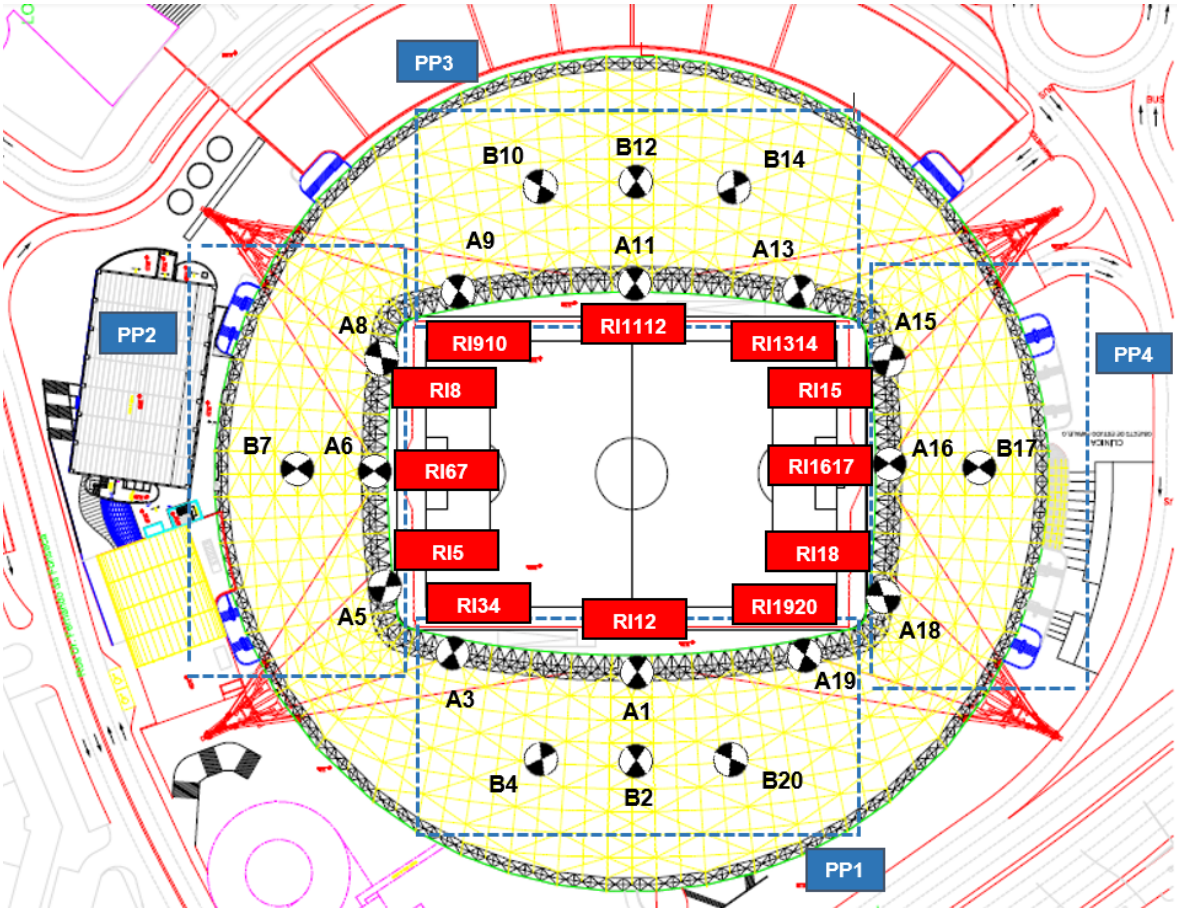


*Figure 3.16 - Stadium representation of the antennas location, the number of RIs and PPs.*

# Chapter 4

# LTE Capacity Dimensioning

This chapter aims to describe the capacity planning for the LTE network. Evaluating the total capacity allows estimation of the number of sites required to carry the anticipated traffic over the coverage area [Syed09]. Capacity planning involves selection of site, and system configuration, e.g. channels used, channel elements and sectors, avoiding under dimensioning that causes poor network performance or over dimensioning that leads to unnecessary costs.

Since the wireless cellular network dimensioning is directly related to the quality and effectiveness of the network, once the number of sites based on the traffic forecast is obtained, the interfaces of the network are dimensioned, and the used techniques are presented. The purpose of this step is to perform the allocation of traffic in such a way that no bottleneck is created in the network.

## 4.1 MIMO

MIMO stands for Multiple Input Multiple Output, where multiple refers to multiple antennas used simultaneously for transmission and reception. The big question is why is desirable to add more antennas? This section answers the question.

Using the multipath signal propagation, that is present in all terrestrial communications, MIMO is used to improve communication performance, capacity with higher spectral efficiency (more bits per second per hertz of bandwidth) and diversity (reduced fading) or link reliability. Offering significant increases in data throughput and link range without using additional bandwidth or transmission power [StGWZ10].

The limit to how much data can be transmitted in a given bandwidth is known as the Shannon-Hartley theorem (Shannon's Law), the channel capacity (bits/s) can be calculated by:

$$C \approx n \times B \times \log_2(1 + \frac{S}{N}) \quad (4.1)$$

Where:

- n is the number of Tx/Rx antennas;
- B is the bandwidth in Hz;
- S/N is the signal-to-noise ratio.

The bandwidth limits how fast the information symbols can be sent over the channel and Signal-to-Noise Ratio (SNR) limits how much information can be squeezed in each transmitted symbol. So, it is possible to affirm that noise impacts the maximum information rate, thus making the separation of cells, in order to have the least amount of overlap, a very important aspect of radio network design and planning. For this reason, chapter 3 is dedicated to antenna placement.

According to [Basil17], MIMO and its usage, there is a significant boost to the number of transmitted information bits, improving the system throughput and spectral efficiency. Applying the definition of MIMO nxn directly to equation (4.1) means increasing the theoretical maximum data transfer speed n times when compared to the use of single-input-single-output (SISO).

One of the primaries reasons to use multiple antennas is to improve link quality and reliability. According to [Estra11], diversity uses two or more antennas on the transmitter and/or the receiver at a certain distance, separating them has desirable effects, and it is called spatial diversity. Both transmit and receive. Diversity can increase the reliability of the link especially when the channel is noisy, the fading will not have an impact because a slightly different version of the signal emitted is transmitted across independent fading channels. Therefore, the usable range increases because repetition due to loss or damage during the signal delivering is lower.

Existence of multiple antennas in a system means the existence of different propagation paths. Aiming at improving the data rate of the system, the spatial multiplexing method is used, since different portions of the data are placed in different propagation paths. This technique consists in sending signals from

two or more different antennas with different data streams. The receiver can distinguish between the various paths and extract independent data streams from each when processing the signals, increasing the peak data rates by a factor of 2 (2x2 configuration).

Based on [HoTo09], MIMO operation also includes pre-coding which means that multiple data streams are emitted from the transmit antennas with independent and appropriate weightings (phase and gain) such that the SNR is maximized at the receiver output.

The basic principle of MIMO is presented in Figure 4.1, where the different data streams are fed to the pre-coding operation and then onwards to signal mapping and OFDMA signal generation. The reference symbols enable the receiver to separate different antennas from each other. The channel estimation needed for separating the MIMO streams can be corrupted when transmission occurs from another antenna. To avoid this, the used reference symbol resource needs to be from a single transmit antenna, so the reference symbols and empty resource elements are mapped to alternate between antennas.

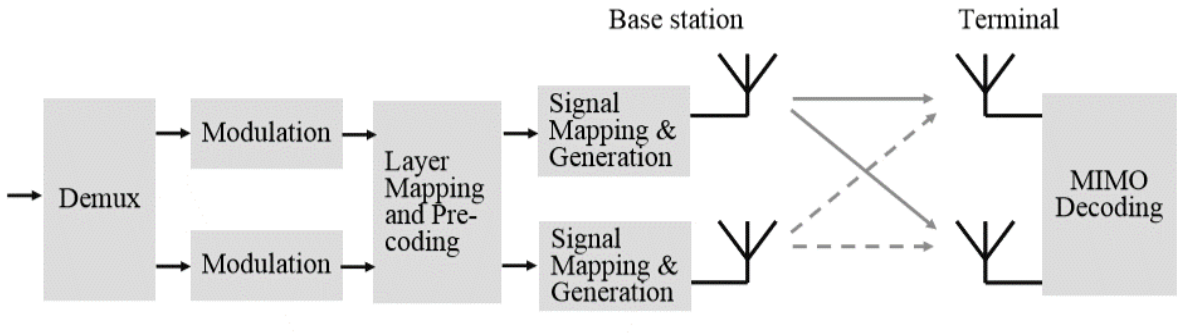


*Figure 4.1 - 2x2 MIMO principle configuration (extracted from [HoTo09]).*

A specific mode of MIMO operation is the Multi-User MIMO (MU-MIMO) where the eNodeB is sending from two (or four depending on the specifications) antenna ports different data streams for different devices. Figure 4.2 illustrates the principle.

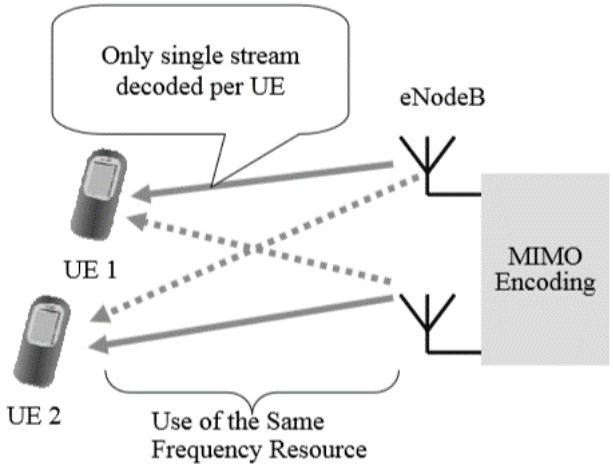


*Figure 4.2 - Principle of Multi-user MIMO transmission (extracted from [HoTo09]).*

An analogy that is usually done is to think of wireless communication as a vehicle traveling on a highway. Each vehicle represents bits of information while the roads are analogous to the wireless

spectrum available. The decks of freeway represent the spatial layers created in multiplexing schemes. The direction is from the mobile tower network to the UE. Figure 4.3 represents the communication over one single LTE band with 2x2 MIMO.

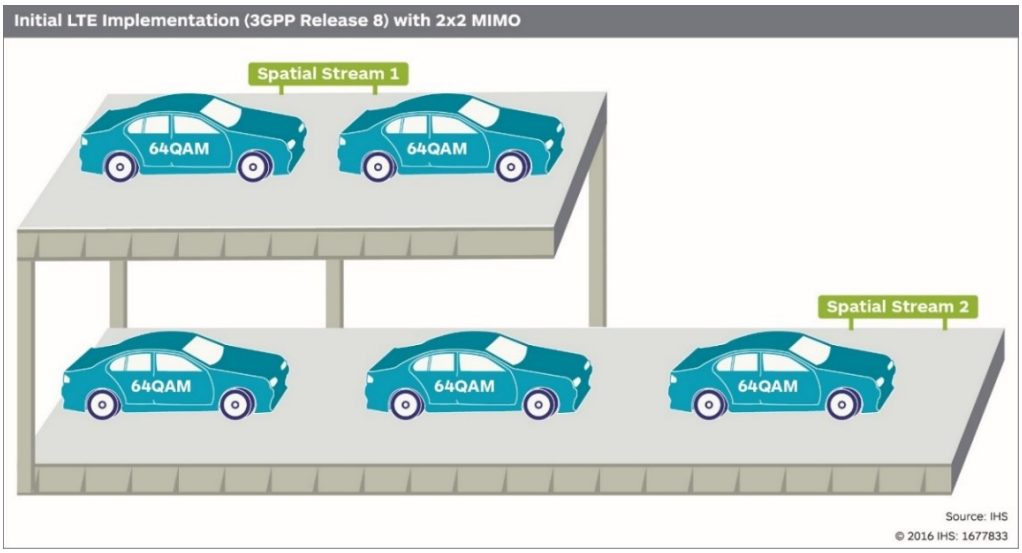


*Figure 4.3 - Analogy between LTE wireless communications over a single LTE band with 2x2 MIMO and automobiles traveling in a highway (extracted from [Lam16]).*

Figure 4.4 is the extension of the analogy with the evolution into LTE Advanced using carrier aggregation and 256-QAM (LTE Category 11).

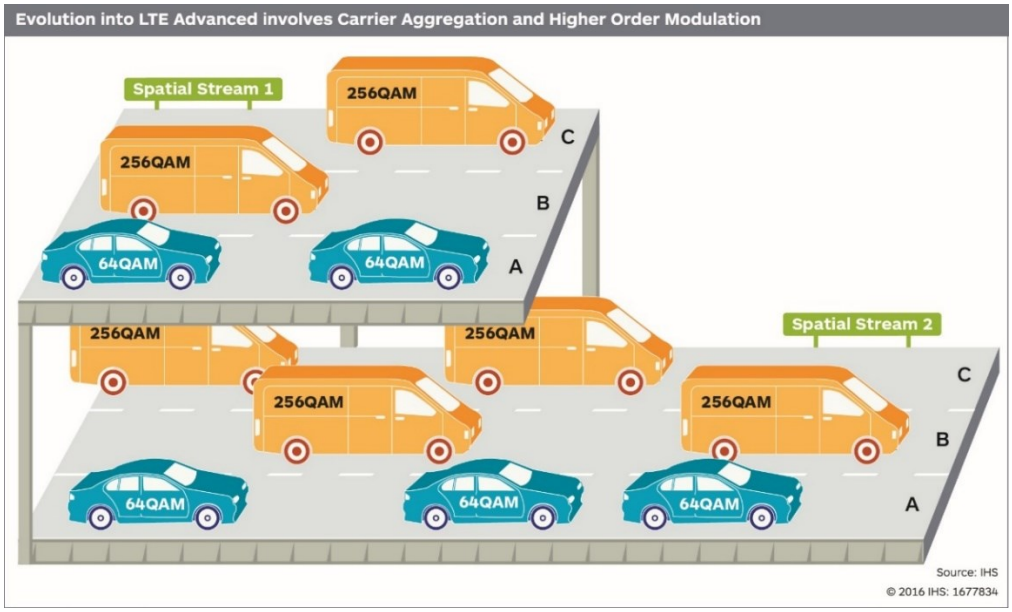


*Figure 4.4 - Analogy between LTE Advanced using carrier aggregation and 256-QAM and automobiles traveling in a highway (extracted from [Lam16]).*

MIMO allows the transmission of parallel data streams from multiple-antenna elements at the transmitter

which are then received and demodulated by multiple-antenna elements at the receiver. So, the more antennas the UE has, the more data can transfer at once, that means faster wireless download and upload speeds. To achieve these faster speeds, it requires that the user is connected with a cellular network that supports 4x4 MIMO.

According to [Hoff18], recent tests have demonstrated that going from 2x2 MIMO to 4x4 MIMO can improve wireless signal strength too. In a downlink connection, the power comes from the antenna, and in the uplink, the power comes from the UEs. When compared to an antenna, the UE power is weaker, so the uplink connection is not as stable as the downlink. For this reason, it is important to have antennas with sensitive receivers (Rx's).

In Table 4.1, UE belonging to category 5 upwards can support 4x4 MIMO. However, a UE with low modulation schemes cannot take full advantage of 4x4 MIMO. This variation of MIMO is now standard on high-end phones like Apple's iPhone XS, iPhone XS Max, Samsung's Galaxy S9 and S9+, Google's Pixel 3 and Pixel 3 XL, these are capable of utilizing it to the maximum. However, this corresponds to a small number of smartphones. Most UE cannot achieve high modulation schemes like 256-QAM, only the ones categorized 10 forwards can and most of the time only in downlink connections. The expression "the more MIMO, the better" is not applicable when the UE is connected to a cellular network that offers more MIMO but does not support this type of system.

*Table 4.1 - UE Category characteristics (extracted from [Tech18]).*

<table>
<tr><th colspan="2" rowspan="2">UE Category</th><th colspan="2">Max. Data Rate</th><th rowspan="2">Min. Number of DL CCs</th><th rowspan="2">DL MIMO Layers</th><th colspan="2">Highest Modulation</th></tr>
<tr><th>DL</th><th>UL</th><th>DL</th><th>UL</th></tr>
<tr><td rowspan="5">Rel 8</td><td>1</td><td>~ 10 Mbps</td><td>~ 5 Mbps</td><td rowspan="5">1</td><td>1</td><td rowspan="9">64 QAM</td><td rowspan="4">16 QAM</td></tr>
<tr><td>2</td><td>~ 50 Mbps</td><td>~ 25 Mbps</td><td rowspan="4">2</td></tr>
<tr><td>3</td><td>~ 100 Mbps</td><td>~ 50 Mbps</td></tr>
<tr><td>4</td><td>~ 150 Mbps</td><td>~ 50 Mbps</td></tr>
<tr><td>5</td><td>~ 300 Mbps</td><td>~ 75 Mbps</td><td>64 QAM</td></tr>
<tr><td rowspan="3">Rel 10</td><td>6</td><td>~ 300 Mbps</td><td>~ 50 Mbps</td><td rowspan="2">1 or 2</td><td rowspan="2">2 or 4</td><td>16 QAM</td></tr>
<tr><td>7</td><td>~ 300 Mbps</td><td>~ 100 Mbps</td></tr>
<tr><td>8</td><td>~ 3000 Mbps</td><td>~ 1500 Mbps</td><td>5</td><td>8</td><td>64 QAM</td></tr>
<tr><td rowspan="4">Rel 11</td><td>9</td><td>~ 450 Mbps</td><td>~ 50 Mbps</td><td rowspan="2">2 or 3</td><td rowspan="4">2 or 4</td><td rowspan="4">16 QAM</td></tr>
<tr><td>10</td><td>~ 450 Mbps</td><td>~ 100 Mbps</td></tr>
<tr><td>11</td><td>~ 600 Mbps</td><td>~ 50 Mbps</td><td rowspan="2">2, 3 or 4</td><td rowspan="2">256 QAM</td></tr>
<tr><td>12</td><td>~ 600 Mbps</td><td>~ 100 Mbps</td></tr>
</table>

According to [JEcon18], the top 3 most sold smartphone brands are: Huawei, Samsung and Apple. Based on the top 8 most sold smartphones in Portugal in 2017 [Marg18], Table 4.2 shows that only 2 out of 8 cannot support more than 2x2 MIMO, only two can take advantage of 4x4 MIMO and that in apple the iPhone 8 was the first one categorized over 10.

*Table 4.2 - Popular smartphone models with the respective UE category.*

| | Model (year) | UE Category |
|---|---|---|
| **Huawei** | P8 Lite (2015) | 4 |
| | P9 Lite (2016) | 4 |
| | P10 Lite (2017) | 12 |
| **Samsung** | Galaxy S7 Edge (2016) | 9 |
| | A5 (2017) | 6 |
| **Apple** | Iphone 6S (2015) | 6 |
| | Iphone 7 (2016) | 9 |
| | Iphone 8 (2017) | 12 |

In stadium environments, it is crucial to think not only in terms of the best theoretical solution but in terms of reaching and providing a good QoE for the biggest number of users. It is important to mention too, that a user that can reach this high modulation (256-QAM) occupies a big part of the band “stealing” from other users that are not capable. Nowadays not only for a question of fairness but of costs too, a 2x2 MIMO system was chosen.

## 4.2 Sectorization and Traffic Profile

Sectorization has a dual purpose in the design of a radio network, increasing network capacity and minimizing the number of signals presented in a specific area by limiting sector coverage. There are three sectorization types: horizontal, vertical and mixed sectorization that corresponds to hybrid horizontal-and-vertical sectorization.

Limiting the coverage also limits interference from non-serving sectors, which improves capacity, signal-to-interference-plus-noise ratio (SINR) and maximum achievable data rate (MADR). In Line-of-Sight (LOS) areas like the seating bowl, sector overlap minimization is achieved by using highly directional and isolated antennas.

Since stadium, *Estádio José Alvalade,* is partly covered by a roof and has a different number of seats in the two levels/rings of sectorization it is not sufficient to use horizontal sectorization. The number of seats at the lower tier (level near the field) is superior to the ones existing at the upper tier. A vertical sectorization will be a better choice to mitigate the different quantity of users on both levels due to its type of coverage. However, the most efficient and expensive too will be the mixed sectorization. For this

solution, a mixed sectorization was selected. Figure 4.5 corresponds to the simulation of the chosen solution where it is possible to observe the resulting distribution of the sectors, a mixed one when using the 1800 MHz band.

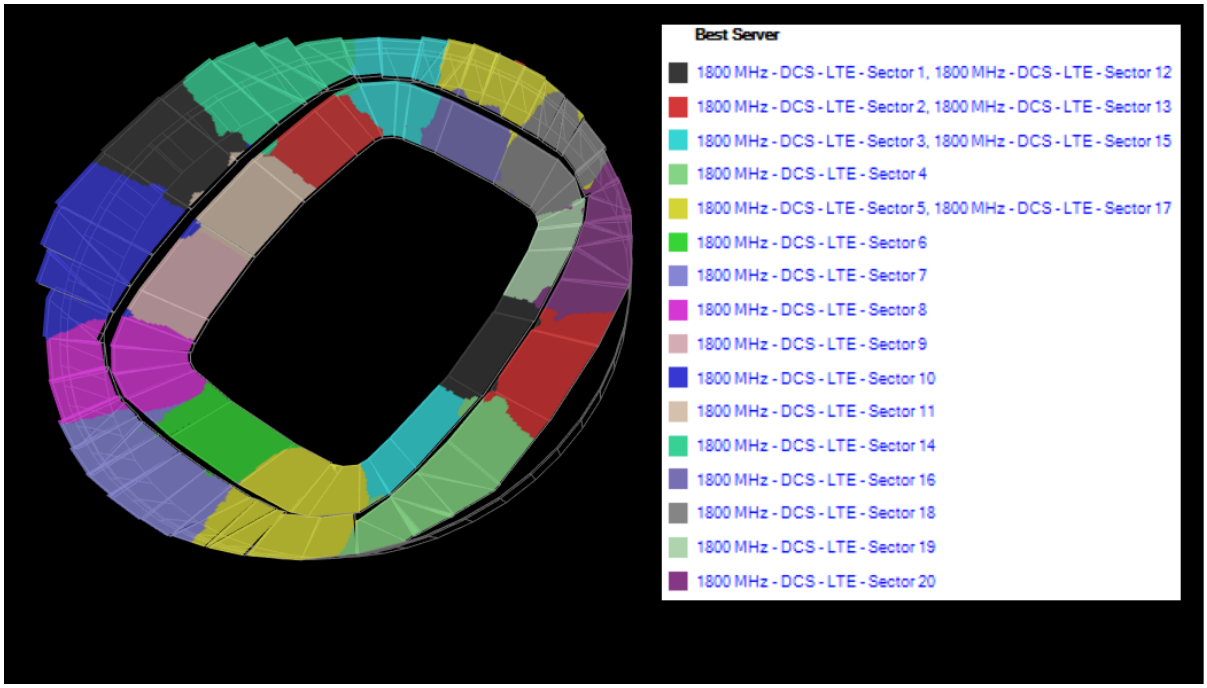


*Figure 4.5 - Final solution iBwave Best server output map considering the 1800 MHz band.*

The number of sectors per carrier depends on the number of seats, the carrier's subscriber penetration rate and the carrier's mobile traffic profile. The case study stadium has 50 095 seats distributed by two different levels/tiers. The first one is level A/ lower tier, and the second one is level B/ upper tier, between them, stands the private box, the VIP area and the presidential box. These central areas are covered by the antennas responsible for covering the users at the lower tier, as mentioned in the subchapter 3.3.1.

In order to not emphasize one of the three mobile network operators in Portugal: MEO, NOS or Vodafone, a subscriber uniform market share was considered, so each operator has 1/3 of the total seats. It is important to have into account that not all terminals support LTE technology, the 4G penetration percentage is about 70% in Portugal UEs, value revealed by Dense Air at the Small Cells World Summit 2019 in London [SCF19].

According to [Zava17], to understand the total number of sectors that should cover the seating area is important to follow some steps. First, a calculation for the maximum number of LTE subscribers inside the stadium is required: 50 095 is the total capacity/number of seats, 1/3 of this is approximately 16 699 seats. Giving a margin of growth until October based on the forecasting presented in Chapter 6, an 80% penetration rate was applied to this number; there will be 13 360 LTE subscribers per operator.

Secondly, the MIMO data rates used to obtain the average data rate per sector were taken from both SINR, and MADR output maps, Figure 4.7 and Figure 5.5 obtained when simulating the chosen solution. Table 4.3 resumes this step.

According to [Cox12], in order to UEs reach the theoretical peak data rates, the following conditions must be fulfilled:

1. The antenna must be transmitting and receiving in its maximum bandwidth of 20MHz;
2. The UE must have the most powerful capabilities that are available at each release, i.e. spatial multiplexing on the downlink or the use of 64-QAM on the uplink;
3. The user should be close to the antenna;
4. The antenna should be well isolated to avoid interference;
5. The UE must be the only one active in that sector. If it is not, then the capacity will be shared amongst all the users, resulting in a large drop in the peak data rate that is available to each one.

The last condition will never be achievable at an event situation (game day). Knowing this, the coverage is based on the maximum achievable data rate (MADR) values obtained with the iBwave Software. From these values, the $datarate_{average}$ was calculated and used to obtain the necessary number of sectors. The highest data rates (165.87 Mbit/s) are only possible near the antenna. The lowest data rates (11.36 Mbit/s) will be where the sectors overlap. And the reasonable data rates will be where the signal is not as strong as in the direction of the antenna but is not an overlapping zone.

*Table 4.3 - Coverage (%) distribution of MADR per modulation based on Figure 4.7 and Figure 5.5.*

| Modulation | MADR (Mbps) | Coverage (%) |
|---|---|---|
| QPSK | 11.36 | 4.6 |
| 16-QAM | 35.27 | 8.4 |
| 64-QAM | 71.73 | 9.7 |
| 64-QAM | 116.56 | 11.15 |
| 64-QAM | 167.87 | 66.15 |

$$datarate_{average} = 11.36 \cdot 0.046 + 35.27 \cdot 0.084 + 71.73 \cdot 0.097 + 116.56 \cdot 0.1115 + 167.87 \cdot 0.6615 \approx 133.16\ Mbps \quad (4.2)$$

Contrary to what happened in outdoor situations, where traffic is considered for the different distribution of calls typical over the day, week and longer cycles; for stadium environments traffic is always designed for the maximum stadium capacity. To ensure that it reaches close to all the expected demand [GraKP06].

According to [Hecht16], data traffic from mobile devices is increasing by an estimated 53% per year. The demand for bandwidth is fast outstripping providers' best efforts to supply it. Generally speaking, the bandwidth can be compared to water flowing pipe. The wider it is, the more water will pass through it at once or the maximum rate at which it can download data. The throughput is the quantity of water

passing through the pipe or how many units of information a system can process in a given amount of time; the maximum throughput can never be higher than the bandwidth.

Data rates correspond to the speed at which data is transferred. As stated by [Wood18], the more Mbps you have, the faster your internet. Although, how much speed is needed depends on the type of usage. Users who want to download High Definition (HD) videos or upload high-resolution photos will need more kbps than someone who wants to browse Facebook or send emails. The speed a user sign up for is not always the speed he gets. The available bandwidth may be affected by other households' network demand, the device own hardware and the provider's infrastructure quality, among other factors [Layt17].

The book [Zava17] presents the duration of the network connection during a busy hour and the fixed data rates in kbps based on a user profile at a stadium environment. However, these values are not considering the today typical social networking service (browsing, file sharing and video streaming). For this reason, the values for data rates considered are the ones presented in Table 4.4. A downlink performance was considered. It is important to note that a subscriber can use more than one service type per busy hour at a stadium environment. The average duration of video conferencing session is shorter than other venues due to crowd noise. The value assumed for video streaming was not the typical average data rate (5120 kbps) since the video traffic appears embedded in social media and web pages. This web applications are built in order that a sufficient quality for video streaming can be achieved with 2000 kbps of data rate.

*Table 4.4 - Average data rate [kbps] per type of service (based on [Pire15] and [Zava17]).*

| **Service** | | **Service Class** | **Average Data Rate [kbps]** |
|---|---|---|---|
| Voice | | Conversational | 12.2 |
| Email | | Background | 100.0 |
| Web Browsing | | Interactive | 500.0 |
| File Sharing | | Interactive | 1024.0 |
| Data Download | | Interactive | 1000.0 |
| Social Networking | | Interactive | 384.0 |
| Video | Calling | Conversational | 384.0 |
| | Streaming | Streaming | 2000.0 |

According to [Mish04], the best way to estimate traffic in the network is in terms of 'erlangs'. The amount of traffic generated by a user in one traffic channel for a busy hour. When a user generates 25 mErl of

traffic during the busy hour is the equivalent to 120 seconds of network usage, i.e., 2 minutes. One Erlang means that a single circuit is used 100% of the time [GraKP07]. The connection duration considered was based on personal experience.

The blocking rate is the percentage of attempted network connections that are denied due to insufficient network resources. In data, connections request is never denied, for this reason, there is a margin license connection for users which limits the entrance of users in each carrier. More users will degrade the cell because the connection will be delayed until resources are not available, this delay will give customers the perception of a “slow” network. If the blocking rate is efficient, a higher wireless utilization rate would be obtained. However, the aim is to guarantee the best possible QoE, so the blocking rate is low. Table 4.5 shows the connection duration, the data rates and the desired blocking for the different types of services.

*Table 4.5 - Data Traffic Distribution at the stadium during the busy hour per service type: duration (milierlangs per user), data rates (kbps) and blocking rate (%) (based on real stadium experience and on [Zava17]).*

| **Type of Service** | | **Connection Duration (mErl/user)** | **Connection Duration (minutes)** | **Data Rate (kbps)** | **Blocking Rate (%)** |
|---|---|---|---|---|---|
| Email | | 12.5 | 1 | 100 | 1 |
| Web Browsing | | 37.5 | 3 | 500 | 2 |
| Video Calling | | 5 | 0.4 | 384 | 1 |
| Data Download | | 50 | 4 | 1000 | 2 |
| Social Networking | Video Streaming | 37.5 | 3 | 2000 | 4 |
| | File Sharing | 50 | 4 | 1024 | 2 |
| | Browsing | 75 | 6 | 384 | 2 |

Duty cycle is defined as the ratio of carried traffic to theoretical maximum traffic when all resources are used for the full hour. Since the carried traffic corresponds to the traffic intensity handled, in a peak situation the cell is loaded, more PRBs are used, so a low value for this parameter was considered, 10% in this study. In this LTE capacity calculation, it was assumed that data is transmitted to each user only once in the LTE frame. Therefore, a subscriber receives that every 10 ms. So, the delay between two consecutive data Tx will be 10 ms, and the transmission duration is 1 ms.

Once again, according to [Zava17], the required data throughput per service type is calculated using the expression:

$$Throughput_{service} = LTE_{Sub} \cdot \frac{Connection_{duration}}{1000} \cdot \left(1 - \frac{Blocking_{rate}}{100}\right) \cdot \frac{data_{rate}}{1000} \cdot \frac{Tx_{delay}}{duty_{cycle}} \quad (4.3)$$

Where:

- $LTE_{Sub}$ is the number of LTE subscribers per operator;
- $Connection_{duration}$ is the duration of the connection in mErl/user;
- $Blocking_{rate}$ is the desired percentage of blocking per service type;
- $data_{rate}$ as the name indicates is the data rate per service type in kbps;
- $Tx_{delay}$ is the delay between consecutive data transmissions (Tx);
- $duty_{cycle}$ represents the duty cycle, and it is always 0.1.

*Table 4.6 - Results obtained from the expression (4.3).*

| Type of Service | Throughput (Mbit/s) |
|---|---|
| Email | 16.53 |
| Web Browsing | 245.49 |
| Video Conferencing | 25.39 |
| Data Download | 654.64 |
| Video Streaming | 961.92 |
| File Sharing | 670.35 |
| Browsing | 502.76 |

$$Throughput_{total} = 3077.08\ Mbit/s$$

Considering the distribution of MADR from Table 4.3 and the expression (4.2), the number of sectors necessary to obtain the required total throughput is:

$$\frac{Throughput_{total}}{datarate_{average}} = 23.11 \approx 24\ sectors \quad (4.4)$$

In order to guarantee a good QoE for the spectators, 24 sectors are necessary. However, the design and implementation of a dedicated solution for a large venue, like the case study, implies a huge investment cost so it cannot be implemented only for nowadays traffic characteristics. The solution needs to be designed in order to make the investment profitable for as long as possible. For this reason, the users will be distributed by 40 sectors.

Forecasting the development of mobile data demand is a challenge. By combining the estimations of annual traffic growth per service and bandwidth demand, an estimation for how long this solution is valid/sufficient is presented in chapter 6.

## 4.3 Load Balancing

One of the most critical aspects when designing a network is the distribution of load over the network. It is necessary to take into account that putting an antenna per used band is quite tricky: too much weight in the infrastructure because of all radio equipment and cables, maintenance will be more demanding, and the price would be much higher. The best way to reduce the number of antennas installed is by creating two LTE layers. So instead of having two antennas, the stadium has one that uses a mechanism called Load Balancing (LB). Not all UE behave in the same way before the different frequency bands (some do not support 2600 MHz band. For example, the iPhone before model 6). So, load balancing has to be done so that in peak situations, everyone has the same level of user experience, whether using a more demanding mobile application or not.

There are two ways of making the load balancing between LTE 1800 and 2600 band:

1. By the number of PRBs being used;
2. By distributing the number of users equally per each band.

In an outdoor network, the indoor penetration of frequencies, such as the band 800, 1800 and 2600 is different (for propagation reasons). So the distribution is made based on the PRB status since the eNodeB knows if the PRB is: being occupied/allocated or free, which involves transferring users from the layer with less free PRBs to the one that has more available resources. However, in stadium environments, more specifically in peak situations like half-time, all PRBs are being used so this balancing option will not be efficient. For this reason, the distribution is made based on the number of users in each band. The BBU has the LB parameterization loaded and is responsible for counting how many users are in one band and the other. How does BBU know this? When the Mobile Terminal (MT) makes an RRC connection setup (that is, establishes an uplink connection - example: when it refreshes a web page) starts counting as a user in that frequency band. The number of users must be equal in both 1800 and 2600 band.

According to [MisM14], the load balancing techniques may be based on the active or idle mode users. The big difference between the two modes is the mobility procedure carried out when real-time traffic or QoS demands increases in a cell. In idle mode, there will be a cell reselection: natural if the MT change his spatial location and the MT loses the cell signal or forced in case of stadium environments because the antennas are in LoS and very close to the bleacher (seating area) so the signal is always strong. In active mode, a handover would take place.

### 4.3.1 Handover vs Reselection

- **Handover (HO):** is a technique that enables the network to provide continuous service to users, especially when they are moving away from the connected cell toward another cell. Happens when the UE is in active mode. For example, the MT is losing the signal of one cell and begins to detect that the signal is better in another cell, the network causes the downlinks, and the

user's connection will be entirely broken with the existing cell before being switched to the better one [Techp19].

- **Reselection:** is a kind of mechanism to change cell after UE is camped on a cell and stay in idle mode. This makes UE get connected to the cell, which has the best condition among all the cells to which the UE is allowed to camp on. The criteria and algorithm for reselection process are complex. The reselection may be natural or forced. The natural reselection happens when the UE starts losing signal from a cell and gain from another. In stadium environments, this type of reselection is not considered since the antennas are very close to the bleacher [Share17].

The cell reselection is a slower process than the hard HO since it does not need to give such a fast response, involves much less signaling and synchronism. This is reflected in the number of occupied PRBs. In the moment of transition from one cell to another, the user doing the HO will count as two, one in the cell that he is abandoning and the other in the destination cell. Since less free PRBs available are reflected in slowness and the objective is to balance the cell load the more efficient way, Inter-Frequency Load Balancing (IFLB) is done in idle mode instead of active mode.

When a user is camped in a cell and sends a message with an mobile application, starting from the moment it waits for the answer and leaves the application running in the background it may enter in idle mode. How? The BBU can be defined to after 10 seconds with low throughputs to force the UE to idle mode. This acceleration of the transition from active to idle mode is desirable since it was defined that the LB will occur in idle mode and that with fewer users in active mode the eNodeB is free for new users to enter.

### 4.3.2 Inter Frequency Load Balancing (IFLB)

The IFLB is the name of the process of sending a user from one band to the other. When a cell has load relations established, every 15 seconds has the following behaviour, as shown in Figure 4.6:

1. Determine her own cell load status;
2. Exchange load information and compares with the one from the target;
3. If the actual cell has a higher load than the target, starts selecting offload UEs candidates;
4. If the target has good Reference Signal Received Power (RSRP), the ones selected before start being sent to the target for balancing the load.

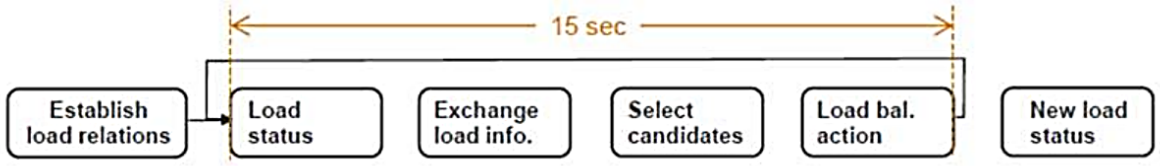


*Figure 4.6 - Feature Process Flow (extracted from [Eric15]).*

According to [Eric15], the percentage load can be calculated as follows:

$$Percentage\ Load = \frac{\sum QCIsubscriptionQuanta}{CellSubscriptionCapacity} \quad (4.5)$$

Where:

- $QCIsubscriptionQuanta$ represents the minimum acceptable downlink bit rate (kbps);
- $CellSubscriptionCapacity$ represents the achievable downlink bit rate (kbps), at maximum load.

For example, for the QoS class 8 presented in Table 2.5, the QCI subscription Quanta is 100 kbps, the default value is 1. Being the site a 20 MHz channel bandwidth site the Cell Subscription Capacity is 16000 kbps, the default value is 10000.

The load information exchanged between the source and target results on the amount, which is off-loaded to the neighbouring cell, known as Load Balancing Action (LBA) Magnitude. This parameter may be calculated using the following expression:

$$LBAmagnitude = \frac{\min(IbCeiling, LoadDiff)}{(NumIFLBrelations+1)} \quad (4.6)$$

Where load difference is obtained from:

$$LoadDiff = Percentage\ Load_{source} - Percentage\ Load_{target} \quad (4.7)$$

And:

- $IbCeiling$ is the maximum load difference taken into account in LBA;
- $NumIFLBrelations$ is the number of IFLB relations.

The $IbThreshold$ is the minimum load difference that triggers the LBA. The UEs are randomly selected for load balancing if $hreshold < LoadDiff < IbCeiling$. Of course, they will only be moved when the UE:

- Is not in an emergency call;
- Can support the frequency of the target cell.

Since one of the main goals of this solution is not limit or restrict the data usage or its type, no data QCI class will have priority over the others.

LTE does not support voice, so when a user is connected to a 4G network and decide to make a voice call, the UE falls back to 2G or 3G networks that support circuit switch calls. This flow describes circuit switched fall back (CSFB) from 4G to 2G or 3G. However, when the mobile user initiates a voice call is registered to an LTE network that does not support voice, UE releases the existing session as it needs

to initiate an extended service request and start going to transition to a 3G or 2G network. Voice always needs to have priority over data. For these reasons QCI class 1 for conversional voice, in Table 2.5, is the only one that will be defined as having priority.

There are two types of load sharing: between layers of adjacent cells/sectors or vertical load sharing (same sector). In stadium environments, there is no interest in a load sharing between adjacent cells/sectors because the users are already evenly distributed by coverage sector. However, that might be 4 or 5 rows of seats that correspond to two cell edges (overlapping zone) in these cases, IFLB between adjacent sectors could be an option. The other users make IFLB between layers of the same sector (vertical load sharing).

The baseband is calculated and dimensioned, giving the maximum of users per cell in reaching this value; no more users enter the cell. When the cell is full, when one user leaves, others enter. At events the LB criteria are adjusted in order to accomplish the following objectives: avoid cell congestion, equitable distribution of users per band and provide QoS. The congestion is avoided with an equal distribution of the users and the QoS results from evaluating the CQI.

## 4.4 SINR

The performance of any radio channel is not only related to the absolute signal level, but also to the quality of the signal. When there are active communications between the base stations (BSs) and the UEs, the interfering power is considered, and the SINR is used to determine the radio channel conditions for a given UE.

Channel Quality Indicator (CQI) is the information sent by UE on the uplink path to the eNodeBs, that indicates the received channel quality, and the packet scheduler uses it for further scheduling purposes.

For LTE capacity dimensioning, an LTE SINR coverage map was calculated using the iBwave Software. As sector overlap affects SINR, an assumption was made about the quantity and position of the sectors. When considering the specifications written above as the final solution (Table 3.1), an SINR coverage map was simulated, and the stadium bowl can be split into 5 SINR ranges with different efficiency (bits/RE), as shown in Figure 4.7. The prediction legends on the right side of the picture are for level A, and the one in the left is for the level B. This simulation was obtained considering the 1800 MHz band.

The relationship between SINR, modulation scheme and spectral efficiency taken from Table 4.7, enable us to calculate the number of resources needed to support each service type listed for busy-hour traffic at stadiums. LTE resources are Physical Resource Blocks (PRB). The number of resources needed varies with SINR.

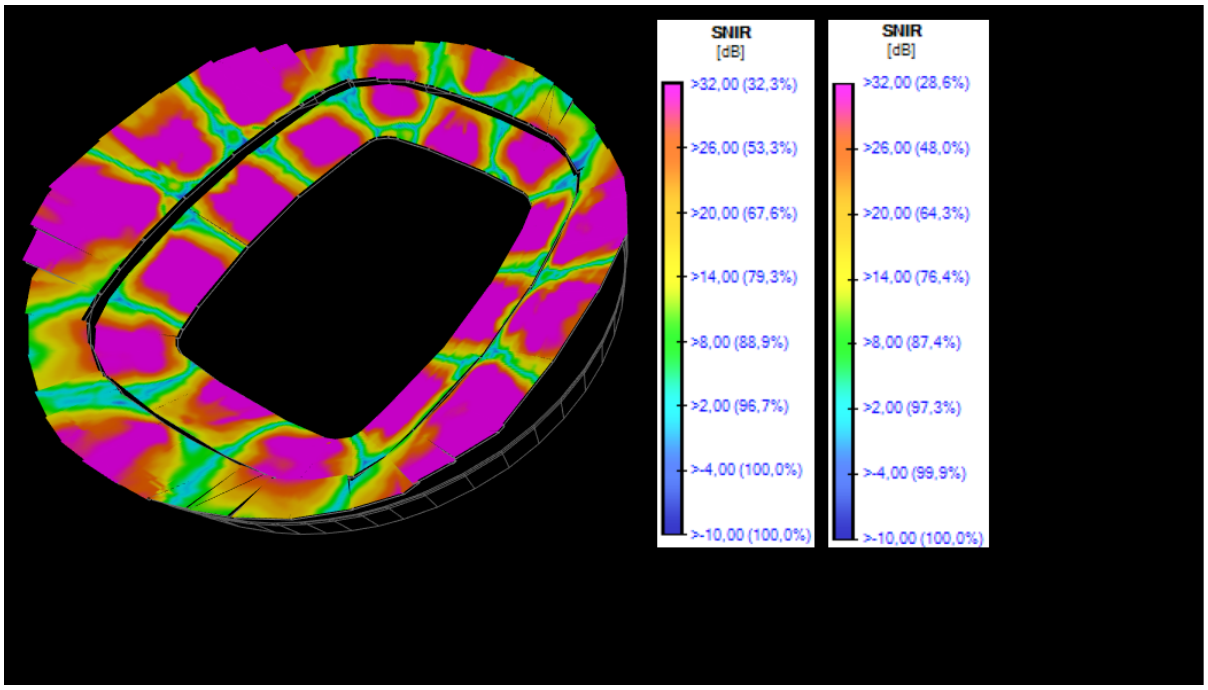


*Figure 4.7 - Final solution iBwave SINR output map considering the 1800 MHz band.*

*Table 4.7 - CQI look-up table considering 10% Block Error Rate (BLER) threshold (extracted from [Basil17]).*

| CQI | Range of SINR (dB) | MCS | | Efficiency (Bits/RE) |
|---|---|---|---|---|
| | | Modulation | Approximate code rate | |
| 0 | SINR < -6.936 | Out of Range | -- | -- |
| 1 | -6.936≤SINR<-5.146 | QPSK | 0.0762 | 0.1523 |
| 2 | -5.147≤SINR<-3.18 | QPSK | 0.1172 | 0.2344 |
| 3 | -3.18≤SINR<-1.253 | QPSK | 0.1885 | 0.3770 |
| 4 | -1.253≤SINR<0.761 | QPSK | 0.3008 | 0.6016 |
| 5 | 0.761≤SINR<2.699 | QPSK | 0.4385 | 0.8770 |
| 6 | 2.699≤SINR<4.694 | QPSK | 0.5879 | 1.1758 |
| 7 | 4.694≤SINR<6.525 | 16 QAM | 0.3691 | 1.4766 |
| 8 | 6.525≤SINR<8.573 | 16 QAM | 0.4785 | 1.9141 |
| 9 | 8.573≤SINR<10.366 | 16 QAM | 0.6016 | 2.4063 |
| 10 | 10.366≤SINR<12.289 | 64 QAM | 0.4551 | 2.7305 |
| 11 | 12.289≤SINR<14.173 | 64 QAM | 0.5537 | 3.3223 |
| 12 | 14.173≤SINR<15.888 | 64 QAM | 0.6504 | 3.9023 |
| 13 | 15.888≤SINR<17.814 | 64 QAM | 0.7539 | 4.5234 |
| 14 | 17.814≤SINR<19.829 | 64 QAM | 0.8525 | 5.1152 |
| 15 | SINR≥19.829 | 64 QAM | 0.9258 | 5.5547 |

The mathematical expression used to calculate the instantaneous data rate of each user is:

$$\mathrm{R\ (t)} = \mathrm{Efficiency\ (t)} * \mathrm{RE} \ / \ \mathrm{RadioFrame_{length}} \tag{4.8}$$

Where:

- $\mathrm{R}$ is the instantaneous data rate at time t (bps);
- $\mathrm{Efficiency}$ correspond to the spectral efficiency (bits/RE) – Table 4.7;
- $\mathrm{RE}$ is the total number of REs specified for downlink data transmission;
- $\mathrm{RadioFrame_{length}}$ is 10 ms because it was assumed that data is transmitted to each subscriber only once in each LTE frame.

Knowing the data rate for each type of service Table 4.5 and the spectral efficiency tabulated in Table 4.7, the total number of Resource Elements (REs) needed for the downlink data transmission can be easily obtained.

According to [Basil17], with the typical cyclic prefix, a PRB contains a total of 168 resource elements (RE). Each PRB has 148 resource elements for 10% Block Error Rate (BLER) threshold and 20 REs are used for control and signalling purposes. With this reference number of RE per PRB and the number of REs obtained from the expression (4.8), the number of necessaries PRB is known, Table 4.8. It is important to have into account that if SINR is high, a single PRB may be enough to support a type of service, if SINR is low, more than one PRB may be required.

The efficiency (Bits/RE) values were calculated using averages based on Table 4.7. For Range 1, 0.5125 bits/RE was considered, for Range 2, 1.5222 bits/RE, for Range 3, 2.8197 bits/RE and Range 4, 4.5136 bits/RE. The efficiency value for Range 5 was directly extracted from Table 4.7, 5.5547 bits/RE.

*Table 4.8 - Based on the ranges obtained from the iBwave SINR output map (Figure 4.6).*

| | | **Number of Physical Resource Blocks (PRB) per connection** | | | | |
|---|---|---|---|---|---|---|
| **Service Type** | **R(t) (kbps)** | **Range 1** | **Range 2** | **Range 3** | **Range 4** | **Range 5** |
| | | -4≤SINR<2 | 2≤SINR<8 | 8≤SINR<14 | 14≤SINR<20 | 20≤SINR<32 |
| Emails | 100 | 12 | 4 | 2 | 1 | 1 |
| Video Conferencing | 384 | 45 | 15 | 8 | 5 | 4 |
| Social Networking | 384 | 45 | 15 | 8 | 5 | 4 |
| Web Browsing | 500 | 58 | 20 | 11 | 7 | 5 |
| Data Download | 1000 | 116 | 39 | 21 | 13 | 11 |
| File Sharing | 1024 | 119 | 40 | 22 | 14 | 11 |
| Video Streaming | 2000 | 232 | 78 | 42 | 26 | 21 |

## 4.5 Performance Optimization – QoS

### Carrier Aggregation

In 2011, the 3GPP Rel.10 introduced the Carrier Aggregation (CA) technique to increase the peak data of a 4G LTE network. Operators could increase the total available bandwidth of a single transmission, and so increase the bitrate and capacity of the network, by aggregating multiple channels together and combine spectrum in low-, mid-, and high-band frequencies.

Each aggregated carrier is referred to as a component carrier (CC). The component carrier can have a bandwidth of 1.4, 3, 5, 10, 15 or 20 MHz and a maximum of five component carriers can be aggregated. So, when it is time to choose the strategy, each mobile network operator can choose a channel bandwidth from Table 2.2 according to his final objective. Since the main purpose is to give a good QoE to the spectators, it is assumed the use of 20 MHz channel bandwidth to provide extra capacity. Hence the maximum aggregated bandwidth is 100 MHz, as shown in Figure 4.8.

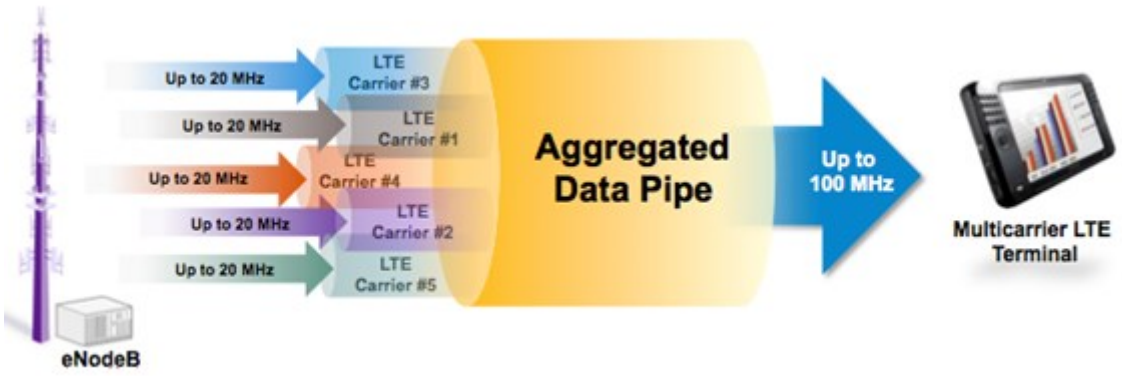


*Figure 4.8 - Carrier Aggregation features (extracted from [Amon11]).*

CA allows carriers to send and receive data over an aggregated data pipeline to increase data rates and to lower latency. This means that carriers will be able to support high-speed data traffic even in times of peak network usage.

According to [Wann13], the easiest way to arrange aggregation would be to use contiguous component carriers within the same operating frequency band, so-called intra-band contiguous however due to operator frequency allocation scenarios; this might not always be possible. For non-contiguous allocation, it could either be intra-band or inter-band. In the first one, the component carriers belong to the same operating frequency band but have a gap, or gaps, in between, as can be observed in Figure 4.9, in the contiguous intra-band aggregation scenario, the component carriers are in the same band and are adjacent to each other. A multiple of 300 kHz separates them in order to not interfere with each other. In non-contiguous intra-band aggregation, the component carriers are in the same band separated by a multiple of 100 kHz.

As state by [Cox12], the most challenging scenario is the inter-band aggregation, where the component carriers are in different frequency bands. The mobile may require different radio components to support each band because the cell's coverage area may be very different. In FDD mode, the allocations on the uplink and downlink can be distinct, but the number of downlink component carriers is always greater than or equal to the number used in the uplink.

Inter-band CA aggregates multiple CCs in different operating bands. Inter-band CA is more complex than intra-band CA because the multi-carrier signal cannot be treated as a single signal and therefore requires a more advanced transceiver in the User Equipment (UE).

In the end, CA will allow mobile to transmit and receive using five component carriers in a variety of frequency bands. Not all UEs can handle this technique only UE category 8 forward.

In carrier aggregation technique, only a limited number of frequency bands are supported, a mobile UEs declares which bands and band combinations it supports. The MT capability is known as the CA bandwidth class which states the number of component carriers that the mobile supports and the total number of resource blocks that it can handle, illustrated in Figure 4.9.

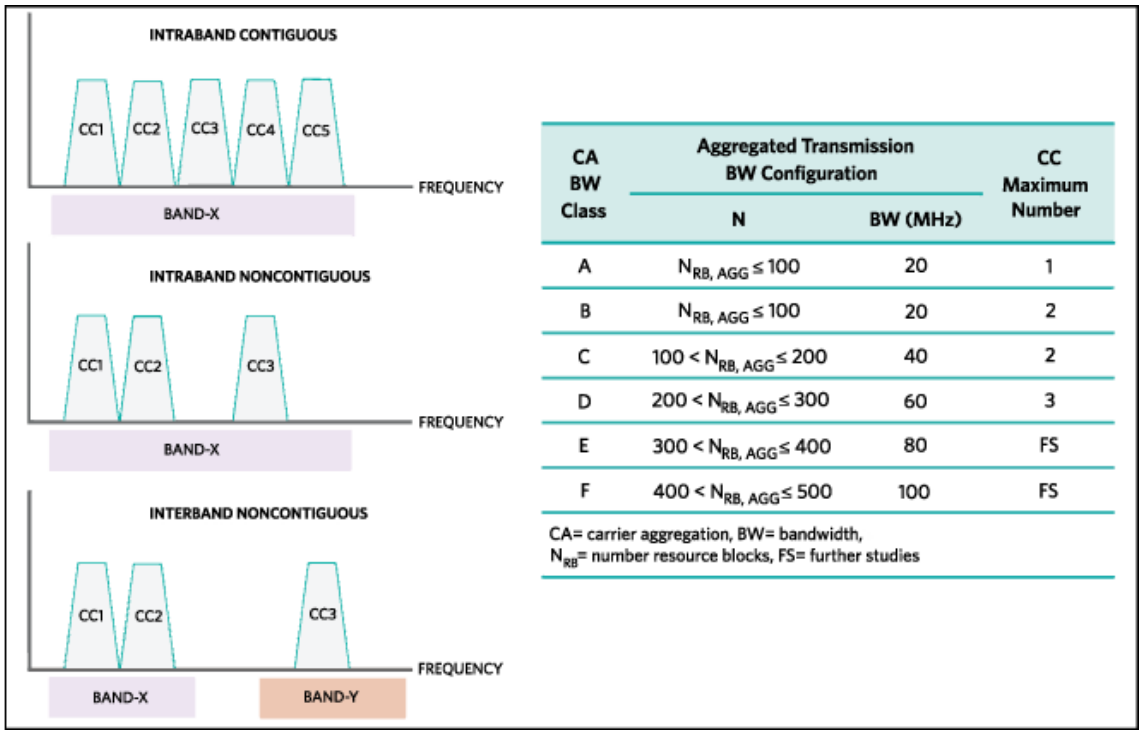


| CA BW Class | Aggregated Transmission BW Configuration | | CC Maximum Number |
|---|---|---|---|
| | N | BW (MHz) | |
| A | $N_{RB, AGG} \leq 100$ | 20 | 1 |
| B | $N_{RB, AGG} \leq 100$ | 20 | 2 |
| C | $100 < N_{RB, AGG} \leq 200$ | 40 | 2 |
| D | $200 < N_{RB, AGG} \leq 300$ | 60 | 3 |
| E | $300 < N_{RB, AGG} \leq 400$ | 80 | FS |
| F | $400 < N_{RB, AGG} \leq 500$ | 100 | FS |

CA= carrier aggregation, BW= bandwidth,
$N_{RB}$= number resource blocks, FS= further studies

*Figure 4.9 - Illustration that summarizes the different types of carrier aggregation, different CA classes and transmission bandwidth configurations (extracted from [Anza14]).*

Carrier aggregation between low- and high-band frequencies is a standard configuration because many operators have valuable low-band spectrum (such as 800 MHz) that has definite coverage advantages. The 4G LTE Frequency Bands usually used in Portugal are B20 (800 MHz), B3 (1800 MHz) and B7 (2600 MHz). Comparing the three possible CA types combinations [Wann13] is possible to conclude that CA_3A-7A (1800-2600 MHz) has a bigger maximum aggregated bandwidth 40 MHz against the 30 MHz obtained with CA_3A-20A (1800-800 MHz) or CA_7A_20A (2600-800 MHz). For this reason, aggregating the band 3 and 7 will support more users at busy-hour situation (half-time).

CA can be used strategically in this type of solution. It works in active mode and seeks to benefit the user experience.

If the 1800 and 2600 band signal levels are balanced/identical, some terminals can synchronize the two frequencies on their internal radius, and the eNodeB is transmitted and received through the two bands. Is almost possible to talk about a kind of “Virtual MIMO” since two paths are used for transmitting and receiving, theoretically providing twice the throughputs.

In this situation, the user counts twice one in the 1800 band and another in the 2600 band, allocating resources from each one, for this reason, the number of users that can use CA must be limited. In this case, a maximum of 400 users will be considered per eNodeB, i.e., per bleacher. It will also be imposed that if the processing capacity in the eNodeB exceeds 50% load, it is no longer allowed for more users to enjoy CA.

# Chapter 5

# iBwave Simulations

The iBwave Design Enterprise Software was used in order to optimize the design of stadium *José Alvalade,* considering outdoor signals and interferences in the indoor signal predictions for data throughput. In the following simulations, the outdoor estimated signal was -75 dBm in order to adequately support the provision of the bandwidth for video streaming, web browsing, social networking and more. The theoretical signal data estimated around the building area was manually introduced, and his impact is reflected in the different output maps.

## 5.1 Output Maps Meaning

The iBwave Design Enterprise is a powerful software for designing large and complex indoor wireless networks. Having access to the blueprints of the venue and after making a site survey, using the advanced 3D modelling it was possible to generate a model of our case study with the help of the AutoCAD tool.

Accordingly to [iBwave], this software presents a database that can be customized with more than 30,000 parts from different vendors/brands. It is an expensive user-friendly tool which I only had access to a trial license for 15 days. With the license, it was possible to generate the 3D modelling of the case study stadium and simulate different LTE solutions. However, only the most relevant simulations will be discussed ahead.

The output maps obtained for each discussed simulation are displayed throughout the dissertation and in section Annex B, as the respective configuration was tabled, and the positioning scheme taken from the software. In each output map figure, the legend on the left or top corresponds to the values that act on the lower level A, the one in the right or the bottom correspond to the level B. If it only appears one legend the values are valid for all stadium.

The iBwave Optimization Module based on outdoor measurements allows the creation of output maps reflecting the impact of these measurements on the indoor environment; for this work, the following output maps were considered relevant:

1. LTE RSRP Map: RSRP is an acronym for LTE Reference Signal Received Power. It is the average of power of a Resource Element (RE) that carry a cell specific Reference Signals (RS) over the entire bandwidth. At the edge of the LTE coverage sector, the signal will have low strength, so it will be closer to -100 dBm.
2. Best Server: This map allows to optimize the design since it enables to identify the interfering sectors at any location quickly. Represents the area of action of each sector;
3. LTE Overlapping Zones: This map represents the number of eNodeB sectors in each pixel for which the condition RSRP > (Best Server RSRP – RSRP_margin) is satisfied. “Number of sectors” equal to 1 means that the user placed on that location receives the signal from only one sector, if the number of sectors is greater than 1, means that is an overlapping zone.
4. SINR: the purpose of this output map is to interpolate both the outdoor signal and the signal provenient from an interfering sector, with the signal strength map to produce the SINR at any given point of the prediction area. Once again, the outdoor signal was manually introduced;
5. Dominance Over Macro Map: As the name indicates, this map calculates and display the dominance of the indoor signals over the macro network. The interference of the outdoor signal is subtracted from the indoor signal strength and mapped. By observing the maps, the green part is where the indoor signal strength is 10 to 15 dB higher than the interference from the outdoor signal. Where it is yellow, the indoor signal strength is between 8 to 10 dB higher than the outside signal. Where it is red, the indoor signal strength is between 0 to 8 dB higher than

the signal interference from the macro network. The primary goal is to have as little as possible areas in black since in that areas the outdoor signal dominates;

6. Maximum Achievable Data Rate Map (MADR): The importance of data rates have increased over the past few years. To create this map the software uses the RSRP Signal Strength and SINR output maps to obtain the throughput distribution indoors. This map makes sure that there are enough antennas to have a good data coverage. In the edges of the building located at the second tier, the outdoor interference is stronger making the data rates drop significantly. The same happens in the areas of sector overlapping but with the interference between sectors;
7. Mobile Tx. Power: It is the only uplink analysis map considered. It displays the required mobile transmit power in each location of the prediction area over the entire RF channel, considering the same path loss both in the uplink and downlink way. The mobile station maximum transmit power is 24 dBm and the minimum transmit power is -40 dBm.

## 5.2 Simulations

The first simulation made was using only the CommScope antenna, designed especially for stadiums, as described in subchapter 3.3.2. However, it is possible to observe in Figure 3.11 and Figure 3.12, that for the level B/upper tier this solution was not so good. So, the main goal was to improve the results obtained in the upper tier without degrading the ones obtained for the lower tier. Identical output map values for both stadium levels were the results to achieve.

As explained before, the antennas covering the corners are closer to the seating area when comparing to other parts of the bleacher. So, to cover both the upper and lower tier, the antenna must present a big vertical beamwidth (VB). For this reason, a second and third simulation were performed using two different antenna models with a wider vertical beamwidth than the stadium antenna.

For simulation 2, the corner antenna model used was the CommScope CMAX-DMH60-43-V53 (datasheet 2) and for simulation 3 was the JMA XGU-FRO-130 (datasheet 3). Both datasheets are presented in Annex A. When comparing the RSRP output maps Figure 5.1 and Figure 5.2, it is possible to observe that the signal strength level is higher and more uniform in simulation 2 than in simulation 3. These results can be justified by the differences between both antenna models characteristics. Despite having a similar VB for the 1800 band, the CommScope antenna presents a 68 degree horizontal beamwidth (HB) versus the 32 degrees of the JMA antenna. Which result in a higher signal strength level in the corners, higher SINR values and, consequently, bigger MADR average value. Figure B.4 and Figure B.5 of Annex B, compare SINR Output Maps obtained from simulation 2 and 3, respectively. Figure B.6 and Figure B.7 compare MADR Output Maps results from simulation 2 and 3. Using the 2600 band, the RSRP Output Maps present drastic differences from one simulation to the other. This happens because both JMA antenna VB and HB are smaller than the beamwidth values of the Commscope antenna. Figure B.8 corresponds to simulation 2 and Figure B.9 to simulation 3.

The signal strength level difference is more visible in the corners, especially on the level A/ lower tier, which reflects on the lower average values of MADR. Although the difference between Figure B.10 and

Figure B.11 is not so accentuated as expected, this may be justified by the high gain value of the JMA antenna. Comparing both Table B.2 and Table B.3, it is possible to conclude that the low gain value of the CommScope CMAX-DMH60-43-V53 was compensated introducing 49 dBm as signal source power input.

Another simulation that results in interesting output maps was simulation 4. Considering the CommScope stadium antenna in all positions except for B2, B7, B12 and B17 antennas where the CommScope CMAX-DMH60-43-V53 model (datasheet 2 – Annex A) was used again. As explained before, the middle part of the grandstand is the tallest point of the level B bleachers meaning more seats constitute it. So, the sector responsible for covering those areas, especially sectors 2 and 12, would cover a large number of people comparing to other sectors. This means more data traffic, more resources (PRB) utilizations and more people sharing capacity, consequently resulting in lower data rates achievable for each user. A sector should cover more or less the same number of persons, in order to guarantee an identical QoE in all parts of the stadium bleachers. Using the B7 band, simulation 4 presents better MADR results than the final simulation, Figure 5.3 and Figure 5.4, respectively. However, as explained, it does not correlate to the real data rates that can be achieved in both 2 and 12 sectors.

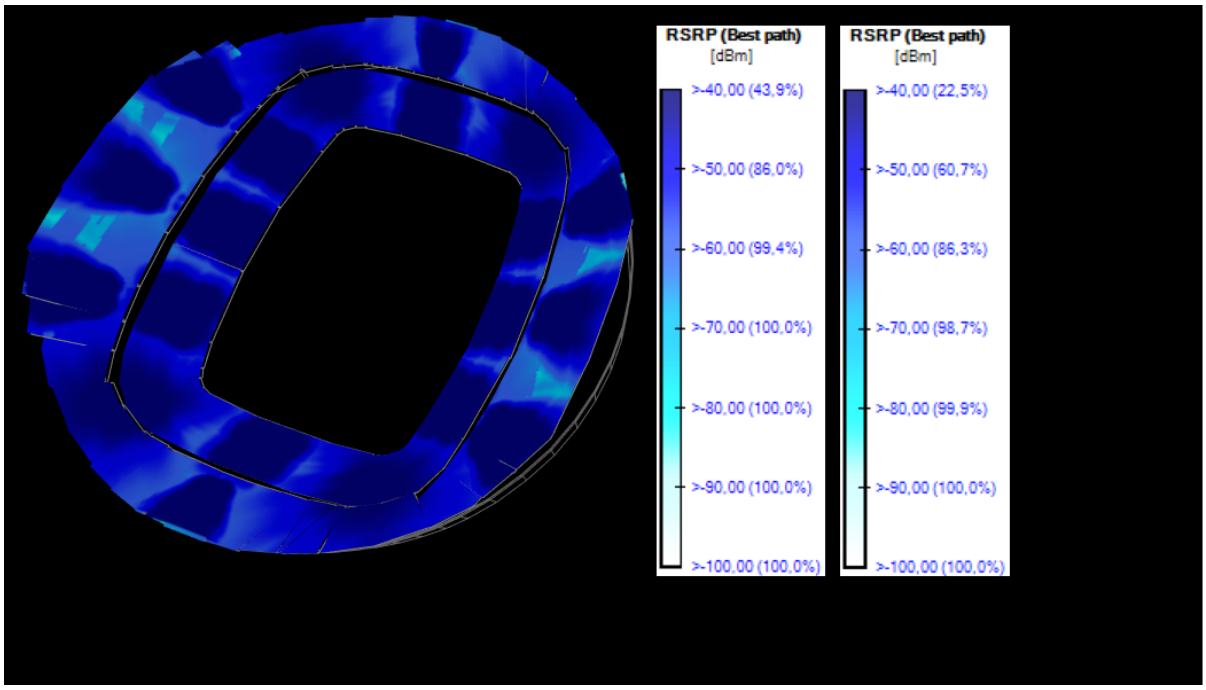


*Figure 5.1 - iBwave RSRP Output Map obtain in simulation 2 considering 1800 MHz band.*

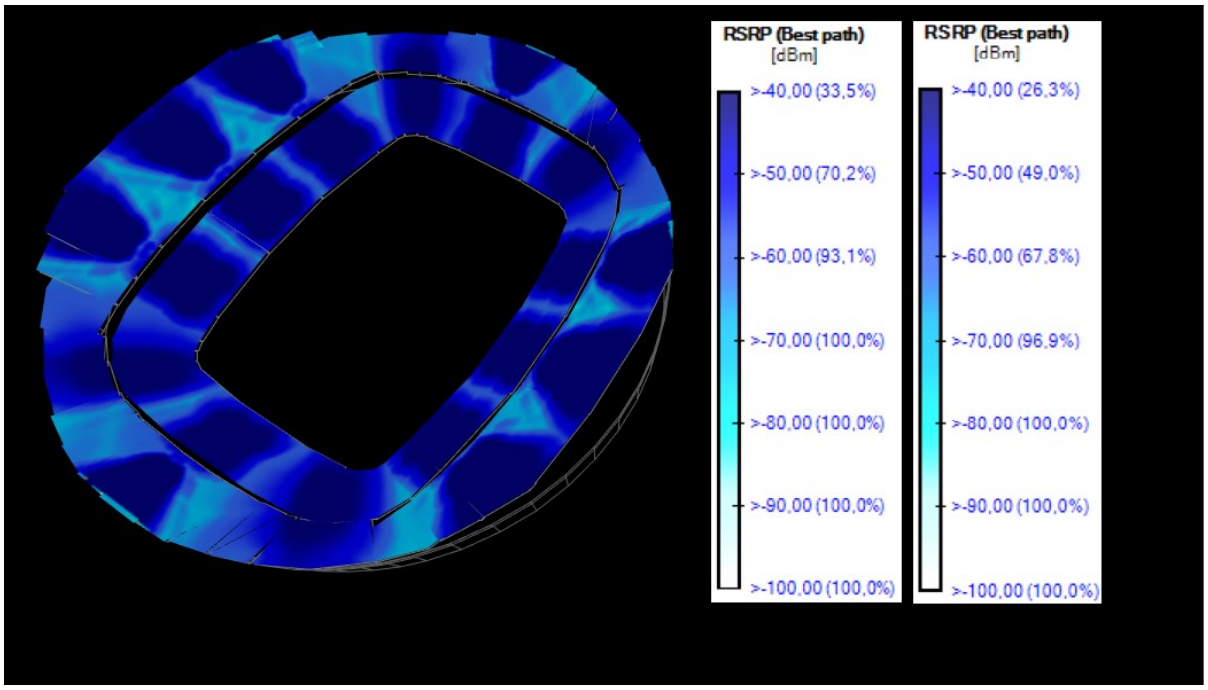


*Figure 5.2 - iBwave RSRP Output Map obtained in simulation 3 considering 1800 MHz band.*

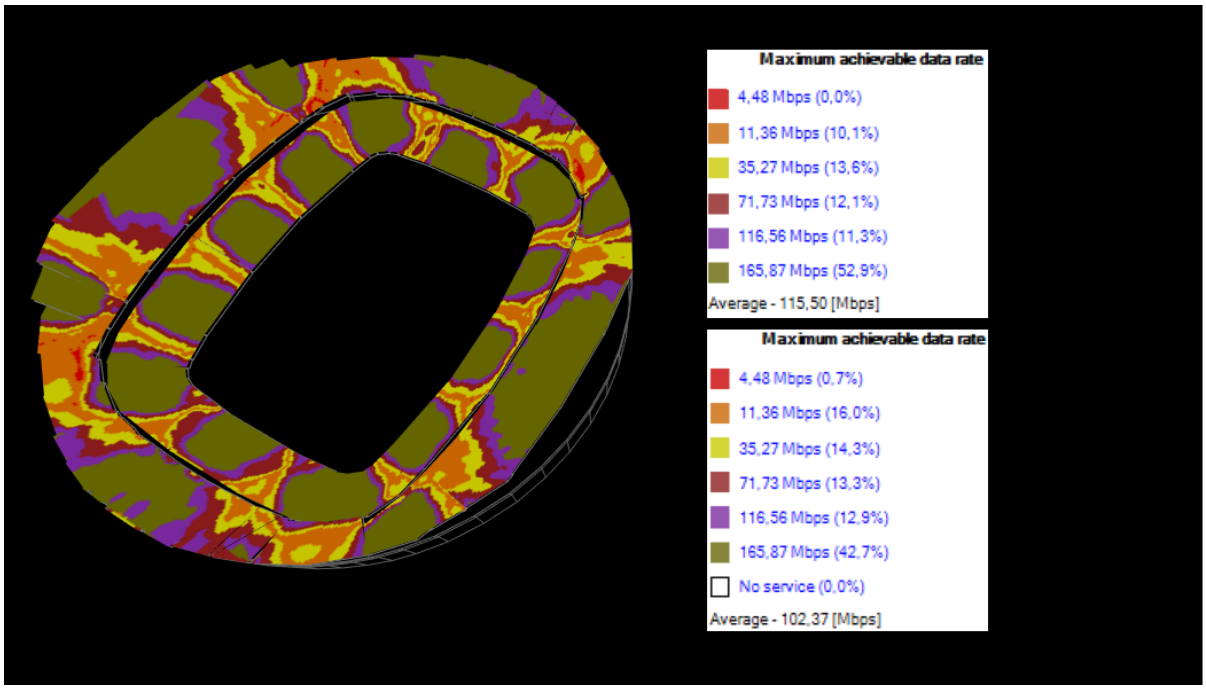


*Figure 5.3 - iBwave MADR output map obtained in simulation 4 using 2600 MHz band.*

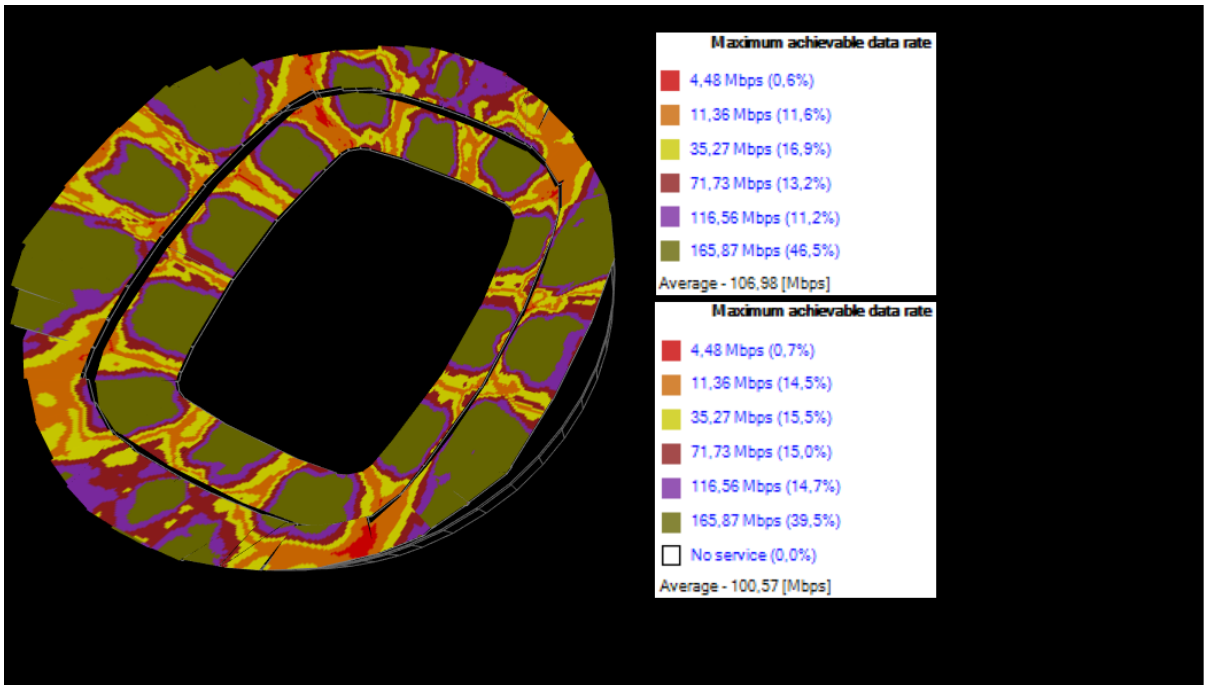


*Figure 5.4 – Final Solution iBwave MADR output map obtained using 2600 MHz band.*

One of the most relevant simulations resulted from using a discontinued antenna model CMAX-DM60-CPUSEi53 (datasheet 4 – Annex A), and the best results were obtained. However, with the same configuration and conditions, Table B.5, the output maps using the actual antenna model CMAX-DM60-CPUEV53 (datasheet 5 – Annex A) were noticeably worse. Analyzing both antennas datasheets, most parameters were similar; however, the actual antenna front-to-back ratio was 3 dB lower. This parameter should have the highest possible value because of the rooftop characteristics.

After this disappointing result, the closest simulation to the results obtained in that failed attempt (simulation 5) were the ones obtained with the final solution. Although, the chosen solution was not so balanced between the results using both bands as simulation 5. When comparing the final solution results obtained using the B3 and B7 band, it is possible to observe the output maps degradation results obtained when changing from the 1800 band to the 2600 band. Simulation 5 presented the most balanced results between bands since the important parameter front-to-back ratio was equal when using both bands. However, the values usually vary from one range of frequencies to the other. It is known that 1800 band provides a broader coverage range than 2600 band and different propagation characteristics. These will not be as relevant as other parameters on the results because of the short distance between the antennas and the seating area.

The RSRP output maps differences, Figure 5.6 and Figure 5.7, are justified by the 3 degree difference in the HB and the 1 degree difference in the VB. The close proximity of the antenna to the users confers relevance to broader beamwidth values in order to accentuate the effect of the radiation pattern and consequently the signal strength level. Another antenna characteristic that leads to lower SINR values is the 2 dB difference in the front-to-back ratio. Figure B.12 corresponds to the output map using 2600 MHz band and Figure 4.7 using the 1800 MHz band.

This parameter must present high values because this specific rooftop is made of a material that blocks

the signal making it impossible for the signal to pass through it and so reflecting the signal to the seating area. The smaller the value, the more unwanted radiation in an undesired direction (back lobe), creating interference in the seats, reflected mostly on the level B corners of the LTE Overlapping Zones output maps using the 2600 MHz band, Figure 5.8. The overlap degrades sharply as a result of the loss of “dominance” of the sectors 5, 8, 15 and 18 (corner sectors). Sector 7 and 17, using the CommScope CMAX-3030S-D-V53 model (datasheet 6 – Annex A), begin to interfere in the area of action of the corner stadium CNLPX305FF antennas (datasheet 1 – Annex A), without being the best server Figure 5.9. The average MADR is lower using the 2600 band for all the reasons described before Figure 5.4, to the values obtained using the 1800 band Figure 5.5.

The output maps, from the final solution, which were not presented before, are displayed on the sub-section B4 of the Annex B. The assumed configuration is presented in Table 3.1 and the final position antenna scheme in Figure 3.8.

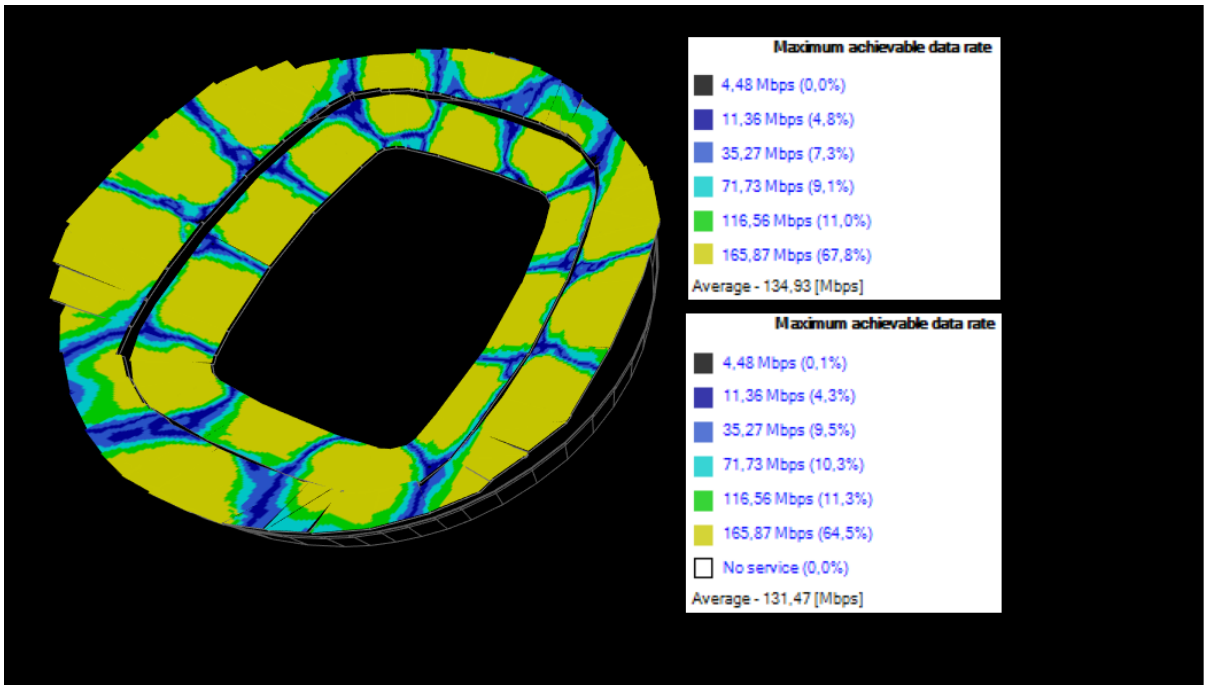


*Figure 5.5 - Final Solution iBwave MADR output map obtained using the 1800 MHz band.*

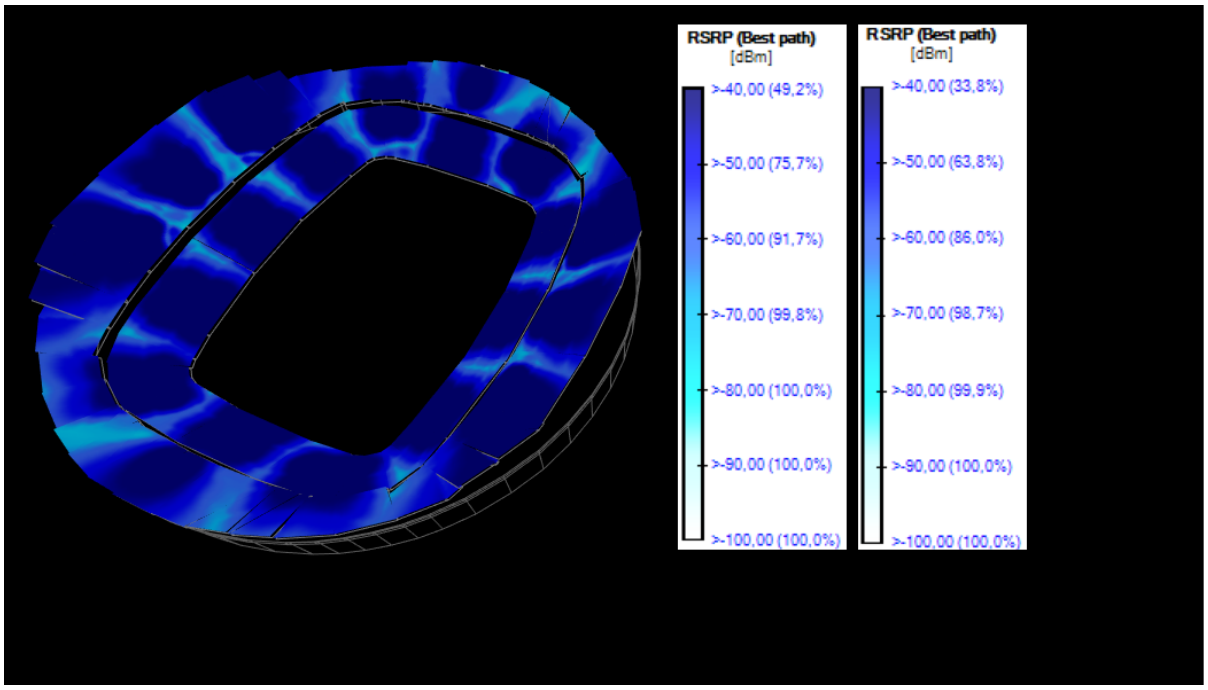


*Figure 5.6 - Final Solution iBwave RSRP output map obtained using the 1800 MHz band.*

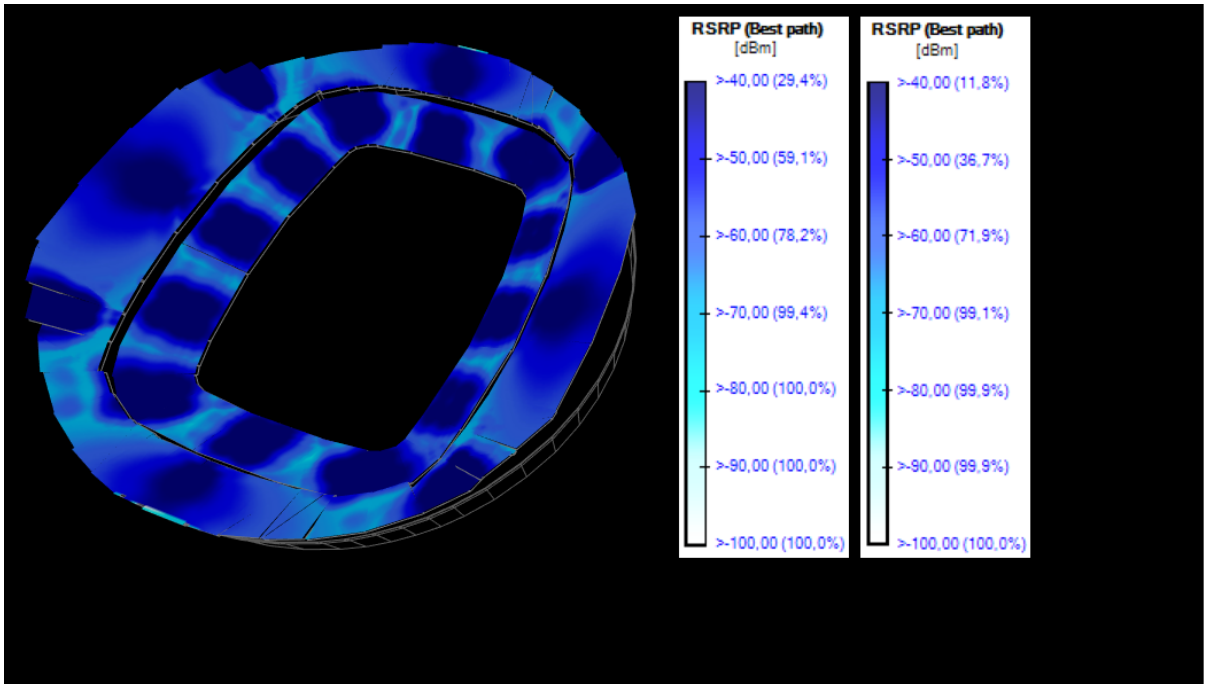


*Figure 5.7 - Final Solution iBwave RSRP output map obtained using the 2600 MHz band.*

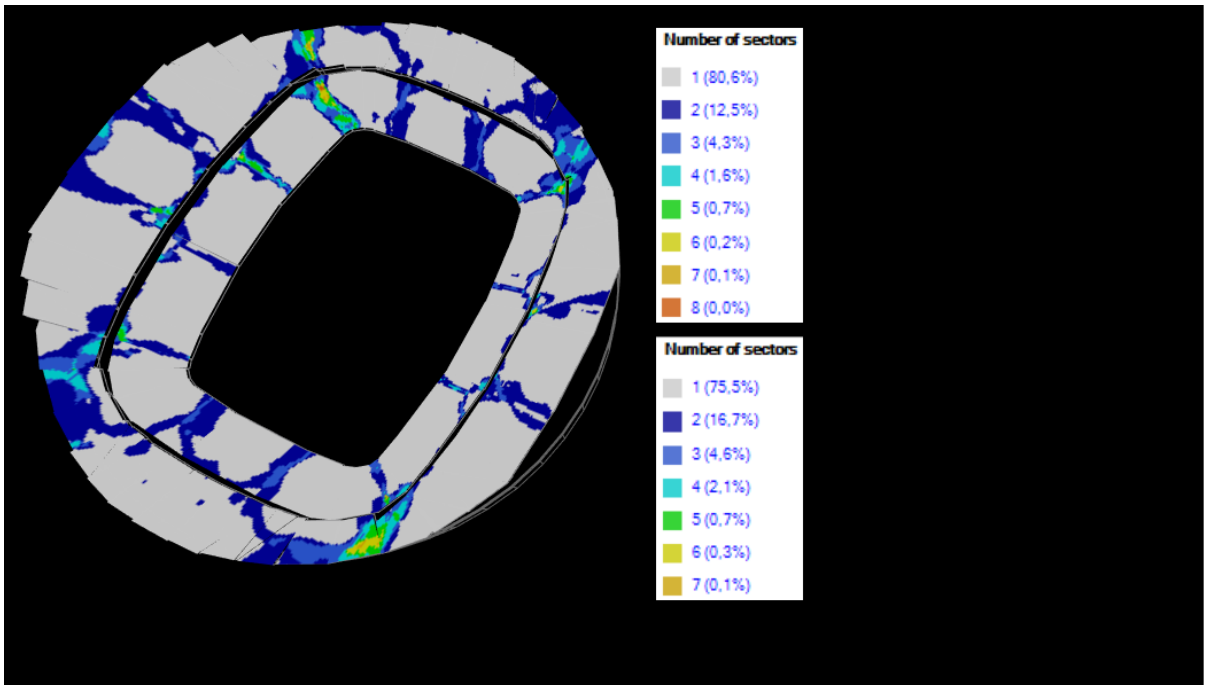


*Figure 5.8 - Final Solution iBwave LTE Overlapping Zones output map obtained using the 2600 MHz band.*

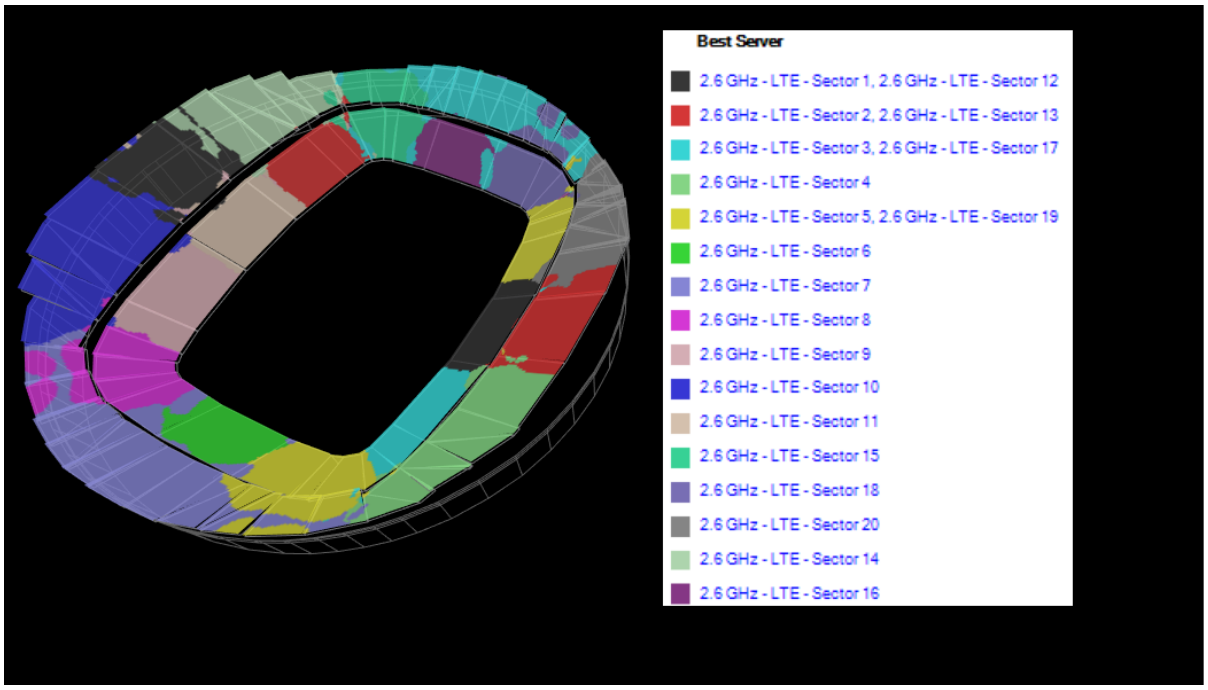


*Figure 5.9 - Final Solution iBwave Best Server output map obtained using the 2600 MHz band.*

# Chapter 6

# Future LTE installations

When planning an LTE installation of this dimension, a considerable investment needs to be made. The total cost is based on the establishment of the technical room, the connection to power and to the backbone network, the base station and RF equipment and all the cables involved. This chapter was inspired in [Flob18] and showed how the designing had as its main priority a scalable solution and the best for as long as possible, with the minimum equipment.

## 6.1 Financial and Physical Limitations

The BBUs cannot support an unlimited number of antennas and, since for each antenna are required 6 RRUs, the weight at the rooftop will be increased with the addition of more antennas. In the case of additional BBUs being required, additional cabinets and power infrastructure will be required escalating the costs.

The use of mobile data applications and services functions is within a set of constraints, established in the subchapter 4.2 and the user demand for mobile data traffic was generalized for the current year. This estimation was considered when calculating the number of sectors and, consequently, the number of antennas. Table 6.1 presents a comparison with the prices and the weights of the different antennas tested in chapter 5.

*Table 6.1 - Approximate Value and Net Weight of the antennas used in the simulations of chapter 5 (prices extracted from [Aliba19] and [Solid19]).*

| Equipment | Brand | Model | Net Weight (kg) | Approximate Value (€) |
|---|---|---|---|---|
| Antenna | Commscope | CNPLX3055F | 37 | 800 |
| Antenna | JMA | XGU-FRO-130 | 8.66 | 1150 |
| Antenna | Commscope | CMAX-3030S-D-V53 | 18 | 2321 |
| Antenna | Commscope | CMAX-DMH60-43-V53 | 1.6 | 522 |

*Table 6.2 - Total weight and price of each simulation (based on Table 6.1 and Annex A information).*

| Simulation | CommScope CNPLX3055F (Quantity) | Another Antenna Model (Quantity) | Total Weight (kg) | Total Price (€) |
|---|---|---|---|---|
| 1 | 20 | 0 | 740 | 16000 |
| 2 | 16 | 4 | 598.4 | 14888 |
| 3 | 16 | 4 | 626.64 | 17400 |
| 4 | 16 | 4 | 598.4 | 14888 |
| Final | 18 | 2 | 702 | 19042 |

The total cost of the chosen antennas' solution is presented in Table 6.2, and the weight is approximately 702 kg distributed along the whole rooftop. When comparing to other simulations, the chosen final solution is the most expensive and the second heaviest. However, it was the only simulation that returned very similar MADR average values in both levels of the stadium (Figure 5.5), when using the 1800 MHz band. And also, an average MADR value higher than 100 Mbps for both levels when using the 2600 MHz band (Figure 5.4). Simulation 4 presents better results than the final solution mainly in sector 2 and 12, using the 2600 MHz band. Yet, in peak situations like the half-time, the final solution LTE network will provide a higher QoE for the users, as explained before in chapter 5.

## 6.2 Forecasting Future Demand

Designing the dedicated 4G solution involving the minimum equipment possible is the ideal scenario. However, the famous Portuguese quote "cheap turns expensive"; applies perfectly to this situation and so building an expandable and lasting network installation will be the best option, reducing the total project costs considerably. The capacity gain going from a 24 sector solution to a final 40 sector solution is considerable but will not be enough for many more years. According to [EricFut16] in Western Europe, due to high penetration in high-end user devices and high-quality LTE networks, complemented with affordable packages of large data volumes, leads to higher data usage per subscription. Considering that mobile data usage is evolving to more data rate demanding categories, it was considered important to present an estimation for how long this solution would be sufficient. In order to do that, two mobile data forecasts were applied.

By combining estimations of annual traffic growth, bandwidth demand of historic traffic data and estimations of LTE penetration rate, two forecasting cases are presented. For each case, a capacity over time was estimated, allowing to calculate the number of necessary sectors.

### 6.2.1 Case 1 – Mobile Traffic by application category evolution 2017-2023

The first forecast was a prediction made based on data collected from the 2017 sports event occurred in Hungary, Figure 1.3. An annual percentage forecasted by Ericsson [EricMT17], presented in Figure 2.4, was applied for those past values collected for mobile traffic category resulting in Figure 6.1. This prediction values were chosen for their complete information, where all application categories are represented. Although there is a more recent prediction, it lacks complete information, only video and social networking were evaluated [Eric19].

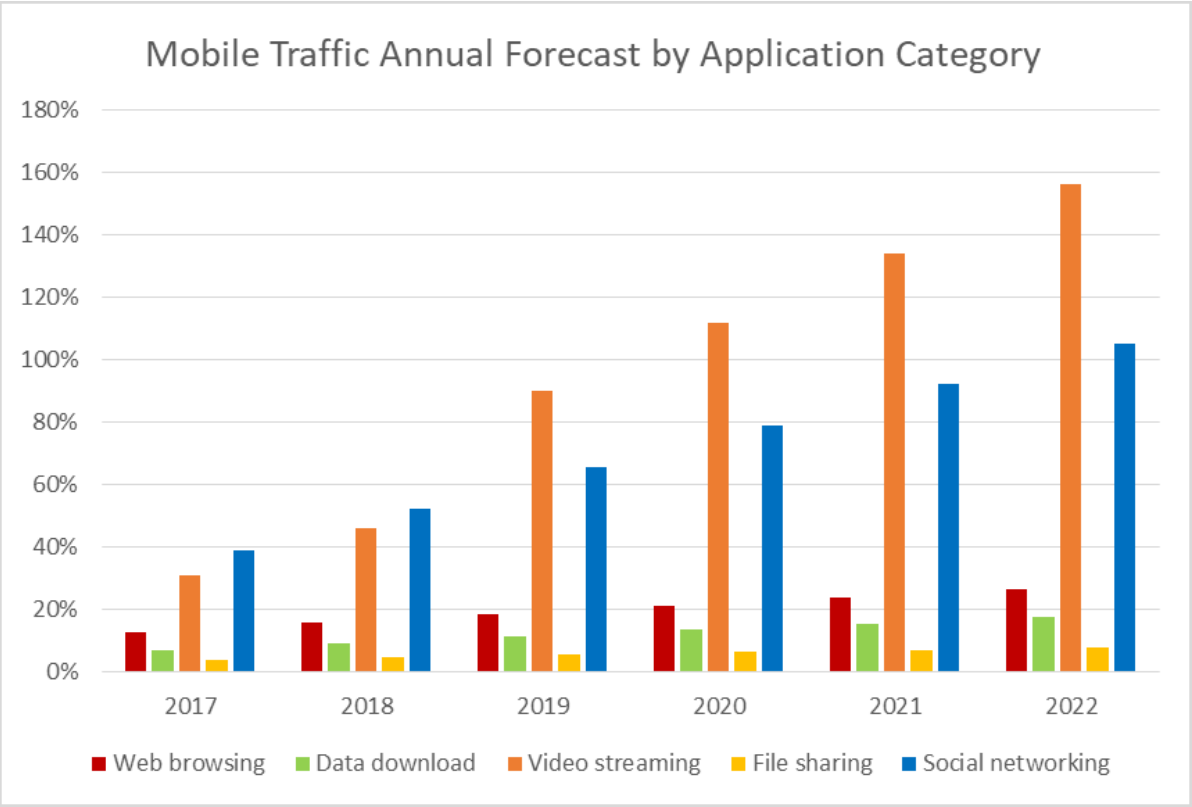


*Figure 6.1 - Mobile Traffic annual forecast by application category.*

*Table 6.3 - Annual forecast for Mobile Traffic by application category (based on Figure 1.3 and Figure 2.4 annual growth).*

| Application Category (%) | 2017 | 2018 | 2019 | 2020 | 2021 | 2022 |
|---|---|---|---|---|---|---|
| **Web browsing** | 13,0% | 15,7% | 18,5% | 21,2% | 23,9% | 26,7% |
| **Data download** | 7,0% | 9,2% | 11,3% | 13,5% | 15,7% | 17,9% |
| **Video streaming** | 31,0% | 45,9% | 89,9% | 111,9% | 134,0% | 156,0% |
| **File sharing** | 4,0% | 4,8% | 5,6% | 6,4% | 7,2% | 8,0% |
| **Social networking** | 39,0% | 52,3% | 65,5% | 78,8% | 92,0% | 105,3% |

In 2017, LTE technology became the most widely used wireless cellular technology worldwide achieving more than 35 percent market share. However, the penetration rate for this technology was not equal in all countries. Knowing that in the current year 2019 the 4G penetration percentage rate in Portugal is 70%, in 2018 was 59% and, according to [Eric19] by the end of 2024, 5G is expected to account for around 40% of mobile subscriptions. By analysing the graph for mobile subscriptions by region and technology, 55% of mobile subscriptions for 4G was assumed for 2024.

Combining all the values, a forecast for LTE penetration rate was obtained through the function poly2sim of MATLAB. The result was transposed to excel in order to obtain a clear graph of the evolution, Figure

6.2.

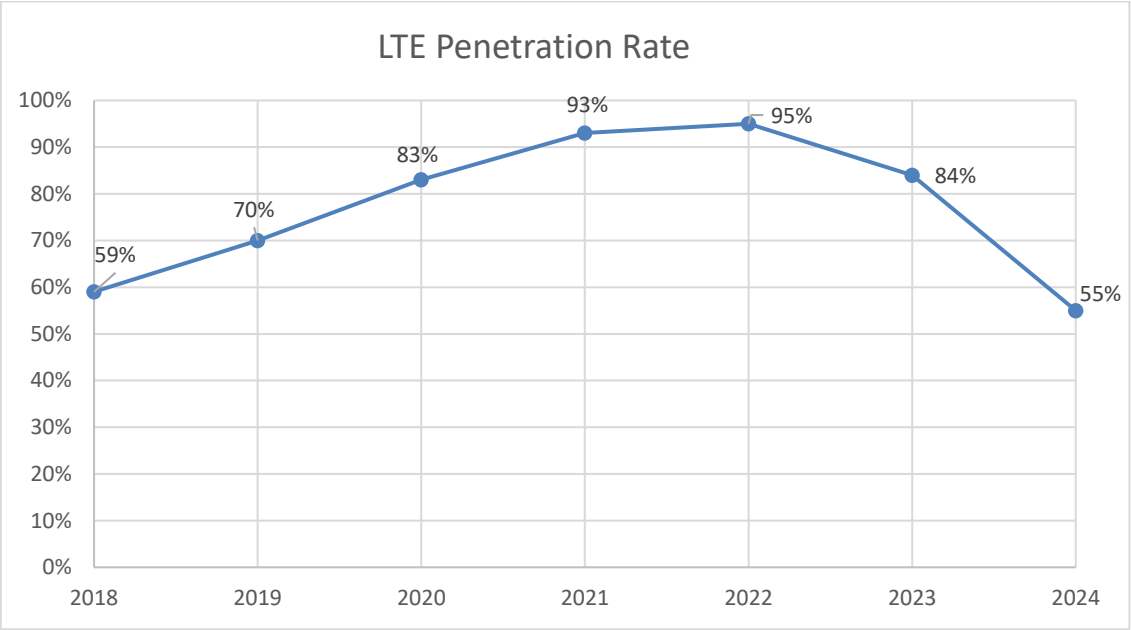


*Figure 6.2 - LTE penetration rate forecast.*

Gathering both forecasts presented in Figure 6.1 and Figure 6.2, the number of sectors were calculated as explained in chapter 4. The throughput per service was obtained, using the expression:

$$Throughput_{year} = Throughput_{2018} \cdot (1 + percentage_{service}) + Throughput_{newsubscriptions} \quad (6.1)$$

Where:

- $Throughput_{year}$ is the throughput per service for the year to predict the number of necessary sectors;
- $Throughput_{2018}$ is the throughput calculated through the expression (4.3) using the LTE penetration rate presented in Figure 6.2 for the year 2018;
- $percentage_{service}$ is the corresponding percentage forecasted - Figure 6.1, for the year to predict;
- $Throughput_{newsubscriptions}$ is the throughput calculated in the expression (6.2).

$$Throughput_{newsubscriptions} = \left(LTE_{subscribersyear} - LTE_{subscribers2018}\right) \cdot \frac{Connection_{duration}}{1000} \cdot \left(1 - \frac{Blocking}{100}\right) \cdot \frac{data_{rate}}{1000} \cdot \frac{Tx_{delay}}{duty_{cycle}} \quad (6.2)$$

Where:

- $LTE_{subscribersyear}$ is the number of LTE subscribers per operator in the year to predict based on the forecasted percentage;
- $LTE_{subscribers2018}$ is the number of LTE subscribers per operator in the year 2018;

- $Connection_{duration}$ is the duration of the connection in mErl/user;
- $Blocking_{rate}$ is the desired percentage of blocking per service type;
- $data_{rate}$ as the name indicates is the data rate per service type in kbps;
- $Tx_{delay}$ is the delay between consecutive data transmissions (Tx);
- $duty_{cycle}$ represents the duty cycle and is always 0.1, as in chapter 4.

After obtaining the throughput per service ($Throughput_{year}$), a total throughput ($Throughput_{total}$) was calculated, adding the estimated throughputs for all services. At least, the number of sectors was calculated using the expression (4.4) with the same $datarate_{average}$ value estimated in chapter 4, resulting in Table 6.4. The forecasting was done only until 2022 due to the big entrance of the 5th Generation expected for that year.

*Table 6.4 - Number of sectors necessary in order to guarantee a good QoE considering case 1.*

| 2020 | 2021 | 2022 |
|---|---|---|
| 34 sectors | 38 sectors | 40 sectors |

### 6.2.2 Case 2 – Video Traffic Growth

The second forecast was predicted using the interactive web application of Ericsson [EricMV19] that contains historical as well as forecast data on mobile data traffic.

Besides the expected growth of mobile traffic, the traffic is evolving to data-intensive applications like video, as shown in Figure 1.2 and Figure 1.3. Counting as video traffic appears the use of embedded video in social media and web pages. This type of traffic continues to grow, increasing upstream data usage on events. For this reason, a particular relevance was given to video traffic, and applications like e-mail and audio streaming, which were not very significant in sports events, were despised. So, from the interactive application resulted a graphic for each year, Figure 6.3, Figure 6.4 and Figure 6.5.

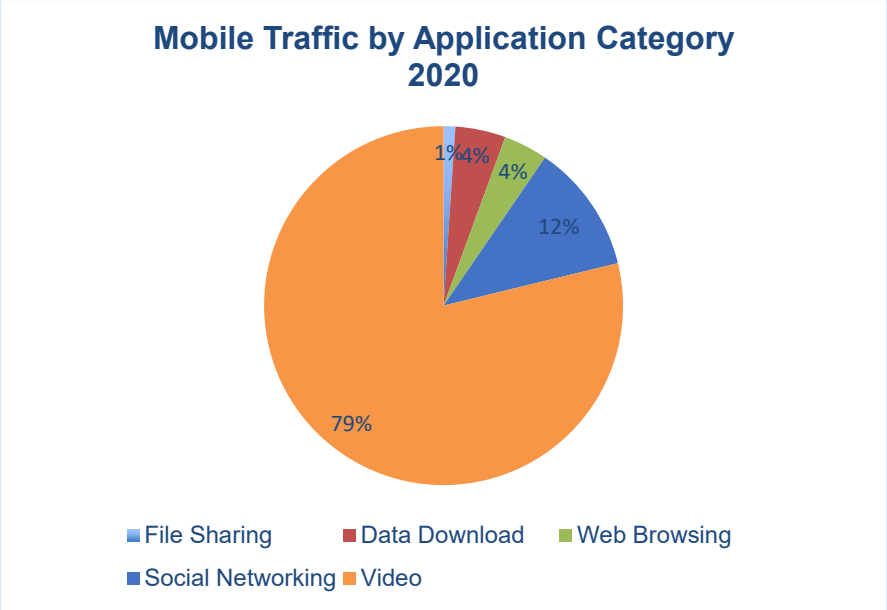


*Figure 6.3 - Video Traffic growth forecasted for 2020 [EricMV19].*

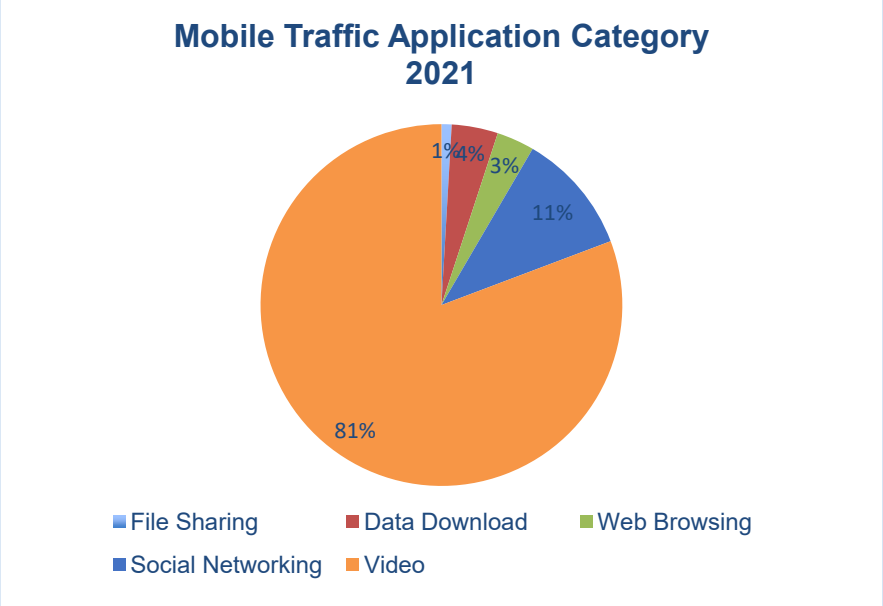


*Figure 6.4 - Video Traffic growth forecasted for 2021 [EricMV19].*

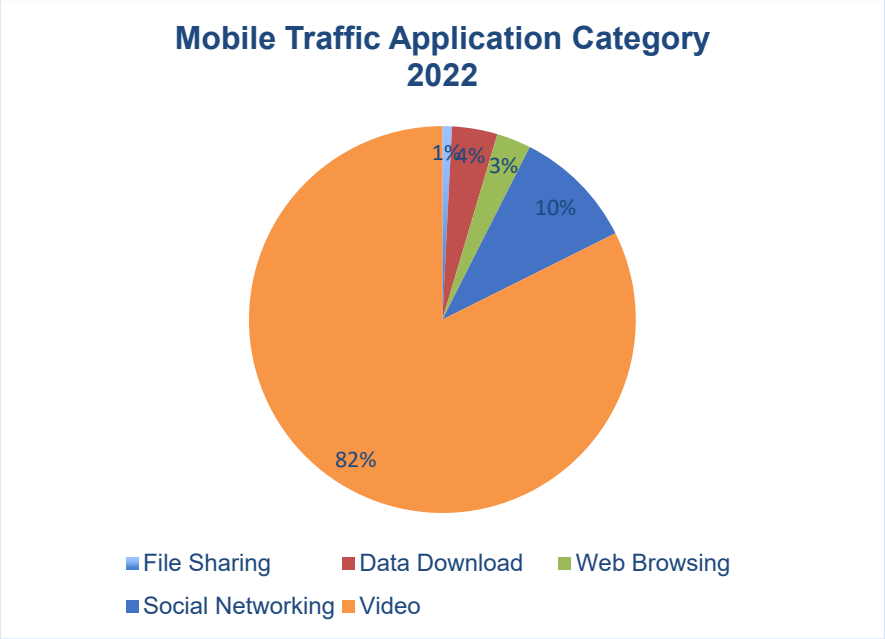


*Figure 6.5 – Video Traffic growth forecasted for 2022 [EricMV19].*

The throughput per service was calculated multiplying the result from the expression (4.3) per $1 + percentage_{service}$, being the $percentage_{service}$ a parameter extracted from Figure 6.3, Figure 6.4 and Figure 6.5 for the year predicted. The $Throughput_{total}$ was calculated, adding the throughputs for all services after applying the percentage forecasted before. At last, the number of sectors was calculated through the expression (4.4), resulting in Table 6.5. For the same reason, explained before the forecasting was done only until 2022.

*Table 6.5 - Number of sectors necessary in order to guarantee a good QoE considering case 2.*

| 2020 | 2021 | 2022 |
|---|---|---|
| 46 sectors | 50 sectors | 51 sectors |

The increase in the number of sectors estimated, considering both the first and the second case, is mostly because the percentage evolution considered is based on an outdoor network characteristic. And not in the specific type of mobile traffic collected in stadium environments for sports events.

Considering the 4G technology using three layers, it is possible to reach 60 sectors for data traffic with the position chosen for the antennas presented in Figure 3.8. 40 sectors with the two layers 1800 and 2600 band and 20 sectors in the 800 band. Adding more sectors will require an increase in the equipment and so, in the weight applied to the rooftop. The design would have to be adjusted to these changes.

# Chapter 7

# Conclusions

The present chapter finalizes this work, summing up the main conclusions per chapter and pointing out aspects that could be considered in future work.

The primary objective of this dissertation was to find an optimal 4G network solution for stadium José Alvalade, placed in Lisbon. This decision should seek to provide good QoE for users in peak situations (game days) and should be designed to be the best for many years since it implies a significant investment. Taking advantage of the site survey made and the blueprints of the stadium, it was possible to obtain the 3D venue model and so, simulate the behaviour of the selected antennas in different positions of the stadium footbridges. In short, this report intended to present all the theoretical thinking behind the decisions made and to show the distinct scenarios simulated.

In the first chapter, a description of the nowadays profile of data traffic consumption in sports events is presented. Followed by an explanation about how challenging it is to meet the user expectations and showing that the problem is real through test results obtained when visiting the case study stadium on a game day.

Chapter 2 provides a theoretical background on LTE's radio interface, coverage and capacity aspects. It was possible to conclude that proper QoE parameters depend on SINR since a reduction on this parameter leads to a sharp reduction on the achievable data rates, which leads to a reduction of the channel capacity. In a stadium scenario, limiting the cell coverage footprint by using highly directional antennas is one of the most important practises to avoid interference and, consequently, achieve higher values of SINR. Moreover, some information about performance parameters were present, mostly focusing on the services and applications QoS Class Identifiers (QCIs) and QoE ways of measurement. Depending on the QCI some services are prioritized over others. For example, in events situations, voice is always prioritized over any data service. Also described in this chapter is a brief state of the art.

Chapter 3 presents a description of the first two rules that need to be followed in order to achieve an optimum design: the site survey and the 3D modelling. After the site survey, it was possible to conclude that in terms of access for future maintenance and a question of radio efficiency, the antennas need to be placed on the rooftop footbridges. The important decision to mount the corner antennas in the green footbridge was made and explained, followed by the representation of the antennas position and the respective configuration, assumed for the final solution. In order to increase capacity, the chosen operating frequencies were the 1800 and 2600 LTE band. Based on the lower tier shape and the number of seatings per sector coverage area, it was concluded that the most suitable antenna for covering the first ring should have an almost squared radiation pattern. However, these allowances were not confirmed for the upper tier and so, having in mind that logically each sector should cover more or less the same number of users another antenna model was considered for occupying the positions behind the beacons. Before the antennas, basic infrastructure needs to guarantee energy, transmission and RF. The RF equipment used for the LTE installation is divided by twelve installation points, and two different installation solutions were presented. One considering only one operator and the other considering the three Mobile Network Operators (MNOs). All the constituents were described, and the choices justified. The connection between the technical rooms' equipment and the radio equipment were established using optical fiber cables, and the radio units are connected to the antennas using coaxial cables. Considering only one operator, the use of directional combiners revealed to be important since it is not common to find a radio that works in both 1800 and 2600 band combination. To finish, a brief

explanation about the supplying power system was given.

Chapter 4 starts by providing a mathematical explanation of why MIMO needs to be implemented over SISO and how SNR parameter limits the maximum information that can be squeezed in each transmitted symbol. A more complete approach than the one presented in chapter 2, was done for the different main MIMO configurations in LTE. Despite, adding complexity to the system was concluded to be essential since it provides significant improvements in performance and spectral efficiency. It has been proved that 4x4 MIMO allows more data to be transferred at the same time, meaning faster wireless download and upload speeds. This can misguide to the idea of “the more MIMO, the better”. However, only a few smartphone models present the capabilities to take full advantage of this type of MIMO configuration and the associated high modulation schemes. If 4x4 MIMO has been considered the users with this type of smartphone, will occupy a big part of the band “stealing” from the other ones. The necessary theoretical number of sectors to satisfy the LTE subscribers were obtained based on the calculation method presented in the [Zava17] book. The distribution of data traffic during the busy-hour per service type was adapted based on real stadium experience, being more demanding and realistic. The average data rate for the video application category was limited to 2000 kbps since it is the limitation of quality introduced by web applications. A theoretical approach of the existing load balancing techniques was presented, followed by an explanation about the chosen one. For the LTE capacity dimensioning, the number of PRBs, needed to support each service type connection, was calculated. The calculations depended on the SINR range corresponding to each user seating area. Lastly, a theoretical explanation was given about the performance optimization technique, carrier aggregation.

Chapter 5 begins with a description of the software license capabilities. Being a trial license had limitations and, although it was possible to generate the desired output maps, the option of creating automated project reports gathering all the conclusions was not available. The output maps functionalities were succinctly described, finishing the first part of the chapter. The second part consisted of analysing the most relevant simulations and describing the comparisons made until reaching the final solution. The first comparison made was using antennas, for the corner antennas positions, a model with a wider vertical beamwidth. Two different antenna models were compared and despite, the presented results not being the best the behaviour of the CommScope CMAX-DMH60-43-V53 model antenna was interesting for those positions. So, if the software license were still active, a new simulation would be made, using the final solution configuration but replacing the corner antennas by the CommScope CMAX-DMH60-43-V53. With 46 dBm power in other to avoid increasing interference by overlapping sectors. This CommScope antenna model support 4x4 MIMO. Another simulation that resulted in intriguing output maps was simulation 4. However, it was concluded that even though the values of the output maps were much better, it does not mean high achievable data rates in reality. Since the covered area have more seats which means more data traffic, more resources (PRB) utilizations and more people sharing the capacity. When comparing all the simulations, it was concluded that the front-to-back ratio parameter should present high values. Due to the stadium rooftop being made of a material that blocks the signal making it impossible for the signal to pass through it and so reflecting the signal to the seating area, creating interference.

Chapter 6 initiate by announcing the physical limitations of the BBUs in terms of number of RRUs supported. So consequently, the necessity of controlling the number of antennas, not only at a financial level (quantity of antennas and BBUs) but also having in mind the physical weight supported by the rooftop. For each antenna, 6 RRUs are used for the LTE technology. Since the antennas are the most differing factor in terms of total solution cost, weight and efficiency of the solution, a comparison between the models used for the simulations were presented. It was possible to conclude, that it was neither the cheapest nor the lightest solution but was the one that presented the most balanced output map results for both stadium levels. It is important, to refer that even though the solution is not cheapest, in the long run, the savings will outweigh the initial investment. So, the longer the solution is reliable, the better. For that reason, two different forecastings were elaborated for the future mobile traffic demand and the respective estimated expiration date of the solution was presented. Finally, it was predicted that considering the first forecasting, the solution was valid for all the years tested. The second solution was never valid. The increase in the number of sectors estimated, from the first case to the second, is a result of the use of an outdoor network profile, not corresponding to the average values of data traffic in indoor network.

Regarding future work, since the time to use the software was very short, a more exhaustive study could be made simulating other types of antennas. For example, simulations could be oriented for using antennas ready to support 4x4 MIMO. With that different approach, the work will be more future-ready. However, efficiency will depend on the evolution of smartphones characteristics. Another topic which could be addressed as future work is the introduction of LTE-Broadcast (LTE-B) mechanisms. As described in [Eric19], using the Multipedia Broadcast Multicast Service-operation-on-Demand (MooD) it is possible to activate and deactivate LTE-B depending on the number of devices streaming the same video in a specific area and when the traffic level reaches the threshold zone. When activated, the traffic is carried to capable UE, improving the network efficiency since less capacity is used to carry traffic. At last, the development of a 5G indoor solution. Accordingly to [Eric18], the combination of 5G NR with LTE, will not be possible since the actual DAS solution is operating frequency limited to bands below 3 GHz. The high bands are particularly effective in LoS deployments, so an indoor solution based on milimiter wave (mmWave) small cells might be an exciting evolution for this work.

# References


[Aliba19] Alibaba, https://m.alibaba.com/product/62116641999/Commscope-CNLPX3055F-2-port-stadium-sector.html. (Accessed on September 2019).

[Alme13] Almeida, D., *Inter-Cell Interference Impact on LTE Performance in Urban Scenarios*, M. Sc. Thesis, Instituto Superior Técnico, Lisbon, Portugal, Oct. 2013.

[Amon11] Amon, C., *LTE: The Road Ahead,* page 3 of 4, https://www.mwee.com/content/lte-road-ahead/page/0/2, Qualcomm, Mar. 2011.

[ANAC16] ANACOM, *Information on multi-band spectrum auction (3)*, https://www.anacom.pt/render.jsp?contentId=1105917, Feb. 2016.

[Anza14] Anzaldo, D., *LTE-Advanced Release-12 Shapes new eNodeB Transmitter Architecture: Part 1, Technology Evolution*, Application Note 6062, Maximum Integrated, 2014.

[Artiza19] Artiza Networks, http://www.artizanetworks.com/resources/tutorials/cran.html, LTE Tutorials. (Accessed on May 2019).

[Basil17] Basilashvili, G., *Study of Spectral Efficiency for LTE Network*, American Scientific Research Journal for Engineering, Technology, and Sciences (ASRJETS) (2017) Volume 29, No 1, pp 21-32.

[Bryd13] Brydon, A., *LTE MIMO theory and practise*, Technical Report, Unwired Insight, Cambridgeshire, UK, 2013 (http://www.unwiredinsight.com/2013/lte-mimo).

[CaAn19] Carolina P. Lopes and António L. Topa, *Design and Optimization for Mobile Networks in Stadium Environments*, EIEC2019, XIII Iberian Meeting on Computacional Electromagnetics, Santander, Spain, October 15-18, 2019.

[Cham15] Chambers, D., *Wembley Stadium Tour: Deep inside EE´s largest DAS Deployment,* THINKSmallCell, Sep. 2015.

[Corr13] Correia, L.M., *Mobile Communications Systems – Lecture Notes,* Instituto Superior Técnico, Lisbon, Portugal, Fev. 2013.

[Cox12] Cox, C*., An Introduction to LTE: LTE, LTE-Advanced, SAE and 4G Mobile Communications*, John Wiley & Sons, Chichester, United Kingdom, March 2012.

[Data13] DATAFLOQ, *Mobile Data Traffic Explosion: Explore IoT, 5G, & VR Opportunities*, https://datafloq.com/read/mobile-data-traffic-explosion-explore-iot-5g-vr/4095, Dec. 2013. (Accessed on November 2018).

[Eric15] Ericsson, *Inter-Frequency Load Balancing,* https://dokumen.tips/documents/inter-frequency-load-balancing.html, Internal Presentation, Dec. 2015. (Accessed on June 2019).

[Eric17] Ericsson, *Enhancing the event experience,* https://www.ericsson.com/en/mobility-

report/reports/november-2017/enhancing-the-event-experience, Nov. 2017. (Accessed on January 2019).

[Eric18] Ericsson, *The advantages of combining 5G NR with LTE,* https://www.ericsson.com/en/ericsson-technology-review/archive/2018/the-advantages-of-combining-5g-nr-with-lte, Nov.18. (Accessed on October 2019).

[Eric19] Ericsson, *https://www.ericsson.com/en/mobility-report/reports/june-2019*, Jun. 2019. (Accessed on September 2019).

[EricFut16] Ericsson, *Future mobile data usage and traffic growth,* https://www.ericsson.com/en/mobility-report/future-mobile-data-usage-and-traffic-growth. (Accessed on July 2019).

[EricMT17] Ericsson, *Mobile traffic analysis by applications,* https://www.ericsson.com/en/mobility-report/reports/november-2017/mobile-traffic-analysis-by-application. (Accessed on January 2019).

[EricMV19] Ericsson, *Ericsson Mobility Visualizer,* https://www.ericsson.com/en/mobility-report/mobility-visualizer?f=8&ft=2&r=1&t=11,12,13,14,15,16,17&s=4&u=3&y=2018&c=4, based on data from the report published on June 2019. (Accessed on July 2019).

[Estra11] Estrada. P, *MIMO: Why Multiple Antennas Matter,* Cisco Meraki Blog, Feb. 2013 (https://meraki.cisco.com/blog/2011/02/mimo-why-multiple-antennas-matter/).

[Even16] eventbriteBlog, *The Evolution (and Bright Future) of Mobile Phones at Live Events,* https://www.eventbrite.com/blog/the-evolution-and-bright-future-of-mobile-phones-at-live-events-ds00/, Dec. 2016. (Accessed on November 2018).

[Floba18] Flobak, E., *LTE in high capacity locations: A case study of Lerkendal Stadium,* M.Sc. Thesis in Communication Technology, Norwegian University of Science and Technology, Norway, Jan.18.

[Foot15] Football Stadiums, https://www.football-stadiums.co.uk/grounds/portugal/estadio-jose-alvalade/, 2015-2018. (Accessed on May 2019).

[Fuji13] Fujitsu Network Communications, *4G Femtocell Solutions for Stadium Environments*, https://www.fujitsu.com/us/Images/4G-Femtocell-for-Football-Stadiums.pdf, 2013.

[GraKP07] Graham, W. A., Kirkman, C. N. and Paul, *Mobile Radio Network Design in the VHF and UHF Bands: A Practical Approach*, John Wiley & Sons, Chichester, United Kingdom, November 2006.

[Hecht16] Hecht, J., *The Bandwith Bottleneck That Is Throttling The Internet*, https://www.scientificamerican.com/article/the-bandwidth-bottleneck-that-is-throttling-the-internet/, Scientific American, Nature Magazine, Aug. 2016. (Accessed on May 2019).

[Hoff18] Hoffman, C., *What is 4x4 MIMO, and Does My Smartphone Need it?*, https://www.howtogeek.com/394266/what-is-4x4-mimo-and-does-my-smartphone-need-it/,

How-To Geek, Nov.2018. (Accessed on June 2019).

[HoTo09] Holma, H., and Toskala, A., *LTE for UMTS: OFDMA and SC-FDMA Based Radio Access,* John Wiley & Sons, Chichester, United Kingdom, Apr. 2009.

[HoTo11] Holma, H., and Toskala, A., *LTE for UMTS: Evolution to LTE-Advanced*, John Wiley & Sons, Chichester, United Kingdom, Mar. 2011.

[iBwave] iBwave, http://www.ibwave.com/ibwave-design-enterprise. (Accessed on August 2019).

[JEcon18] Jornal Económico Multimédia, *Smartphones: estas são as marcas mais vendidas em Portugal*, https://jornaleconomico.sapo.pt/noticias/smartphones-estes-sao-os-modelos-mais-vendidos-em-portugal-321463, Jun. 2018. (Accessed on April 2019).

[Jevre15] Jevremovic, V., *How to Design Better Wireless Networks for Stadiums*, iBwave Case Study, Sep. 2015.

[Lam16] Lam, W., *Scaling LTE Advanced Beyond Carrier Aggregation; Exploring New Terrains with 4x4 MIMO*, https://technology.ihs.com/580694/scaling-lte-advanced-beyond-carrier-aggregation-exploring-new-terrains-with-4x4-mimo, Market Insight, IHS Markit, Jun. 2016. (Accessed on June 2019).

[Layt17] Layton, S., *How to Decide What Internet Speed You Need*, https://www.nerdwallet.com/blog/utilities/how-to-decide-what-internet-speed-you-need/, Internet Buyer's Guide, NerdWallet, Jan. 2017. (Accessed on May 2019).

[Marg18] Margarido, N., *Os 10 smartphones mais vendidos em Portugal em 2017*, https://www.e-konomista.pt/artigo/smartphones-mais-vendidos-em-portugal/, Ekonomista, Jan. 2018. (Accessed on May 2019).

[Mish04] Mishra, R. A., Fundamentals of Cellular Network Planning and Optimisation: 2G/2.5G/3G… Evolution to 4G, John Wiley & Sons, Chichester, United Kingdom, Apr. 2004.

[MisM14] Mishra, S., Mathur, N., *Load Balancing Optimization in LTE/LTE-A Cellular Networks: A Review*, Article, Amity School of Engineering and Technology, Dec. 2014.

[NSN13] NSN, *High Capacity Mobile Broadband for Mass Events*, White Paper, https://pt.slideshare.net/allabout4g/high-capacity-mobile-broadband-for-mass-events, Oct. 2013.

[Pire15] Pires, J., *LTE Fixed to Mobile Subscribers QoE evaluation,* M.Sc. Thesis, Instituto Superior Técnico, Lisbon, Portugal, Nov. 2015.

[SCF19] Small Cells World Summit 2019, Post-Event Resources, Dense Air Presentation, *4G and 5G: The Densification opportunity*, slide number 5, https://www.smallcells.world/post-event/?utm_medium=email&utm_campaign=Small%20Cell%20World%20Summit%20slides&utm_content=Small%20Cell%20World%20Summit%20slides+CID_0188838ad538dc8cf9f3fdc63b0314f1&utm_source=eshot&utm_term=Download%20Conference%20Report, May. 2019.

[SeTB11] Sesia, S., Toufik, I. and Baker, I., *LTE – The UMTS Long Term Evolution: From Theory to Practice (2nd Edition),* John Wiley & Sons, Chichester, United Kingdom, Agu. 2011.

[Share16] ShareTechnote, http://www.sharetechnote.com/html/FrameStructure_DL.html, Feb. 2016.

[Share17] ShareTechnote, https://www.sharetechnote.com/html/Handbook_LTE_Cell_Reselection.html, Jan. 17. (Accessed on April 2019).

[Shet18] Shetty, A., *Getting to better QoE: The Evolution of Communications Network Performance Assurance*, Accedian Blog, Feb. 2018.

[Solid19] Solid Signal, https://www.solidsignal.com/. (Accessed on September 2019)

[Sport19] Sporting Clube de Portugal Oficial Site, https://www.sporting.pt/pt/bilhetes-e-gamebox/gamebox, Jul. 2018.

[SoLC06] Soldani, D., Li, M. and Cuny, R., *QoS and QOE Management in UMTS Cellular Systems*, John Wiley & Sons, Chichester, United Kingdom, 2006.

[StGWZ10] Stasiak, M., Głąbowski, M., Wiśniewski, A. and Zwierzykowski, P, *Modeling and Dimensioning of Mobile Networks: from GSM to* LTE *(1st Edition),* John Wiley & Sons, Chichester, United Kingdom, Nov. 2010.

[Syed09] Syed, A.B., *Dimensioning of LTE Network3GPP, Description of Models and Tool, Coverage and Capacity Estimation of 3GPP Long Term Evolution radio interface*, M.Sc. Thesis, Helsinki University of Technology, Espoo, Finland, Feb. 2009.

[Tech18] Techplayon, 3GPP Release-15 Cat Types, Throughput, Modulation and Supported UE DL/UL Combinations, *http://www.techplayon.com/3gpp-release-15-ue-category-types-throughput-performance-modulation-and-supported-ue-dl-ul-combinations/*, Jul. 2018. (Accessed on June 2019).

[Techp19] Techopedia, *Hard-Handoff*, *https://www.techopedia.com/definition/7522/hard-handoff*. (Accessed on April 2019).

[Twilio19] Twilio Docs, *Mean Opinion Score (MOS)*, https://www.twilio.com/docs/glossary/what-is-mean-opinion-score-mos. (Accessed on September 2019).

[Wann13] Wannstrom, J., *Carrier Aggregation explained*, https://www.3gpp.org/technologies/keywords-acronyms/101-carrier-aggregation-explained, 3GPP, Jun. 2013. (Accessed on May 2019).

[Wood18] Woodall, M., *What are Mbps and How Many Do I Need*, https://www.reviews.org/internet-service/what-are-mbps/, REVIEWS.org, Jun. 2018. (Accessed on May 2019).

[Yout17] Youtube, *Indroduction to 4G-LTE Air Interface (42890 L4), https://www.youtube.com/watch?v=ayW3knsr-AY,* Mar. 2017. (Accessed on November 2018).

[Zava17] Aragon-Zavala, A., *Indoor Wireless Communications: From Theory to Implementation (1st Edition),* John Wiley & Sons, Chichester, United Kingdom, Aug. 2017.

# Annex A

## Antennas Datasheets

This section presents the important datasheets pages of each antenna mentioned before in the dissertation.

# CNLPX3055F

2-port stadium sector antenna, 2x (790–960, 1710–2170, & 2300–2690 MHz), 50° HPBW. This triband antenna produces rectangular patterns with sharp cutoff for illuminating a section of the crowd. The three bands are internally triplexed, allowing a dual connector interface to be used.

- The antenna includes an internal triplexer for a set of ±45° RF input ports for 2x2 MIMO capabilities

## Electrical Specifications

| Frequency Band, MHz | 790–960 | 1710–2170 | 2300–2690 |
|---|---|---|---|
| Gain, dBi | 11.2 | 11.4 | 11.7 |
| Beamwidth, Horizontal, degrees | 55 | 49 | 47 |
| Beamwidth, Horizontal at 20 dB, degrees | 90 | 81 | 79 |
| Beamwidth, Vertical, degrees | 55.0 | 48.5 | 47.4 |
| Beam Tilt, degrees | 0 | 0 | 0 |
| USLS (First Lobe), dB | 25 | 20 | 22 |
| Front-to-Back Ratio at 180°, dB | 39 | 40 | 38 |
| CPR at Boresight, dB | 20 | 23 | 18 |
| CPR at 3 dB Horizontal Beamwidth, dB | 18 | 15 | 18 |
| Isolation, Cross Polarization, dB | 30 | 30 | 30 |
| Isolation, Inter-band, dB | 30 | 30 | 30 |
| VSWR \| Return Loss, dB | 1.5 \| 14.0 | 1.5 \| 14.0 | 1.5 \| 14.0 |
| PIM, 3rd Order, 2 x 20 W, dBc | -150 | -150 | -150 |
| Input Power per Port, maximum, watts | 100 | 100 | 100 |
| Polarization | ±45° | ±45° | ±45° |
| Impedance | 50 ohm | 50 ohm | 50 ohm |

## Electrical Specifications, BASTA*

| Frequency Band, MHz | 790–960 | 1710–2170 | 2300–2690 |
|---|---|---|---|
| Gain by all Beam Tilts, average, dBi | 10.9 | 11.4 | 11.4 |
| Gain by all Beam Tilts Tolerance, dB | ±0.7 | ±0.9 | ±0.9 |
| Beamwidth, Horizontal Tolerance, degrees | ±4 | ±5 | ±4.3 |
| Beamwidth, Vertical Tolerance, degrees | ±4.3 | ±5.3 | ±4.2 |
| USLS, beampeak to 20° above beampeak, dB | 25 | 15 | 16 |
| Front-to-Back Total Power at 180° ± 30°, dB | 32 | 34 | 34 |
| CPR at Boresight, dB | 20 | 19 | 20 |

* CommScope® supports NGMN recommendations on Base Station Antenna Standards (BASTA). To learn more about the benefits of BASTA, download the whitepaper Time to Raise the Bar on BSAs.

## General Specifications





*Figure A.1 - Datasheet 1 (Page 1) – Datasheet of the especially designed for stadiums CommScope antenna, used in all simulations.*

# CNLPX3055F

| | |
|---|---|
| **Operating Frequency Band** | 1710 – 2170 MHz \| 2300 – 2690 MHz \| 790 – 960 MHz |
| **Antenna Type** | Sector |
| **Band** | Multiband |
| **Performance Note** | Outdoor usage |

## Mechanical Specifications

| | |
|---|---|
| **RF Connector Quantity, total** | 2 |
| **RF Connector Interface** | 7-16 DIN Female |
| **Grounding Type** | RF connector inner conductor and body grounded to reflector and mounting bracket |
| **Radiator Material** | Brass \| Low loss circuit board |
| **Radome Material** | Fiberglass, UV resistant |
| **Reflector Material** | Aluminum |
| **RF Connector Location** | Rear \| Side |
| **RF Connector Quantity, diplexed low and high bands** | 2 |
| **Wind Speed, maximum** | 160 km/h \| 99 mph |

## Dimensions

| | |
|---|---|
| **Length** | 1354.0 mm \| 53.3 in |
| **Width** | 853.0 mm \| 33.6 in |
| **Depth** | 210.0 mm \| 8.3 in |
| **Net Weight, without mounting kit** | 37.0 kg \| 81.6 lb |

## Packed Dimensions

| | |
|---|---|
| **Length** | 1464.0 mm \| 57.6 in |
| **Width** | 990.0 mm \| 39.0 in |
| **Depth** | 411.0 mm \| 16.2 in |
| **Shipping Weight** | 55.0 kg \| 121.3 lb |

## Regulatory Compliance/Certifications

| **Agency** | **Classification** |
|---|---|
| RoHS 2011/65/EU | Compliant by Exemption |
| ISO 9001:2015 | Designed, manufactured and/or distributed under this quality management system |
| China RoHS SJ/T 11364-2014 | Above Maximum Concentration Value (MCV) |
| CE | Compliant with the relevant CE product directives |





*Figure A.2 - Datasheet 1 (Page 2) – Datasheet of the especially designed for stadiums CommScope antenna, used in all simulations.*

# CMAX-DMH60-43-V53

Cell-Max™ Low PIM Directional High Capacity Venue MIMO Antenna, 1690–2700 MHz, 60°, 4x4 MIMO, 4.3-10

## Electrical Specifications

| Frequency Band, MHz | 1690–2170 | 2200–2700 |
|---|---|---|
| Gain, dBi | 7.7 | 8.3 |
| Beamwidth, Horizontal, degrees | 68 | 62 |
| Beamwidth, Vertical, degrees | 66.0 | 62.0 |
| Front-to-Back Ratio at 180°, dB | 30 | 30 |
| CPR at Boresight, dB | 15 | 15 |
| Isolation, Cross Polarization, dB | 24 | 24 |
| VSWR \| Return Loss, dB | 1.5 \| 14.0 | 1.5 \| 14.0 |
| PIM, 3rd Order, 2 x 20 W, dBc | -153 | -153 |
| Input Power per Port, maximum, watts | 50 | 50 |
| Polarization | ±45° | ±45° |
| Impedance | 50 ohm | 50 ohm |

## Product Classification

| | |
|---|---|
| **Brand** | Cell-Max™ |
| **Product Type** | Indoor/outdoor antenna |

## General Specifications

| | |
|---|---|
| **Antenna Type** | Directional |
| **Application** | Indoor \| Outdoor |
| **Includes** | Mounting bracket |
| **Number of Ports, all types** | 4 |
| **Package Quantity** | 1 |
| **Pigtail Cable** | 670-141SXE, plenum rated |

## Mechanical Specifications

| | |
|---|---|
| **Color** | White |
| **Pigtail Length** | 910.0 mm \| 35.8 in |
| **Radome Material** | ABS, UV resistant |
| **RF Connector Interface** | 4.3-10 Male |

## Environmental Specifications





*Figure A.3 - Datasheet 2 (Page 1) – Datasheet of the CommScope antenna used specifically in simulations 2 and 4.*

## CMAX-DMH60-43-V53

| | |
|---|---|
| **Ingress Protection Test Method** | IEC 60529:2001, IP65 |
| **Operating Temperature** | -40 °C to +60 °C (-40 °F to +140 °F) |
| **Relative Humidity** | Up to 100% |
| **Vibration Test Method** | ASTM D4169 \| IEC 60068-2-6 |

### Dimensions

| | |
|---|---|
| **Height** | 100.00 mm \| 3.94 in |
| **Length** | 310.0 mm \| 12.2 in |
| **Width** | 180.0 mm \| 7.1 in |
| **Net Weight** | 1.6 kg \| 3.5 lb |

### Packed Dimensions

| | |
|---|---|
| **Height** | 230.00 mm \| 9.06 in |
| **Length** | 420.0 mm \| 16.5 in |
| **Width** | 400.0 mm \| 15.7 in |
| **Shipping Weight** | 4.8 kg \| 10.6 lb |

### Outline Drawing

### Regulatory Compliance/Certifications

| **Agency** | **Classification** |
|---|---|
| RoHS 2011/65/EU | |





*Figure A.4 - Datasheet 2 (Page 2) – Datasheet of the CommScope antenna used specifically in simulations 2 and 4.*

*Product Specifications*

# XGU-FRO-130

Antenna Systems Group

JMA WIRELESS

X-pol Dual Band Antenna, 698-960/1695-2700 MHz

24", 30° horizontal beamwidth

Fixed electrical tilt

- Fast Roll-Off (FRO) improves intra- and inter-cell SINR
- Separate housing and reflector construction optimizes RF performance while maximizing mechanical strength
- Good passive intermodulation (PIM) performance reduces harmful interference
- Integrated diplexers minimizes cabling costs and improves aesthetics
- Included multi-position stadium bracket accommodates most mounting surfaces
- Suitable for LTE/CDMA/UMTS/GSM

**Includes integrated diplexers**

Reduces mainline cables

Eliminates external tower devices

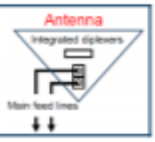


**ELECTRICAL SPECIFICATIONS**

| Frequency band, MHz | 698-745 | 746-896 | 897-960 | 1695-2180 | 2181-2360 | 2496-2700 |
|---|---|---|---|---|---|---|
| Horizontal beamwidth, 3 dB points† (average) | 35° | 30° | 26° | 32° | 26° | 27° |
| Gain, dBi | 10.2 | 10.4 | 10.4 | 11.7 | 12.0 | 11.5 |
| Vertical beamwidth, 3 dB points (average) | 72° | 68° | 60° | 61° | 46° | 47° |
| Azimuth sidelobe suppression, typical, dB | >15 | >11 | >11 | >15 | >15 | >12 |
| VSWR / return loss, dB, maximum | 1.7/11.7 | 1.5/14.0 | 1.7/11.7 | 1.5/14.0 | 1.7/11.7 | 1.7/11.7 |
| Polarization | +/-45° | | | +/-45° | | |
| Electrical down tilt | 0° | | | 0° | | |
| Isolation between ports, dB, minimum | >28 | | | >28 | | |
| Intermodulation (2 x 20 w), IM3, dBc, maximum | -153 | | | -153 | | |
| Impedance, ohms | 50 | | | 50 | | |
| Maximum power per connector, CW (w) | 250 @ 850 MHz | | | 125 @ 1900 MHz | | |

†Beamwidth refers to antenna in orientation shown. Upright installation will reverse H/V beamwidths.





*Figure A.5 - Datasheet 3 (Page 1)– Datasheet of the JMA antenna used specifically in simulation 3.*

*Product Specifications*

# XGU-FRO-130

Antenna Systems Group

JMA WIRELESS

| MECHANICAL SPECIFICATIONS | |
|---|---|
| Dimensions, length/width/depth | 12.6/24.3/7.9 in. (319/616/200 mm) |
| Connector (quantity) type | (2) 7-16 DIN female |
| Connector torque | 220-265 lbf·in (23-30 N-m) |
| Connector location | Back |
| Antenna weight | 14.0 lb (6.36 kg) |
| Bracket weight | 5.0 lb (2.3 kg) |
| Standard bracket kit | P/N 919050 (included) |
| Mechanical down tilt range | +/- 25° lateral (azimuth) and +/- 55° vertical (up/down tilts) |
| Radome material | High strength Luran®, UV stabilized, ASTM D1925 |
| Wind survival | 120 mph (193 km/h) |
| Front wind load @ 100 mph | 52.5 lbf (233.3 N) |
| Equivalent flat plate @ 100 mph | 1.05 sq ft (c=2) |

| ORDER INFORMATION | |
|---|---|
| **MODEL** | **DESCRIPTION** |
| XGU-FRO-130 | 2' X-pol LB/HB 30° HBW, 0°/0° EDT with four DIN connectors |
| XGU-FRO-130-I | 2' X-pol LB/HB 30° HBW, 0°/0° EDT with two DIN connectors and integrated diplexers |
| 919055 | Optional inverted mounting kit for 4.0-10.0 in. OD pole. |
| 91900313 | Optional bracket kit for extended horizontal and vertical tilt ranges. |





*Product Specifications*

XGU-FRO-130

Antenna Systems Group

JMA WIRELESS

*Figure A.6 - Datasheet 3 (Page 2) – Datasheet of the JMA antenna used specifically in simulation 3.*

# CMAX-DM60-CPUSEi53

Cell-Max™ Low PIM Directional High Capacity Venue MIMO Antenna, 698–960 MHz and 1710–2700 MHz, 60°, 8.0 dBi

**OBSOLETE**
**This product was discontinued on: April 15, 2018**

**Replaced By**

| | |
|---|---|
| CMAX-DM60-CPUSEV53 | Cell-Max™ Low PIM Directional High Capacity Venue MIMO Antenna, 698–960 MHz and 1710–2700 MHz, 60°, 8.0 dBi |

## Electrical Specifications

| Frequency Band, MHz | 698–800 | 800–960 | 1695–1880 | 1850–1990 | 1920–2180 | 2200–2700 | 2300–2360 |
|---|---|---|---|---|---|---|---|
| Gain, dBi | 8.5 | 9.2 | 9.3 | 9.6 | 9.8 | 9.2 | 8.9 |
| Beamwidth, Horizontal, degrees | 62 | 59 | 55 | 52 | 55 | 62 | 70 |
| Beamwidth, Vertical, degrees | 62.0 | 58.0 | 55.0 | 54.0 | 55.0 | 59.0 | 65.0 |
| Front-to-Back Total Power at 180° ± 30°, dB | 26 | 26 | 27 | 28 | 29 | 27 | 29 |
| CPR at Boresight, dB | 24 | 24 | 20 | 20 | 20 | 20 | 20 |
| Isolation, Cross Polarization, dB | 30 | 30 | 30 | 30 | 30 | 30 | 30 |
| VSWR \| Return Loss, dB | 1.9 \| 10.1 | 1.9 \| 10.1 | 1.8 \| 10.9 | 1.8 \| 10.9 | 1.8 \| 10.9 | 1.8 \| 10.9 | 1.8 \| 10.9 |
| PIM, 3rd Order, 2 x 20 W, dBc | -153 | -153 | -153 | -153 | -153 | -153 | -153 |
| Input Power per Port, maximum, watts | 200 | 200 | 200 | 200 | 200 | 200 | 200 |
| Polarization | ±45° | ±45° | ±45° | ±45° | ±45° | ±45° | ±45° |
| Impedance | 50 ohm | 50 ohm | 50 ohm | 50 ohm | 50 ohm | 50 ohm | 50 ohm |

## Product Classification

| | |
|---|---|
| **Brand** | Cell-Max™ |
| **Product Type** | Indoor/outdoor antenna |

## General Specifications

| | |
|---|---|
| **Antenna Type** | Directional |
| **Application** | Indoor \| Outdoor |
| **Includes** | Mounting bracket |
| **Number of Ports, all types** | 2 |
| **Package Quantity** | 1 |





*Figure A.7 - Datasheet 4 (Page 1)– Datasheet of the CommScope discontinued model antenna used specifically in simulation 5.*

## CMAX-DM60-CPUSEi53

### Mechanical Specifications

| | |
|---|---|
| **Color** | White |
| **Radome Material** | ABS, UV resistant |
| **RF Connector Interface** | 7-16 DIN Female |
| **Wind Loading, maximum** | 294.0 N @ 216 km/h<br>66.1 lbf @ 216 km/h |
| **Wind Loading, maximum (temporary)** | 294.0 N @ 216 km/h \| 66.1 lbf @ 216 km/h |
| **Wind Speed, maximum** | 216 km/h \| 134 mph |

### Environmental Specifications

| | |
|---|---|
| **Ingress Protection Test Method** | IEC 60529:2001, IP65 |
| **Operating Temperature** | -40 °C to +60 °C (-40 °F to +140 °F) |
| **Relative Humidity** | Up to 100% |
| **Vibration Test Method** | ASTM D4169 \| IEC 60068-2-6 |

### Dimensions

| | |
|---|---|
| **Depth** | 124.5 mm \| 4.9 in |
| **Length** | 299.7 mm \| 11.8 in |
| **Width** | 299.7 mm \| 11.8 in |
| **Net Weight** | 2.9 kg \| 6.4 lb |

### Packed Dimensions

| | |
|---|---|
| **Depth** | 230.0 mm \| 9.1 in |
| **Length** | 520.0 mm \| 20.5 in |
| **Width** | 350.0 mm \| 13.8 in |
| **Shipping Weight** | 7.3 kg \| 16.1 lb |





*Figure A.8 - Datasheet 4 (Page 2)– Datasheet of the CommScope discontinued model antenna used specifically in simulation 5.*

# CMAX-DM60-43-V53

Cell-Max™ Low PIM Directional High Capacity Venue MIMO Antenna, 698–960 MHz and 1710–2700 MHz, 60°, 8.0 dBi

## Electrical Specifications

| Frequency Band, MHz | 698–800 | 800–960 | 1695–1880 | 1850–1990 | 1920–2180 | 2200–2700 | 2300–2360 |
|---|---|---|---|---|---|---|---|
| Gain, dBi | 8.6 | 9.2 | 9.3 | 9.1 | 9.3 | 9.7 | 9.4 |
| Beamwidth, Horizontal, degrees | 60 | 59 | 55 | 54 | 56 | 59 | 61 |
| Beamwidth, Vertical, degrees | 61.0 | 58.0 | 56.0 | 58.0 | 58.0 | 57.0 | 59.0 |
| Front-to-Back Total Power at 180° ± 30°, dB | 24 | 26 | 24 | 26 | 28 | 26 | 28 |
| CPR at Boresight, dB | 24 | 24 | 20 | 20 | 20 | 20 | 20 |
| Isolation, Cross Polarization, dB | 30 | 30 | 30 | 30 | 30 | 30 | 30 |
| VSWR \| Return Loss, dB | 1.5 \| 14.0 | 1.5 \| 14.0 | 1.5 \| 14.0 | 1.5 \| 14.0 | 1.5 \| 14.0 | 1.5 \| 14.0 | 1.5 \| 14.0 |
| PIM, 3rd Order, 2 x 20 W, dBc | -153 | -153 | -153 | -153 | -153 | -153 | -153 |
| Input Power per Port, maximum, watts | 200 | 200 | 200 | 200 | 200 | 200 | 200 |
| Polarization | ±45° | ±45° | ±45° | ±45° | ±45° | ±45° | ±45° |
| Impedance | 50 ohm | 50 ohm | 50 ohm | 50 ohm | 50 ohm | 50 ohm | 50 ohm |

## Product Classification

| | |
|---|---|
| **Brand** | Cell-Max™ |
| **Product Type** | Indoor/outdoor antenna |

## General Specifications

| | |
|---|---|
| **Antenna Type** | Directional |
| **Application** | Indoor \| Outdoor |
| **Includes** | Mounting bracket |
| **Number of Ports, all types** | 2 |
| **Package Quantity** | 1 |

## Mechanical Specifications

| | |
|---|---|
| **Color** | White |
| **Radome Material** | ABS, UV resistant |
| **RF Connector Interface** | 4.3-10 Female |
| **Wind Loading, maximum** | 294.0 N @ 216 km/h \| 66.1 lbf @ 216 km/h |





*Figure A.9 - Datasheet 5 (Page 1)– Datasheet of the replacing CommScope model antenna used specifically in simulation 5.*

## CMAX-DM60-43-V53

| | |
|---|---|
| **Wind Speed, maximum** | 216 km/h \| 134 mph |

### Environmental Specifications

| | |
|---|---|
| **Ingress Protection Test Method** | IEC 60529:2001, IP65 |
| **Operating Temperature** | -40 °C to +60 °C (-40 °F to +140 °F) |
| **Relative Humidity** | Up to 100% |
| **Vibration Test Method** | ASTM D4169 \| IEC 60068-2-6 |

### Dimensions

| | |
|---|---|
| **Depth** | 124.5 mm \| 4.9 in |
| **Length** | 299.7 mm \| 11.8 in |
| **Width** | 299.7 mm \| 11.8 in |
| **Net Weight** | 2.9 kg \| 6.4 lb |

### Packed Dimensions

| | |
|---|---|
| **Depth** | 230.0 mm \| 9.1 in |
| **Length** | 520.0 mm \| 20.5 in |
| **Width** | 350.0 mm \| 13.8 in |
| **Shipping Weight** | 7.3 kg \| 16.1 lb |





*Figure A.10 - Datasheet 5 (Page 2)– Datasheet of the replacing CommScope model antenna used specifically in simulation 5.*

# CMAX-3030S-D-V53

Cell-Max™ Low PIM Directional High Capacity Venue MIMO Antenna, 698–960 MHz and 1710–2700 MHz, 30-Deg,

## Electrical Specifications

| Frequency Band, MHz | 698–800 | 800–960 | 1695–1880 | 1850–1990 | 1920–2180 | 2200–2700 | 2300–2360 |
|---|---|---|---|---|---|---|---|
| Gain, dBi | 13.1 | 13.9 | 12.4 | 13.0 | 13.2 | 14.4 | 14.3 |
| Beamwidth, Horizontal, degrees | 39 | 35 | 39 | 36 | 35 | 29 | 30 |
| Beamwidth, Vertical, degrees | 38.0 | 33.0 | 38.0 | 35.0 | 34.0 | 29.0 | 29.0 |
| Horizontal Sidelobe, dB | 17 | 17 | 17 | 17 | 17 | 17 | 17 |
| Front-to-Back Ratio, Copolarization 180° ± 30°, dB | 28 | 30 | 30 | 30 | 30 | 30 | 30 |
| Isolation, Cross Polarization, dB | 30 | 30 | 30 | 30 | 30 | 30 | 30 |
| VSWR \| Return Loss, dB | 1.5 \| 14.0 | 1.5 \| 14.0 | 1.5 \| 14.0 | 1.5 \| 14.0 | 1.5 \| 14.0 | 1.5 \| 14.0 | 1.5 \| 14.0 |
| PIM, 3rd Order, 2 x 20 W, dBc | -153 | -153 | -153 | -153 | -153 | -153 | -153 |
| Input Power per Port, maximum, watts | 200 | 200 | 200 | 200 | 200 | 200 | 200 |
| Polarization | ±45° | ±45° | ±45° | ±45° | ±45° | ±45° | ±45° |
| Impedance | 50 ohm | 50 ohm | 50 ohm | 50 ohm | 50 ohm | 50 ohm | 50 ohm |

## Product Classification

| | |
|---|---|
| **Brand** | Cell-Max™ |

## General Specifications

| | |
|---|---|
| **Antenna Type** | Directional |
| **Application** | Indoor \| Outdoor |
| **Includes** | Mounting bracket |
| **Number of Ports, all types** | 2 |
| **Package Quantity** | 1 |

## Mechanical Specifications

| | |
|---|---|
| **Color** | White |
| **Radome Material** | Fiberglass, UV resistant |
| **RF Connector Interface** | 7-16 DIN Female |
| **Wind Loading, maximum** | 2128.0 N @ 216 km/h<br>478.4 lbf @ 216 km/h |
| **Wind Loading, maximum (temporary)** | 2128.0 N @ 216 km/h \| 478.4 lbf @ 216 km/h |
| **Wind Speed, maximum** | 216 km/h \| 134 mph |





COMMSCOPE®

*Figure A.11 - Datasheet 6 (Page 1)– Datasheet of the CommScope model antenna used specifically in the final solution simulation.*

## CMAX-3030S-D-V53

### Environmental Specifications

| | |
|---|---|
| **Ingress Protection Test Method** | IEC 60529:2001, IP65 |
| **Operating Temperature** | -40 °C to +60 °C (-40 °F to +140 °F) |
| **Relative Humidity** | Up to 100% |
| **Vibration Test Method** | ASTM D4169 \| IEC 60068-2-6 |

### Dimensions

| | |
|---|---|
| **Depth** | 120.0 mm \| 4.7 in |
| **Length** | 760.0 mm \| 29.9 in |
| **Width** | 760.0 mm \| 29.9 in |
| **Net Weight** | 12.0 kg \| 26.5 lb |
| **Net Weight, with mounting kit** | 18.0 kg \| 39.7 lb |

### Packed Dimensions

| | |
|---|---|
| **Depth** | 218.0 mm \| 8.6 in |
| **Length** | 942.0 mm \| 37.1 in |
| **Width** | 805.0 mm \| 31.7 in |
| **Shipping Weight** | 20.0 kg \| 44.1 lb |

### Outline Drawing

### Regulatory Compliance/Certifications

| **Agency** | **Classification** |
|---|---|
| RoHS 2011/65/EU | |





*Figure A.12 - Datasheet 6 (Page 2)– Datasheet of the CommScope model antenna used specifically in the final solution simulation.*

# Annex B

## Simulations Complement

This section presents additional results for Chapter 5. The configuration taken into account is tabled for each simulation and the position scheme is presented. The output maps that have not been presented before and are considered important are exhibited in this section.

# B1. Simulations General Configuration

*Table B.1 - Configuration considered for the antennas used in simulation 1.*

| Antenna | Sector | Antenna Brand | Antenna Model | Azimuth (degree) | Tilt (degree) | Signal Source Power (dBm) |
|---|---|---|---|---|---|---|
| A1 | 1 | Commscope | CNPLX3055F | 180 | 60 | 49 |
| B2 | 2 | Commscope | CNPLX3055F | 180 | 20 | 49 |
| A3 | 3 | Commscope | CNPLX3055F | 185 | 60 | 49 |
| B4 | 4 | Commscope | CNPLX3055F | 190 | 20 | 49 |
| A5 | 5 | Commscope | CNPLX3055F | 240 | 45 | 49 |
| A6 | 6 | Commscope | CNPLX3055F | 270 | 60 | 49 |
| B7 | 7 | Commscope | CNPLX3055F | 270 | 20 | 49 |
| A8 | 8 | Commscope | CNPLX3055F | 300 | 45 | 49 |
| A9 | 9 | Commscope | CNPLX3055F | 355 | 60 | 49 |
| B10 | 10 | Commscope | CNPLX3055F | 350 | 20 | 49 |
| A11 | 11 | Commscope | CNPLX3055F | 0 | 60 | 49 |
| B12 | 12 | Commscope | CNPLX3055F | 0 | 20 | 49 |
| A13 | 13 | Commscope | CNPLX3055F | 5 | 60 | 49 |
| B14 | 14 | Commscope | CNPLX3055F | 10 | 20 | 49 |
| A15 | 15 | Commscope | CNPLX3055F | 75 | 45 | 49 |
| A16 | 16 | Commscope | CNPLX3055F | 90 | 60 | 49 |
| B17 | 17 | Commscope | CNPLX3055F | 90 | 30 | 49 |
| A18 | 18 | Commscope | CNPLX3055F | 110 | 45 | 49 |
| A19 | 19 | Commscope | CNPLX3055F | 175 | 60 | 49 |
| B20 | 20 | Commscope | CNPLX3055F | 170 | 20 | 49 |

*Table B.2 - Configuration considered for the antennas used in simulation 2.*

| Antenna | Sector | Antenna Brand | Antenna Model | Azimuth (degree) | Tilt (degree) | Signal Source Power (dBm) |
|---|---|---|---|---|---|---|
| A1 | 1 | Commscope | CNPLX3055F | 180 | 60 | 49 |
| B2 | 2 | Commscope | CNPLX3055F | 180 | 20 | 49 |
| A3 | 3 | Commscope | CNPLX3055F | 185 | 60 | 49 |
| B4 | 4 | Commscope | CNPLX3055F | 200 | 20 | 49 |
| A5 | 5 | Commscope | CMAX-DMH60-43-V53 | 220 | 45 | 49 |
| A6 | 6 | Commscope | CNPLX3055F | 270 | 65 | 49 |
| B7 | 7 | Commscope | CNPLX3055F | 270 | 20 | 49 |
| A8 | 8 | Commscope | CMAX-DMH60-43-V53 | 325 | 35 | 49 |
| A9 | 9 | Commscope | CNPLX3055F | 0 | 60 | 49 |
| B10 | 10 | Commscope | CNPLX3055F | 340 | 20 | 49 |
| A11 | 11 | Commscope | CNPLX3055F | 0 | 65 | 49 |
| B12 | 12 | Commscope | CNPLX3055F | 0 | 20 | 49 |
| A13 | 13 | Commscope | CNPLX3055F | 0 | 60 | 49 |
| B14 | 14 | Commscope | CNPLX3055F | 20 | 20 | 49 |
| A15 | 15 | Commscope | CMAX-DMH60-43-V53 | 35 | 45 | 49 |
| A16 | 16 | Commscope | CNPLX3055F | 90 | 60 | 49 |
| B17 | 17 | Commscope | CNPLX3055F | 90 | 30 | 49 |
| A18 | 18 | Commscope | CMAX-DMH60-43-V53 | 150 | 45 | 49 |
| A19 | 19 | Commscope | CNPLX3055F | 175 | 60 | 49 |
| B20 | 20 | Commscope | CNPLX3055F | 160 | 20 | 49 |

*Table B.3 - Configuration considered for the antennas used in simulation 3.*

| Antenna | Sector | Antenna Brand | Antenna Model | Azimuth (degree) | Tilt (degree) | Signal Source Power (dBm) |
|---|---|---|---|---|---|---|
| A1 | 1 | Commscope | CNPLX3055F | 180 | 60 | 46 |
| B2 | 2 | Commscope | CNPLX3055F | 180 | 20 | 49 |
| A3 | 3 | Commscope | CNPLX3055F | 185 | 60 | 46 |
| B4 | 4 | Commscope | CNPLX3055F | 195 | 15 | 49 |
| A5 | 5 | JMA | XGU-FRO-130 | 225 | 45 | 46 |
| A6 | 6 | Commscope | CNPLX3055F | 270 | 60 | 46 |
| B7 | 7 | Commscope | CNPLX3055F | 270 | 10 | 49 |
| A8 | 8 | JMA | XGU-FRO-130 | 310 | 45 | 46 |
| A9 | 9 | Commscope | CNPLX3055F | 355 | 60 | 46 |
| B10 | 10 | Commscope | CNPLX3055F | 350 | 20 | 49 |
| A11 | 11 | Commscope | CNPLX3055F | 0 | 60 | 46 |
| B12 | 12 | Commscope | CNPLX3055F | 0 | 20 | 49 |
| A13 | 13 | Commscope | CNPLX3055F | 5 | 60 | 46 |
| B14 | 14 | Commscope | CNPLX3055F | 5 | 20 | 49 |
| A15 | 15 | JMA | XGU-FRO-130 | 65 | 45 | 46 |
| A16 | 16 | Commscope | CNPLX3055F | 90 | 60 | 46 |
| B17 | 17 | Commscope | CNPLX3055F | 90 | 10 | 49 |
| A18 | 18 | JMA | XGU-FRO-130 | 130 | 45 | 46 |
| A19 | 19 | Commscope | CNPLX3055F | 175 | 60 | 46 |
| B20 | 20 | Commscope | CNPLX3055F | 170 | 15 | 49 |

*Table B.4 - Configuration considered for the antennas used in simulation 4.*

| Antenna | Sector | Antenna Brand | Antenna Model | Azimuth (degree) | Tilt (degree) | Signal Source Power (dBm) |
|---|---|---|---|---|---|---|
| A1 | 1 | Commscope | CNPLX3055F | 180 | 65 | 49 |
| B2 | 2 | Commscope | CMAX-DMH60-43-V53 | 180 | 12 | 49 |
| A3 | 3 | Commscope | CNPLX3055F | 185 | 65 | 46 |
| B4 | 4 | Commscope | CNPLX3055F | 230 | 15 | 49 |
| A5 | 5 | Commscope | CNPLX3055F | 210 | 45 | 49 |
| A6 | 6 | Commscope | CNPLX3055F | 270 | 65 | 49 |
| B7 | 7 | Commscope | CMAX-DMH60-43-V53 | 270 | 15 | 49 |
| A8 | 8 | Commscope | CNPLX3055F | 330 | 45 | 49 |
| A9 | 9 | Commscope | CNPLX3055F | 355 | 65 | 49 |
| B10 | 10 | Commscope | CNPLX3055F | 340 | 15 | 49 |
| A11 | 11 | Commscope | CNPLX3055F | 0 | 65 | 49 |
| B12 | 12 | Commscope | CMAX-DMH60-43-V53 | 0 | 12 | 49 |
| A13 | 13 | Commscope | CNPLX3055F | 10 | 65 | 49 |
| B14 | 14 | Commscope | CNPLX3055F | 25 | 15 | 49 |
| A15 | 15 | Commscope | CNPLX3055F | 30 | 45 | 49 |
| A16 | 16 | Commscope | CNPLX3055F | 90 | 65 | 49 |
| B17 | 17 | Commscope | CMAX-DMH60-43-V53 | 90 | 15 | 49 |
| A18 | 18 | Commscope | CNPLX3055F | 150 | 45 | 46 |
| A19 | 19 | Commscope | CNPLX3055F | 175 | 65 | 49 |
| B20 | 20 | Commscope | CNPLX3055F | 130 | 15 | 49 |

*Table B.5 - Configuration considered for the antennas used in simulation 5.*

| Antenna | Sector | Antenna Brand | Antenna Model | Azimuth (degree) | Tilt (degree) | Signal Source Power (dBm) |
|---|---|---|---|---|---|---|
| A1 | 1 | Commscope | CNPLX3055F | 180 | 60 | 49 |
| B2 | 2 | Commscope | CNPLX3055F | 180 | 20 | 49 |
| A3 | 3 | Commscope | CNPLX3055F | 204 | 60 | 49 |
| B4 | 4 | Commscope | CNPLX3055F | 195 | 20 | 49 |
| A5 | 5 | Commscope | CMAX.DM60-CPUSEi53 | 220 | 45 | 49 |
| A6 | 6 | Commscope | CNPLX3055F | 270 | 60 | 49 |
| B7 | 7 | Commscope | CMAX-DMH60-43-V53 | 270 | 15 | 49 |
| A8 | 8 | Commscope | CMAX.DM60-CPUSEi53 | 320 | 45 | 49 |
| A9 | 9 | Commscope | CNPLX3055F | 340 | 60 | 49 |
| B10 | 10 | Commscope | CNPLX3055F | 355 | 20 | 49 |
| A11 | 11 | Commscope | CNPLX3055F | 0 | 60 | 49 |
| B12 | 12 | Commscope | CNPLX3055F | 0 | 20 | 49 |
| A13 | 13 | Commscope | CNPLX3055F | 15 | 60 | 49 |
| B14 | 14 | Commscope | CNPLX3055F | 20 | 10 | 49 |
| A15 | 15 | Commscope | CMAX.DM60-CPUSEi53 | 40 | 45 | 49 |
| A16 | 16 | Commscope | CNPLX3055F | 90 | 60 | 49 |
| B17 | 17 | Commscope | CMAX-DMH60-43-V53 | 90 | 15 | 49 |
| A18 | 18 | Commscope | CMAX.DM60-CPUSEi53 | 130 | 15 | 49 |
| A19 | 19 | Commscope | CNPLX3055F | 145 | 60 | 49 |
| B20 | 20 | Commscope | CNPLX3055F | 160 | 20 | 49 |

# B2. Antenna Position Scheme for all simulations

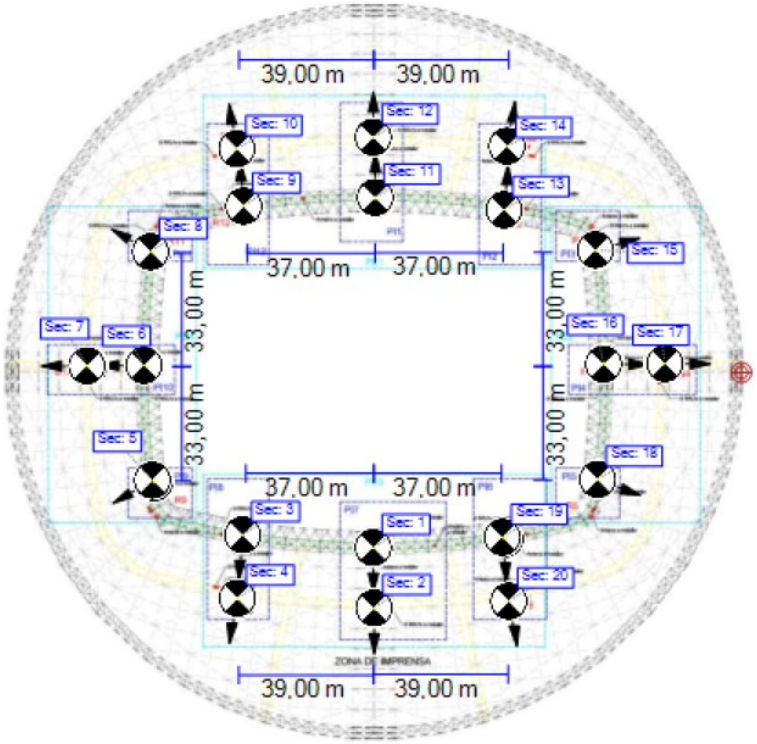


*Figure B.1 - Antenna position scheme extracted from the software for simulation 1, 3 and 5.*

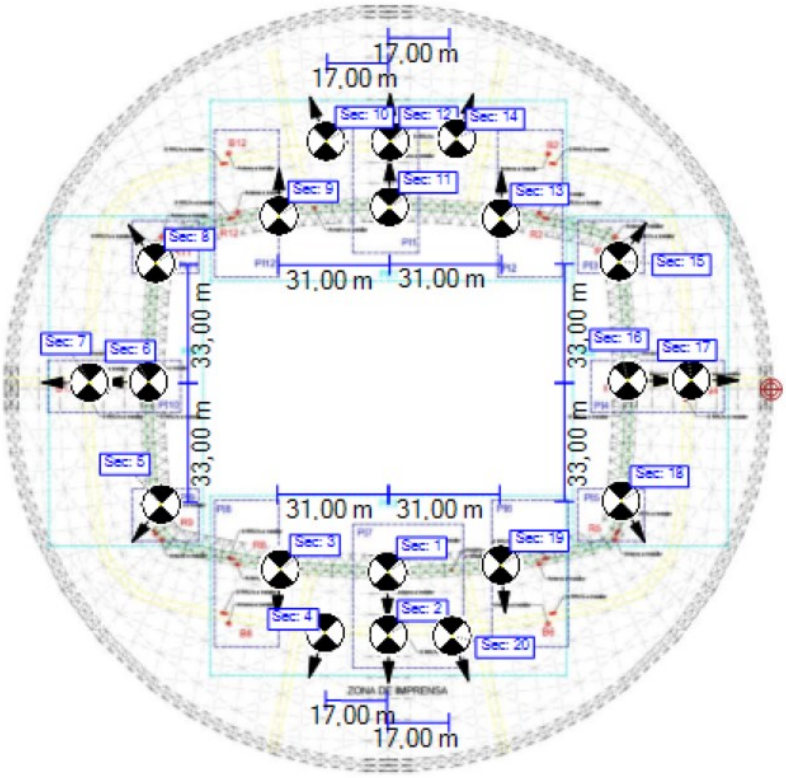


*Figure B.2 - Antenna position scheme extracted from the software for simulation 2.*

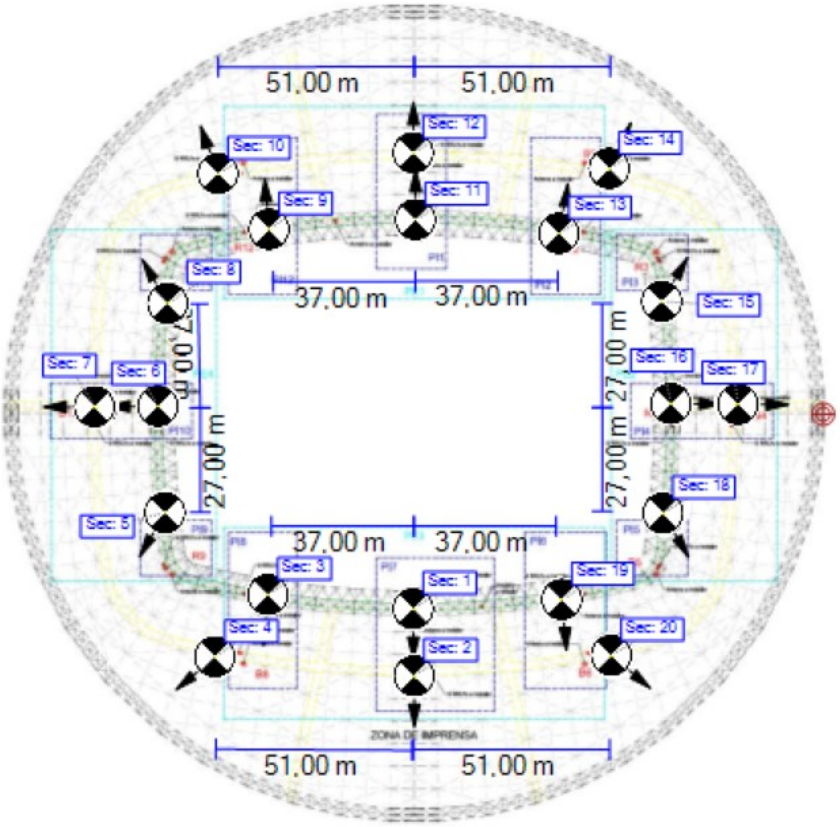


*Figure B.3 - Antenna position scheme extracted from the software for simulation 4.*

# B3. Output Maps of Simulation 2 and 3

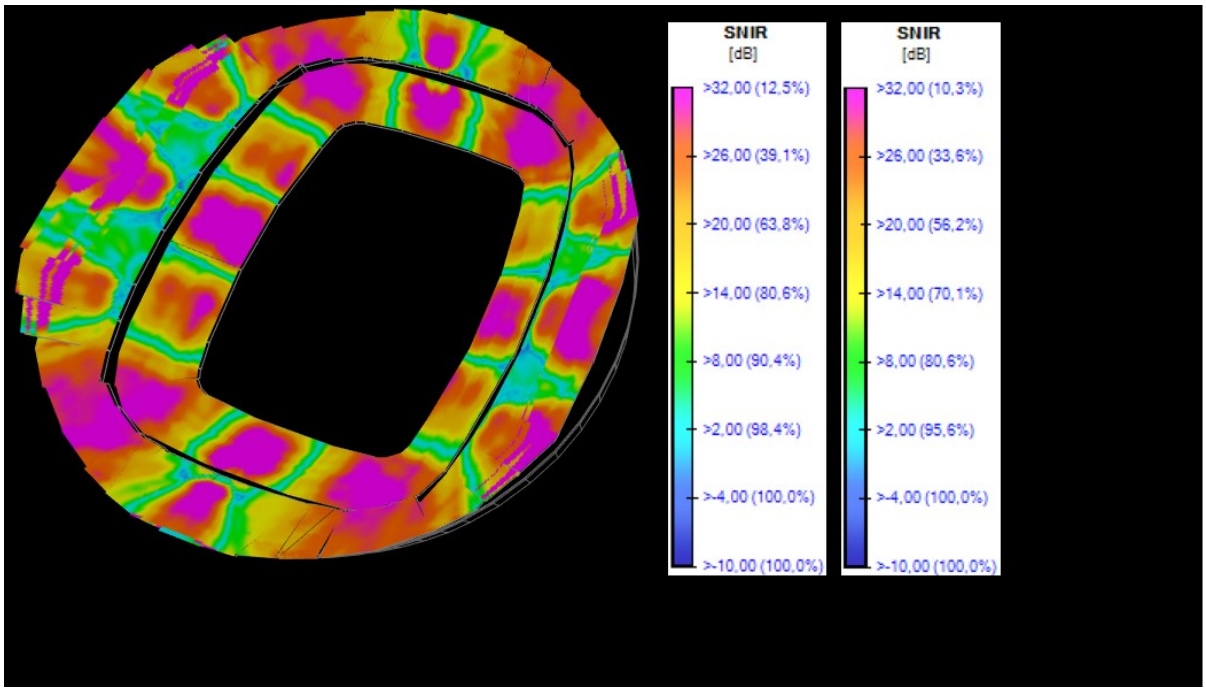


*Figure B.4 - iBwave SINR Output Map obtained in simulation 2 considering 1800 MHz band.*

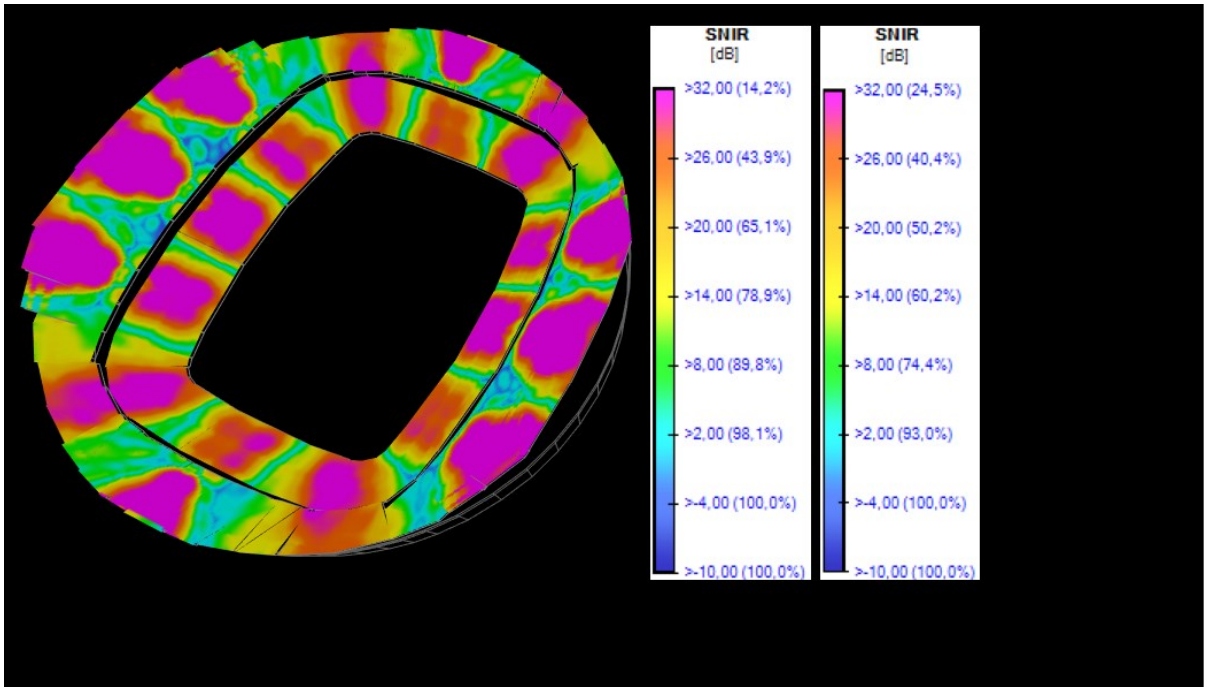


*Figure B.5 - iBwave SINR Output Map obtained in simulation 3 considering 1800 MHz band.*

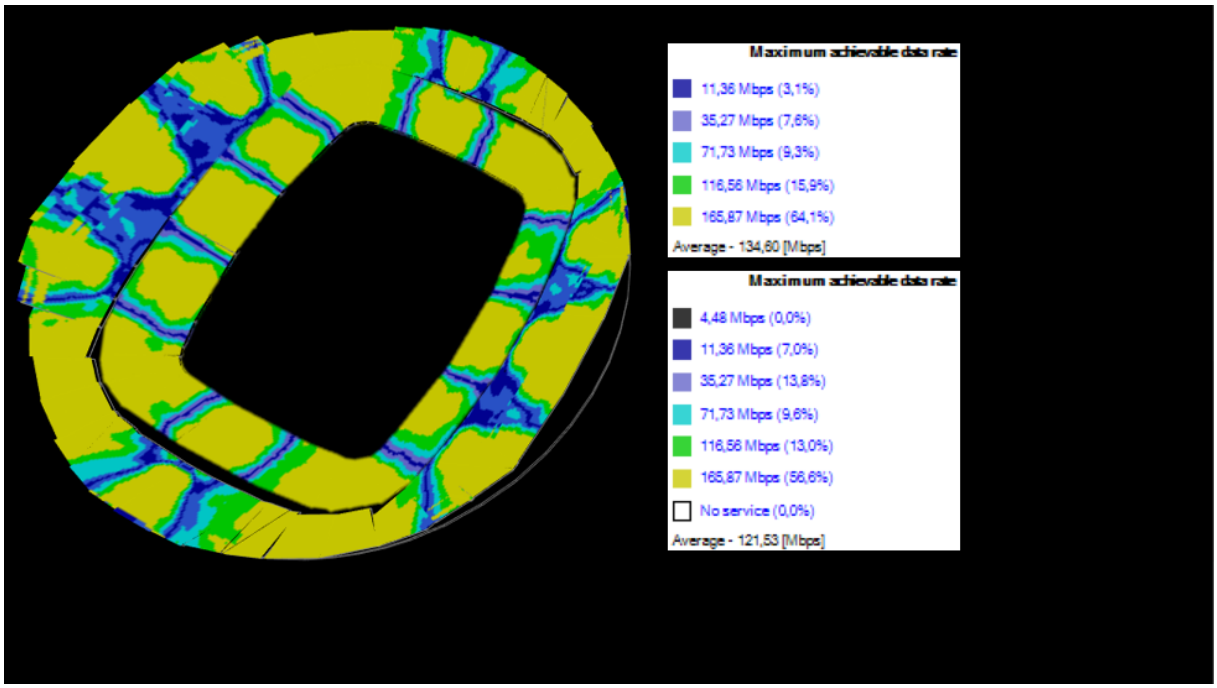


*Figure B.6 - iBwave MADR Output Map obtained in simulation 2 considering 1800 MHz band.*

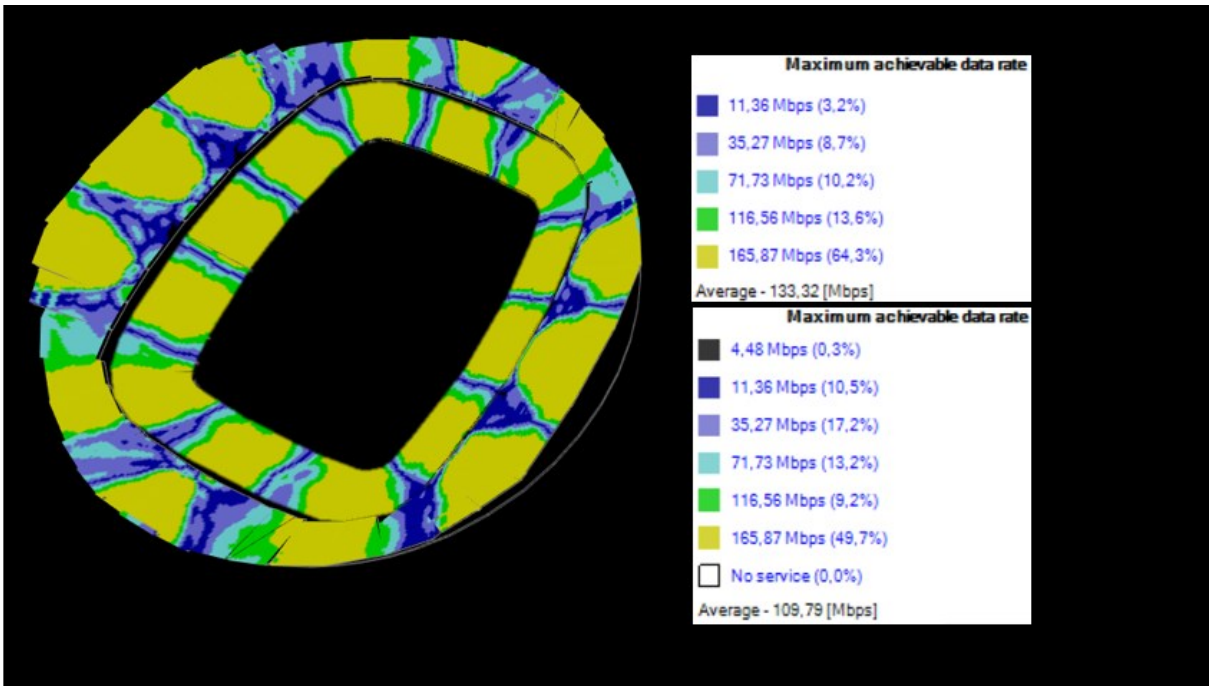


*Figure B.7 - iBwave MADR Output Map obtained in simulation 3 considering 1800 MHz band.*

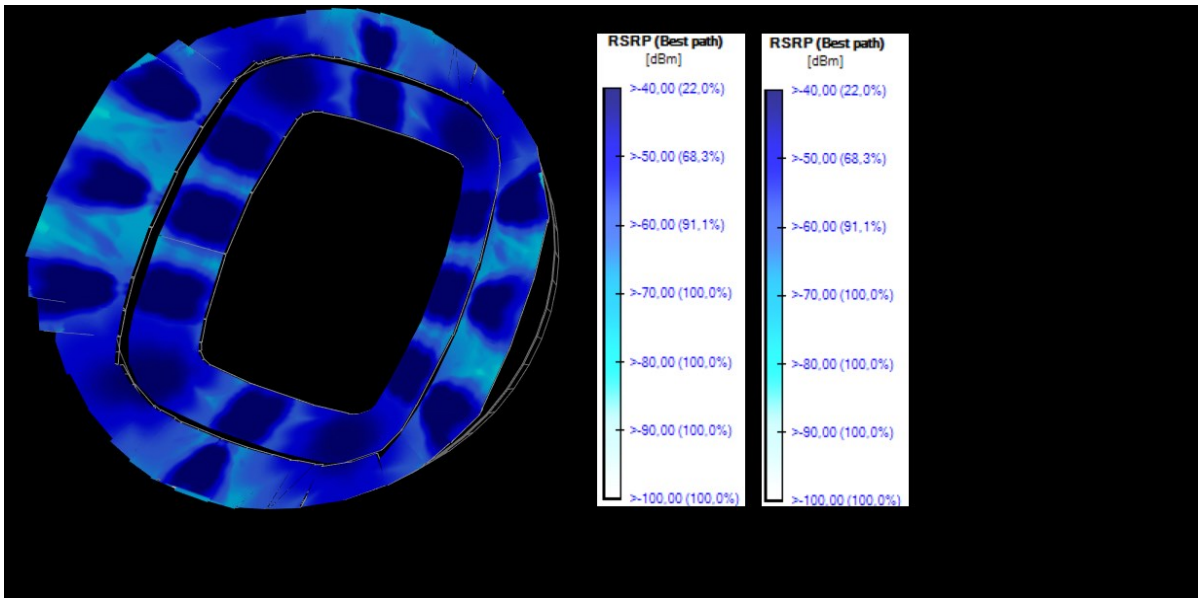


*Figure B.8 - iBwave RSRP Output Map obtained in simulation 2 considering 2600 MHz band.*

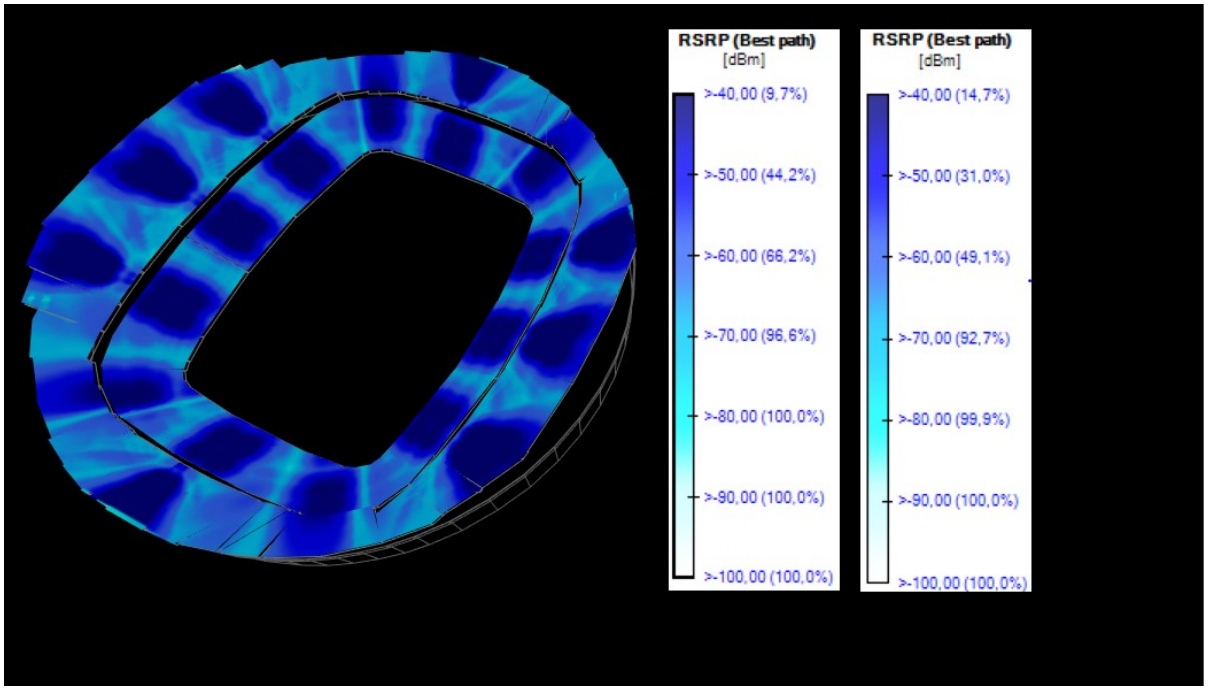


*Figure B.9 - iBwave RSRP Output Map obtained in simulation 3 considering 2600 MHz band.*

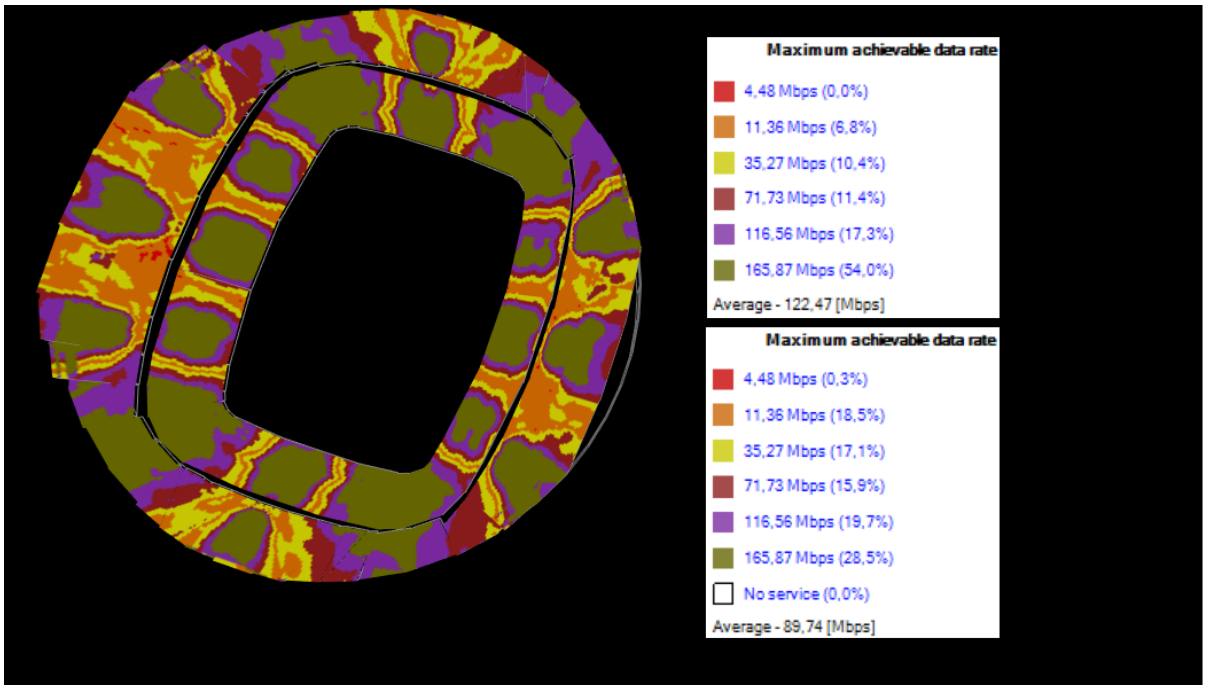


*Figure B.10 - iBwave MADR Output Map obtained in simulation 2 considering 2600 MHz band.*

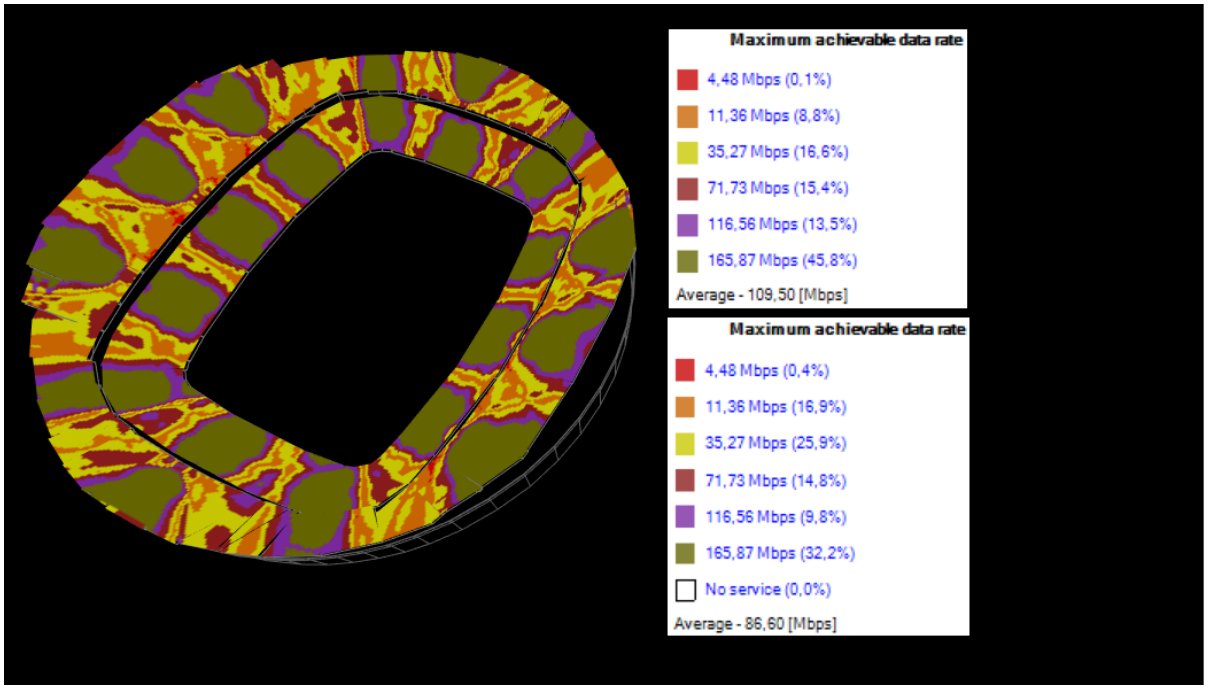


*Figure B.11 - iBwave MADR Output Map obtained in simulation 3 considering 2600 MHz band.*

# B4. Final Solution Output Maps

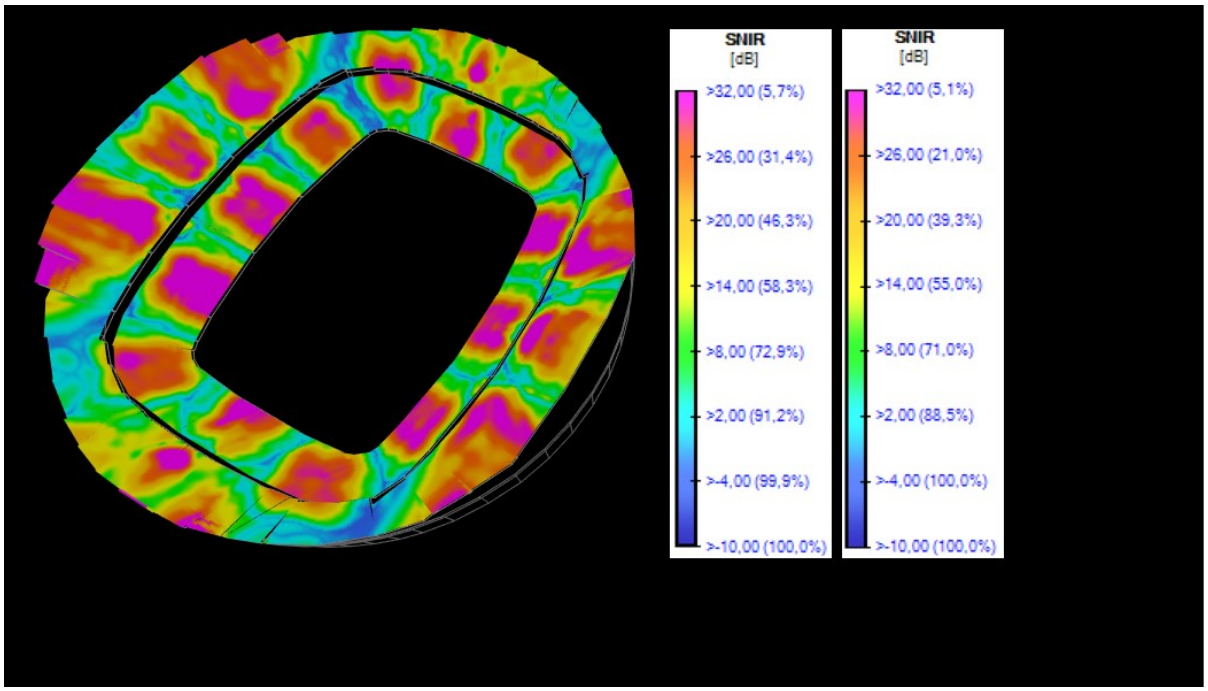


*Figure B.12 - Final Solution iBwave SINR output map obtained using 2600 MHz band.*

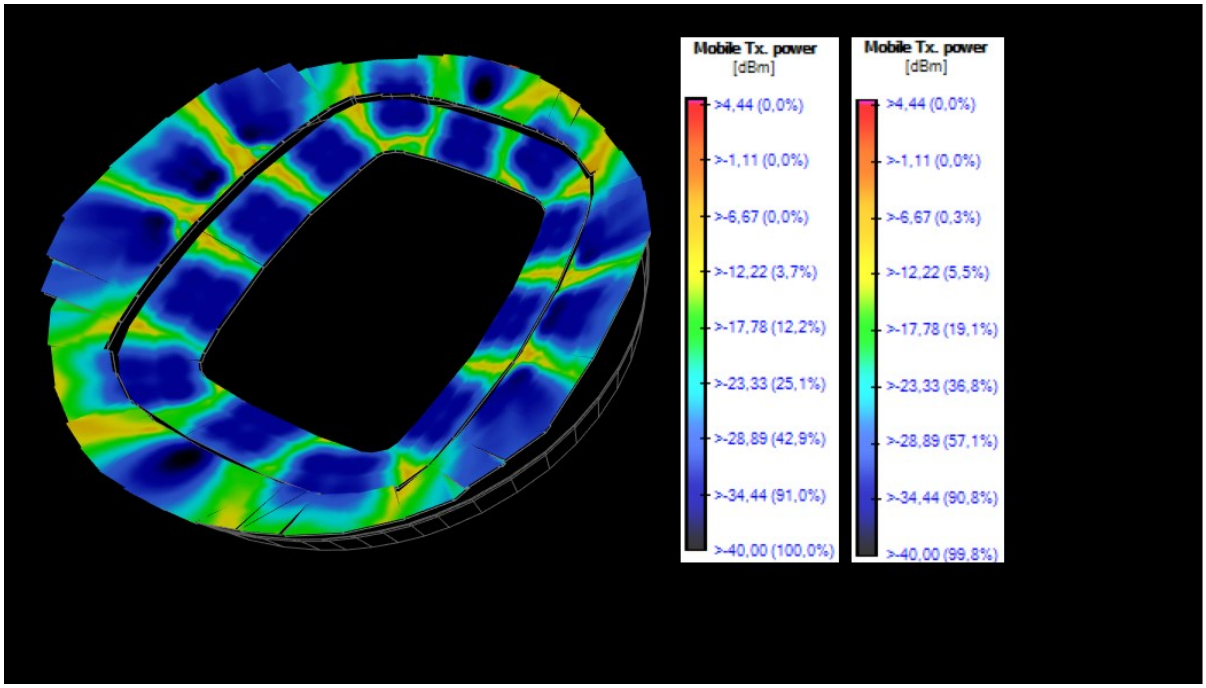


*Figure B.13 - Final Solution iBwave Mobile Tx Power Output Map obtained using 1800 MHz band.*

.

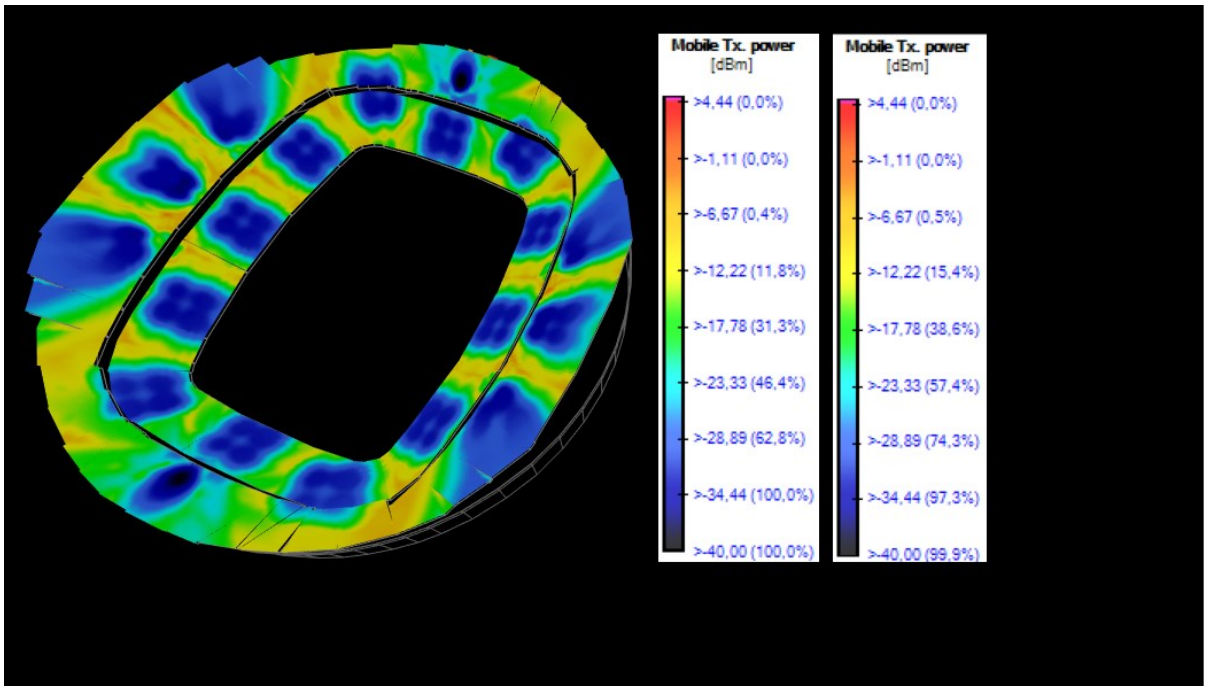


*Figure B.14 - Final Solution iBwave Mobile Tx Power Output Map obtained using 2600 MHz band.*

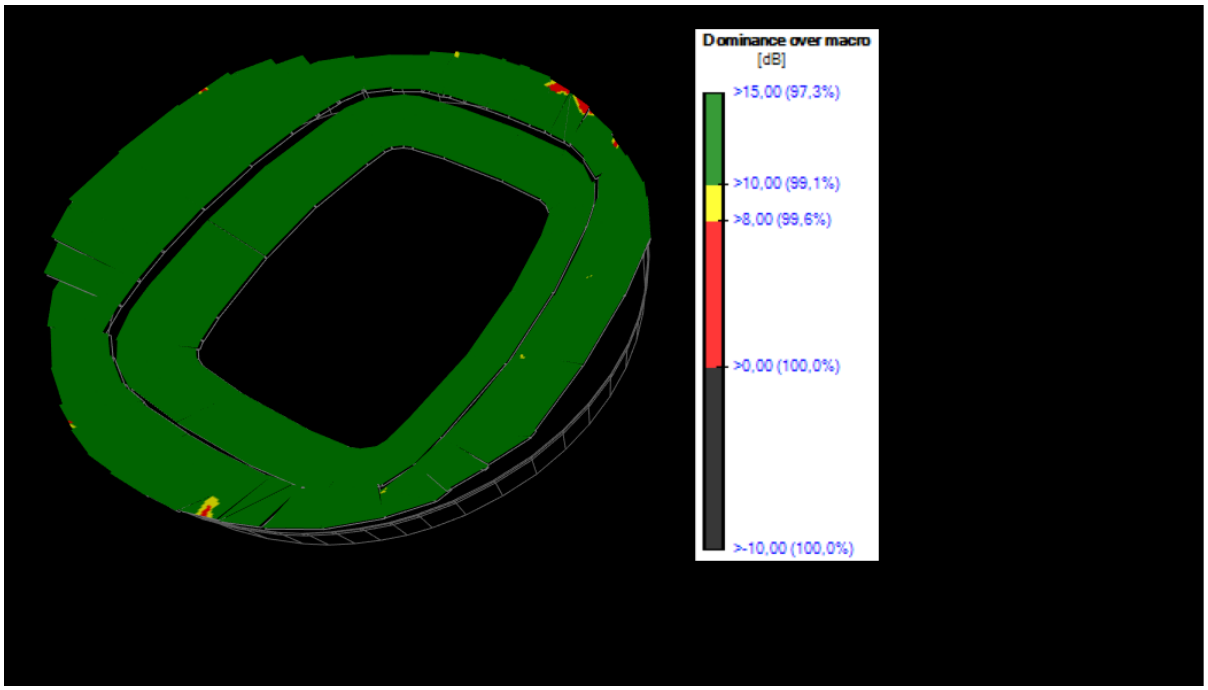


*Figure B.15 - Final Solution iBwave Dominance Over Macro Output Map obtained using 1800 MHz band.*

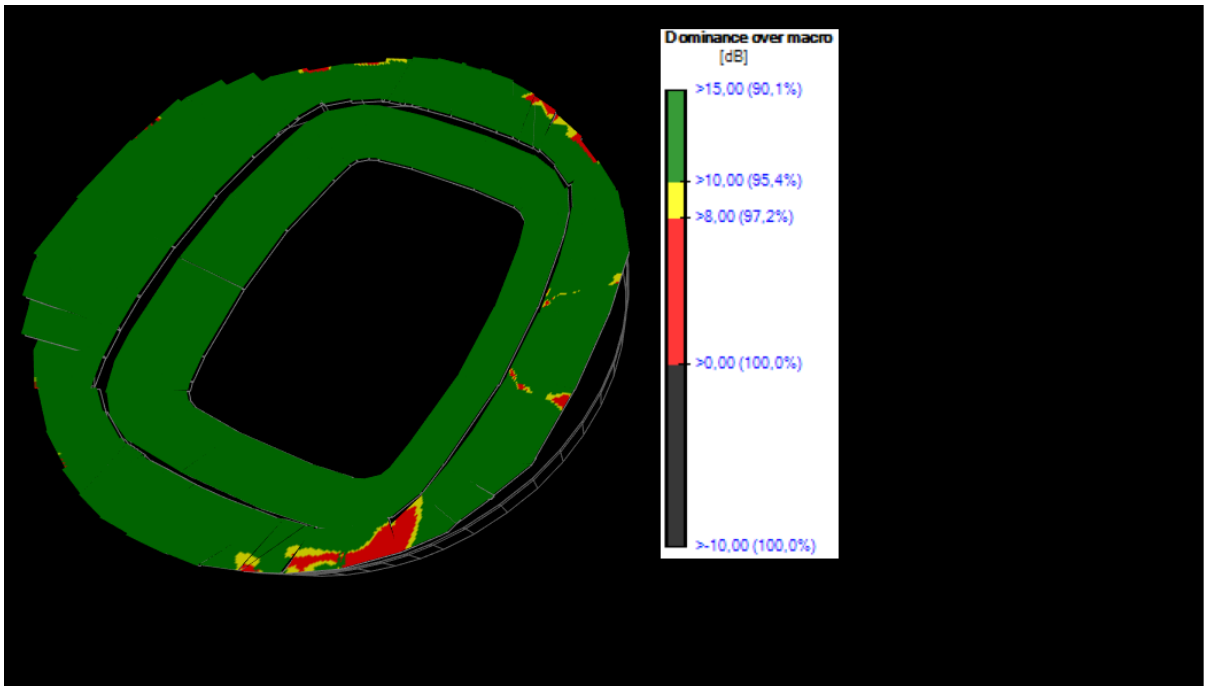


*Figure B.16 - Final Solution iBwave Dominance Over Macro Output Map obtained using 2600 MHz band.*